

STUDIES DIRECTED TOWARD THE USE OF ELECTRON  
IMPACT MASS SPECTROMETRY FOR ISOTOPIC ANALYSIS  
OF CARBON 13 ENRICHED BIOLOGICAL COMPOUNDS

Bari Shown Earl  
B.S., University of Nevada, Las Vegas, 1968  
M.S., Oregon Graduate Center, 1972

A dissertation submitted to the faculty  
of the Oregon Graduate Center  
in partial fulfillment of the  
requirements for the degree  
Doctor of Philosophy  
in  
Organic Chemistry  
January, 1979

This dissertation has been examined and approved by the following  
Examination Committee:

---

G. Doyle Daves, Jr., Thesis Advisor  
Professor

---

Jon Orloff, Examination Committee Chairman  
Assistant Professor

---

Douglas E. Barofsky  
Associate Professor

---

Thomas M. Loehr  
Professor

---

Richard A. Elliott  
Associate Professor

DEDICATION

To my daughters

Melissa

Melinda

Molly

and

Emily

### Acknowledgements

The author wishes to express special appreciation to Dr. G. Doyle Daves, Jr. for his long suffering guidance and encouragement during the course of this investigation, and to Dr. Warren E. Buddenbaum for his contributions of insight and effort. She also wishes to express appreciation to William Anderson for his help and suggestions in obtaining the mass spectral data, Dr. Thomas Loehr for suggestions and critical review, and Drs. A. G. McInnes and D. G. Smith for the  $^{13}\text{C}$  enriched samples of sepedonin and fusaryl alcohol.

The author also feels special gratitude for the efforts of Maureen Seaman in collecting many of the reference materials which contributed to the initial concepts of this work and to Dorothy Malek for the hours spent in typing and organizing this manuscript.

The financial support of the Board of Trustees of the Oregon Graduate Center for Study and Research is acknowledged with thanks.

Finally, the author wishes to thank her husband and family. Without their support, encouragement and active effort this work could not have been accomplished.

Table of Contents

	Page
Abstract .....	xviii
Introduction .....	1
Part I. Historical Review and Evaluation.....	
A. Data Reduction - Methods of Computation	5
B. Application of Carbon-13 Labeling.....	14
1. Introduction .....	14
2. Qualitative Determinations .....	15
3. Quantitative Determinations.....	
a. Singly-labeled compounds.....	19
b. Multiply-labeled compounds.....	40
C. Applications of <sup>13</sup> C mass spectral analysis to problems of biological significance.....	48
D. Conclusion.....	58
Part II. Development of the Polynomial Data Reduction Technique .....	59
A. Introduction.....	59
1. Generality of mass spectral theory.....	59
2. Traditional approach - a model of isotopic isomers.....	60
3. General approach - a statistical model....	62

	Page
B. Considerations for general application of mass spectral carbon isotopic analysis.....	64
1. Preliminary remarks.....	64
2. Kinetic isotope effects alter isotopic content of fragment ion regions.....	64
3. Complex regions contain overlapping ion clusters.....	66
4. Complexity of spectral processes results in carbon skeleton ambiguity.....	66
C. Mathematical formulation.....	67
1. Ion cluster - general.....	67
2. Ion cluster - isotopically enriched sample	68
3. Complex ion regions - overlapping clusters	70
4. Residual ion intensities as monitoring parameters - the factor method.....	70
Part III. Model Calculations Describing the Utility of the Polynomial Data Reduction Technique.....	74
A. Introduction - a rationale for model calculations	74
B. A discussion of some difficulties involved in the interpretation of isotopic mass spectra	74
1. Carbon-13 content - a quantity in need of definition.....	74
a. Four models containing "20% <sup>13</sup> C"	74
b. Model D - a true isomeric mixture	78

	Page
2. M+1/M ratio measurements for determination of isotopic content - a potential for abuse	78
a. A mathematical expression of the relationship between the isotopic abundance and M+1/M.....	78
b. Solutions to the equations relating isotopic abundance and mass spectral ion intensity.....	80
(1) Overview.....	80
(2) Assumption 1 - Natural abundance and isotopically enriched samples yield comparable spectra.....	81
(3) Assumption 2 - All enriched sites are equally enriched.....	82
(4) Determination of the number of enriched sites.....	82
c. Ion intensity ratios in spectra of highly enriched compounds.....	84
d. The potential for abuse of data reduction procedures.....	84
C. An investigation of the interrelationship of variables relating isotopic content and ion cluster appearance.....	85

	Page
1. The ion cluster contour.....	85
a. A concept of uniqueness.....	85
b. Interrelationship of variables in predicting ion cluster contour	86
2. Four variables important to the ion cluster contour.....	90
a. Total isotopic content.....	90
b. Distribution of enrichment.....	90
c. Molecular size.....	95
d. Dynamic range of measurement.....	96
3. Experimental guidelines through Ion Cluster Contour Diagrams.....	97
D. Two illustrations of the use of the polynomial data reduction techniques.....	101
1. One parameter approach.....	101
2. Factor approach.....	106
Part IV. Application of the Polynomial Data Reduction Technique to Data Previously Analyzed by Other Methods.....	111
A. Introduction.....	111
1. A rationale for this investigation.....	111
2. Scope of this investigation.....	111
B. The data reduction technique of Vandenhoevel and Cohen.....	112
1. Derivation of data reduction equation	112
2. Discussion of assumptions and limitations	114

	Page
C. Use of other current methodology.....	115
1. Overview.....	115
2. Derivation of exact analytical expressions	115
3. Application to amino acid analysis.....	116
D. Application of the method of Vandenhoevel and Cohen to model data.....	119
1. Overview.....	119
2. Variables for consideration.....	119
3. Conclusion.....	122
E. Application of the polynomial approach to observa- tion of biological isotope effects.....	123
1. Overview.....	123
2. ICCD evaluation.....	123
3. Advantages of the polynomial approach	125
a. Individual <sup>13</sup> C abundance values.....	125
b. Treatment of overlapping ion clusters.....	125
F. Conclusion.....	127
Part V. Application of the Polynomial Data Reduction Technique to Experimentally Obtained Data	128
A. Introduction.....	128
B. Fusaric Acid - a biosynthetic product.....	128
1. Introduction.....	128
2. Results and discussion.....	131
a. Mass spectral fragmentation pattern	131
b. High resolution mass spectrum.....	134

	Page
c. Analysis - sample with natural isotopic abundance.....	137
(1) Determination of ionic intensity identity from unit resolution data	137
(2) Calculation of $^{13}\text{C}$ natural abundance - a test of accuracy.....	140
d. Analysis - isotopically enriched sample	141
(1) ICCD evaluation.....	141
(2) Determination of $^{13}\text{C}$ abundance levels.....	142
3. Conclusion.....	147
C. Sepedonin - a fungal tropolone.....	147
1. Introduction.....	147
2. Results and discussion.....	148
a. Mass spectral fragmentation pattern	148
b. High resolution mass spectrum.....	149
c. Biosynthetic hypothesis.....	153
d. Ion cluster contributions from natural $^{13}\text{C}$ abundance data.....	155
e. Analysis - sample isotopically enriched by formate $^{-13}\text{C}$ precursor.....	156
(1) ICCD evaluation.....	156
(2) Determination of the number of different $^{13}\text{C}$ abundance levels	157

	Page
f. Analysis - sample isotopically enriched by acetate-2- <sup>13</sup> C precursor	160
(1) ICCD evaluation.....	160
(2) Quantitative determination of <sup>13</sup> C enrichment level	162
3. Conclusion.....	163
References.....	164
Appendix.....	175
A. Computer analysis technique.....	176
1. Preliminary remarks.....	176
2. One parameter approach - a limited application of the polynomial formulation.....	176
3. Factor approach - a more general application of the polynomial formulation.....	179
B. Experimental.....	180
1. Instrumentation.....	180
a. Mass spectrometer and related systems.....	180
b. Computing system.....	181
2. Methods.....	181
a. Mass spectral recording techniques.....	181
b. Computational techniques.....	184
3. Materials.....	184
a. Fusaryl alcohol.....	184
b. Sepedonin.....	187
Vita.....	188

## Figures

	Page
Figure I-1. Gliotoxin .....	17
Figure I-2. Asperlin .....	18
Figure I-3. 1-Deutero-3-ethyl-3-phenylpentane.....	23
Figure I-4 and I-5. Phenylethyl Ions.....	23
Figure I-6. Tropylium ion .....	23
Figure I-7. Benzyl ion .....	23
Figure I-8. Benzenium ion .....	24
Figure I-9. Phenyl ion .....	24
Figure I-10. Linear intermediate .....	24
Figure I-11. Neopentane .....	25
Figure I-12. (2- <sup>13</sup> C)-Furocoumarin.....	31
Figure I-13 and I-14. Electron ions .....	31
Figure I-15. Azepinium ion .....	32
Figure I-16. Oxaziridine .....	34
Figure I-17. m/z 98 .....	34
Figure I-18. 2-Methyl-quinoline-2- <sup>13</sup> C.....	36
Figure I-19. Methylated cyclopropane ion.....	37
Figure I-20. Hydroxylated " " .....	37
Figure I-21. Aminolated " " .....	37
Figure I-22. Tertiary immonium ion .....	37
Figure I-23. Intermediate ion .....	37

	Page
Figure I-24. Kaurene .....	39
Figure I-25. Kaurane .....	39
Figure I-26. Carbon-13 labeling of the pyronocoumarin	41
Figure I-27. Toluene- $\alpha,1$ - $^{13}\text{C}_2$ .....	43
Figure I-28. Randomization .....	44
Figure I-29. Symmetry .....	45
Figure I-30. Dewar benzene .....	47
Figure I-31. Prismane .....	47
Figure I-32. Benzvalene .....	47
Figure I-33. Phiebiarbrone .....	55
Figure I-34. Biosynthesis and EIMS Fragmentation of Ricinine	56
Figure II Observed Mass Spectra Can Be Viewed As Composites	61
Figure III-1 Four 3-carbon Models with isotopically enriched sites .....	75
Figure III-2 Molecular Ion Mass Spectra of Models A-D (Figure III-1) .....	76
Figure III-3 Three 3-carbon samples isotopically enriched at all sites .....	84
Figure III-4 Relationships of factors.....	89
Figure III-5 Plot for molecules.....	91
Figure III-6 Effect of increasing relative separation	92
Figure III-7 Relative separation values.....	93
Figure III-8 Separation values plotted.....	94
Figure III-9 Summary of data .....	95
Figure III-10 Summary .....	95

	Page
Figure III-11 Summary .....	96
Figure III-12 Fourth Variable .....	97
Figure III-13 Summary .....	98
Figure III-14 Summary .....	99
Figure III-15 Determination of value of $b_x$ for Model (Table III-2) .....	103
Figure III-16a Ion Cluster Contour Diagram $^{13}\text{C}_2(15.0,14.1)$	104
Figure III-16b Ion Cluster Contour Diagram $^{13}\text{C}_2(12.3,11.4)$	106
Figure III-17 Model Spectrum $^{13}\text{C}_3(4,3,2)$ 1 ion cluster.	107
Figure III-18 Model Spectrum $^{13}\text{C}_3(4,3,2)$ 2 ion clusters (99.3, 07) .....	108
Figure III-19 Model Spectrum $^{13}\text{C}_3(4,3,2)$ 3 ion clusters (98.3, 1.0, 0.7) .....	109
Figure IV-2 Effect of variables.....	120
Figure IV-3 Magnitude of isotope effect.....	121
Figure IV-4 Effect on deviation.....	122
Figure IV-5 ICCD for sample $^{13}\text{C}$ abundance values....	123
Figure IV-6 Comparison .....	126
Figure V-1 Fusaric Acid .....	128
Figure V-2 Biosynthetic Hypothesis for Fusaric Acid	130
Figure V-3 Principle ions in the EIMS Fragmentation of Fusaryl Alcohol .....	132
Figure V-4 EI Mass Spectrum of Fusaryl Alcohol.....	134
Figure V-5 Polynomial Factor Analysis of Fusaryl Alcohol, Natural Isotopic Abundance, Spectra.	141

	Page
Figure V-6	142
Ion Cluster Contour Diagram Fusaryl Alcohol(acetate-1- <sup>13</sup> C precursor) model <sup>13</sup> C <sub>2</sub> (9,4) .....	142
Figure V-7	143
Computer Print-out: Determination of <sup>13</sup> C Abundance Fusaryl Alcohol(acetate- 1- <sup>13</sup> C precursor) .....	143
Figure V-8	147
Sepedonin .....	147
Figure V-9	148
EI Mass Spectrum of Sepedonin.....	148
Figure V-10	148
Resonance Structures of Sepedonin.....	148
Figure V-11	149
EIMS Fragmentation Pathway of Sepedonin - Principal Ions .....	149
Figure V-12	153
Biosynthetic Hypothesis for Sepedonin...	153
Figure V-13	155
<sup>13</sup> CMR Results for <sup>13</sup> C-Enriched Sepedonins	155
Figure V-14	157
Ion Cluster Contour Diagram Sepedonin (formate- <sup>13</sup> C precursor).....	157
Figure V-15	159
Computer Print out: Determination of <sup>13</sup> C Abundance Sepedonin (formate- <sup>13</sup> C precursor)	159
Figure V-16	160
Ion Cluster Contour Diagram Sepedonin (acetate-2- <sup>13</sup> C precursor).....	160

Tables

	Page	
Table I-1	The Number of Possible Isomers Increases Geometrically With the Number of Labeled Sites	7
Table I-2	.....	26
Table III-1	Relative EIMS ion intensity values for eight model ion clusters.....	87
Table III-2	EIMS Isotopic Analysis of a Model System	102
Table III-3	EIMS Isotopic Analysis of a Model System	105
Table IV-1	Results of EIMS Isotopic Analysis of Various Amino Acid Fragment Ions.....	117
Table V-1	High Resolution Ion Intensity Recordings for Selected Ions of the Fusaryl Alcohol EI Mass Spectrum .....	133
Table V-2	High Resolution EI Mass Spectrum of Fusaryl Alcohol .....	135
Table V-3	Relative EIMS Ion Cluster Intensities of the Fusaryl Alcohol Molecular Ion Region.....	138
Table V-4	EIMS Ion Intensity Data of the Fusaryl Alcohol Molecular Ion Region.....	139
Table V-5	Polynomial Factor Analysis of Fusaryl Alcohol, Natural Isotopic Abundance, Spectra	141
Table V-6	Isotopic Analysis of the EIMS Ion Regions of <sup>13</sup> C Enriched Fusaryl Alcohol.....	144

	Page	
Table V-7	Isotopic Analysis of the EIMS C <sub>10</sub> Ion Region of a <sup>13</sup> C Enriched Fusaryl Alcohol.....	146
Table V-8	High Resolution Electron Impact Mass Spectrum of Sepedonin.....	150
Table V-9	Proton Magnetic Resonance Results for Carbon- 13 Enriched Sepedonins.....	153
Table V-10	EIMS Ion Cluster Intensity Results for m/z 206 Region Sepedonin-Natural <sup>13</sup> C Abundance.	155
Table V-11	EIMS Ion Cluster Intensity Results for m/z 206 Region - Sepedonin - Formate <sup>13</sup> C Pre- cursor .....	157
Table V-12	<sup>13</sup> C Isotopic Enrichment Results for Three EIMS Spectra Sepedonin-Formate- <sup>13</sup> C Precursor	158
Table V-13	EIMS Ion Cluster Intensity Results for m/z 206 Region-Sepedonin-Acetate-2- <sup>13</sup> C Precursor	160
Table V-14	<sup>13</sup> C Isotopic Enrichment Results for Four EIMS Spectra Sepedonin-Acetate-2- <sup>13</sup> C Precursor	161
Table A-1	M/M+1 Ion Intensity Ratios From Mass Spectra of Acetyl Acetone Parent Ion Region Demonstrat- ing Change in M/M+1 with Change in Slit Width	184
Table A-2	Ion Intensity Ratios From Mass Spectra of Fusaryl Alcohol Parent Ion Region Demonstrat- ing Quality of Visual Averaging Possible with Use of Wide Slit Widths.....	185

## ABSTRACT

The use of electron impact mass spectrometry for isotopic analysis is an established technique; however, its application to problems involving biologically produced molecules enriched in  $^{13}\text{C}$  has been severely limited. This limitation is shown to arise because of data reduction techniques which are, for practical purposes, incapable of dealing with the complex situation of multiple enrichment sites, limited isotope abundance, and complex spectral regions. Two approaches for detailed isotopic analysis of EIMS intensity are presented and illustrated using model data, literature data, and original data from biosynthetically enriched compounds. The first approach which allows for sequential variation of any one parameter is shown to be of value in experimental design through construction of ion cluster contour diagrams which summarize the variation of isotopic distribution, molecular size, and uncertainty in measurement with total isotopic content. The second approach differs in concept from previous methods and is especially promising for application to problems involving multiple sites of enrichment, limited isotopic abundance, and complex spectral regions. The key concept of this approach is that the roots of the polynomials constructed from observed spectral intensities are analytically related to the isotopic content and the isotopic distribution of the ions giving rise to the intensities.

## INTRODUCTION

Mass spectrometry has been applied almost from the very beginning of its development to the detection of stable isotopes and the measurement of their abundance. As early as 1907 a primitive instrument was utilized in the search for isotopes of the very elements of primary concern in this present investigation - carbon, hydrogen, oxygen and nitrogen - elements of significant biological importance (1). Of historical interest and certain amusement is the conclusion of that study: No isotopes exist for these elements!

Fortunately, since that time, the work of numerous investigators has greatly increased the sophistication and sensitivity of mass spectral instruments. Stable and even radioactive isotopes have been detected for these and other elements, the exact masses obtained,<sup>1</sup> and the relative natural abundances accurately and precisely measured for samples from various sources.<sup>2</sup> Such measurements are now done routinely on advanced isotope ratio mass spectrometers by first converting the sample to an appropriate gas.

Methods for isolation of elemental isotopes have been and are currently being developed. Mass spectral analysis of compounds of

---

<sup>1</sup>Exact mass tables of the elements are kept and annually reviewed and revised by the International Union of Pure and Applied Chemistry (IUPAC). As an example, see ref. (2).

<sup>2</sup>For examples of natural abundance measurements made from specific sources, see refs. (3-5).

differing isotopic proportions has found application in many and diverse fields including studies of mass spectral fragmentation pathways (7,8), reaction mechanisms (8), structure (8), biosynthesis (8,9) and metabolism (8,10-13), archeological dating (14), and more recently, outer space exploration (15). Artificial enrichment or labeling with deuterium combined with mass spectral analysis has found most extensive application and use of oxygen-18 and nitrogen-15 have followed in frequency of use (8). Carbon-13 labeling has found valuable although limited application in the past for a number of reasons: Carbon-13 enriched precursors of high isotopic purity have been of limited availability (16). Carbon-13 occurs in relatively high natural abundance (17). High resolving power is needed to separate  $^{13}\text{C}$  isotopic ions from  $^{12}\text{CH}$  ions which commonly interfere (1 in 40,000 at mass 200). Perhaps, most importantly, many experiments would result in enrichment at numerous multiple sites, a problem for which data reduction techniques have had minimal development. (See Part IA).

Advances in other techniques for isotopic analysis and the practical limitations of mass spectrometric isotopic analysis have currently shifted analytical emphasis for  $^{13}\text{C}$  enriched molecules away from mass spectrometry. However, there remain many appealing properties which have preserved interest in its application: Mass spectrometry is a general approach to isotopes of all elements. It appears to be an idealized example for automation of the traditional analysis techniques

involving degradation to component parts.<sup>3</sup> It is capable, particularly in combination with gas chromatography, of analysis of mixtures.<sup>4</sup> Its inherent degradation mechanism and its ability to accept mixtures limits reagents, sample preparation time, and contamination. It is potentially fast, sensitive, accurate and precise (20).

To date, however, due to practical limitations, these favorable properties have been of limited advantage for use of the mass spectrometer in isotopic analysis. The limitations may be grouped into three general classes:

- (1) those that are related to the mass spectral behavior of the molecule;
- (2) those that are instrumental in nature; and
- (3) those that are related to data reduction techniques.

Therefore, applications of mass spectral analysis to problems involving <sup>13</sup>C have been very selective so far. Most have, in general, (1) made use of only a tiny fraction of the available information, (2) made assumptions which degrade the quality of the data available, and/or (3) limited the number of enrichment sites within the molecule to not more than two. Applications to analysis of biologically produced, intact samples have been particularly scarce. (See Part IC)

---

<sup>3</sup>For a discussion of the limitations in the picture of mass spectrometry as an automatic degradation technique for isotopic analysis, see ref. (18).

<sup>4</sup>Some care must be taken, however, when use of gas chromatography is made during isotopic analysis, since separation of isotopes within the column is a real possibility (19).

Experience in this research has convinced us that the detailed analysis of isotopic mass spectrometric data will require the following elements:

- (1) improved data reduction techniques;<sup>5</sup>
- (2) computer aids;<sup>6</sup>
- (3) instrumental modifications;
- (4) use of high resolution data.

It is the intention of this investigation to explore the feasibility of an exhaustive isotopic description of a biologically-produced, <sup>13</sup>C enriched molecule based on mass spectral data alone using the limited instrumentation available in this particular laboratory. In so doing, a new and unique data reduction technique is developed which shows great promise for analysis of compounds with multiple sites of isotopic enrichment, limited isotopic abundance, and/or complex spectral regions.

---

<sup>5</sup>Theoretical investigation of data reduction techniques for isotopic electron impact mass spectral data is an area of current interest. For a discussion of the literature pertaining to this subject, see Part IA herein.

<sup>6</sup>The increasing availability of computers has greatly enlarged their use in the field of EIMS isotopic analysis. Computer techniques have been applied in the areas of construction of model spectra (21,22), real data acquisition and processing (23-25), reduction of acquired data (26-30), and interpretation of data to yield chemical information (31-33). For a review of the principles involved in the selection of a laboratory computer see "Computers for Spectroscopists" (34). For an exhaustive application of computer techniques to EIMS including isotopic analyses, see (35).

## PART I

## HISTORICAL REVIEW AND EVALUATION

## A. Data Reduction - Methods of Computation

To the uninitiated the limited application of mass spectrometry for the determination of  $^{13}\text{C}$  enrichment in complex molecules is not easily understood. It appears obvious that this technique should be adaptable to compounds enriched in isotopes of any element. In fact, its use has been severely limited. Relative neglect of an element such as germanium is understandable. Compounds containing this element are relatively few. Carbon, however, is an abundant and important element. Voluminous experiments incorporating carbon-14 enrichment stand in evidence. Parts IB and IC of this work attempt to be an exhaustive review of the literature pertaining to electron impact mass spectral isotopic analysis of complex molecules containing carbon-13<sup>7</sup>. It is obvious from the review that applications of this technique have been extremely limited in both scope and number. The limited development of data reduction techniques for  $^{13}\text{C}$  mass spectral analysis may be one reason. Why is  $^{13}\text{C}$  data reduction uniquely difficult? The most obvious reason is the possibility which exists for enrichment at multiple sites within a single molecule. Discussions of selected references will here be presented to illustrate the evolution of current data reduction techniques.

---

<sup>7</sup>The term "complex molecules" is intended to exclude mass spectral isotopic analysis techniques which require the sample to be in the form of a simple gas. Development of instruments for measurement of isotope ratios in simple gases was an early advance in EIMS (36-38).

The earliest work to detail a method for isotopic analysis of  $^{13}\text{C}$  enriched molecules was that of D. P. Stevenson in 1951 (39). He pointed out that since pure specimens of  $^{12}\text{C}$  or  $^{13}\text{C}$  compounds are not available,  $^{13}\text{C}$  enriched compounds will, of a necessity, be mixtures of several isotopic compounds, hereafter called "isotopic isomers", differing from each other in both the relative number of  $^{12}\text{C}$  and  $^{13}\text{C}$  atoms in the molecule and in the positions of the isotopic atoms. Stevenson proposed beginning the interpretation of the mass spectrum of an isotopically enriched specimen by determining the concentrations of the various isotopic species and thereby constructing individual mass spectra for each pure isotopic isomer. That is, using an example from his work, a spectrum taken for a sample of propane-1- $^{13}\text{C}$  produced from potassium cyanide (ca. 50%  $^{13}\text{C}$ ) with ethyl bromide would actually be viewed as a composite of the spectra of propane- $^{13}\text{C}_0$ , propane-1- $^{13}\text{C}$ , propane-2- $^{13}\text{C}$ , propane-1,2- $^{13}\text{C}_2$ , propane-1,3- $^{13}\text{C}_2$ , and propane- $^{13}\text{C}_3$ . Six formulas are presented for calculating the concentrations of the possible  $^{13}\text{C}$  enriched propane isomers (reduced from 8 by symmetry) from the  $^{13}\text{C}$  content of the enriched starting material and the natural abundance of  $^{13}\text{C}$ . Individual spectra for each isotopic isomer are then constructed from the observed mass spectrum and the spectrum of naturally occurring propane. From the constructed mass spectra, the isotope effect of the  $^{13}\text{C}$  substitution on the mass spectral fragmentation processes is clearly visible. A similar procedure is followed for the enriched butanes.

This approach is clearly quite complex. It is not applicable to spectra of biologically produced  $^{13}\text{C}$ -enriched molecules where dilution

effects render the  $^{13}\text{C}$  content of the "reagents" unknown. Even for cases where the  $^{13}\text{C}$  content of the starting material is fixed the complexity of the method increases rapidly with the size of the molecule (see Table I-1). For a molecule with only 10 possible sites of  $^{13}\text{C}$  enrichment over 1000 isotopic isomers are possible. It is clear why

TABLE I-1

THE NUMBER OF POSSIBLE ISOMERS INCREASES EXPONENTIALLY  
WITH THE NUMBER OF LABELED SITES

<u>NO. OF SITES</u>	<u>NO. OF ISOMERS</u>
0	1
1	2
2	4
3	8
6	64
10	1024
15	32768

the great majority of the mass spectral analyses of  $^{13}\text{C}$ -enriched intact molecules deal with  $^{13}\text{C}$  enrichment at a single site. (See Part IB3) Stevenson's data reduction procedure seems to have greatly influenced the general view of isotopically enriched mass spectra and resulted in widespread application of an approach referred to herein as the method of isotopic isomers.

In 1962 Biemann included a detailed description of an isotopic mass spectral data reduction technique in his book "Mass Spectrometry - Organic Chemical Applications" (40). His approach again considers the spectrum to be a mixture of isotopic isomers, but it is based on knowledge

of the spectrum of the naturally occurring sample. He recommends a stepwise procedure multiplying the measured ion intensities of the enriched spectrum by the normalized ion intensities of the natural abundance spectrum (intensity of the parent  $^{13}\text{C}_0$  ion = 1.0) and then subtracting the results from the intensities in that enriched spectrum. The portions due to the  $^{13}\text{C}_0$  isotope and its associated ions resulting from the naturally present  $^{13}\text{C}$  are thus removed. This procedure is then successively repeated with the ion intensity remainders until all ion intensities approach zero. As Biemann points out such a technique could also utilize a set of simultaneous equations.

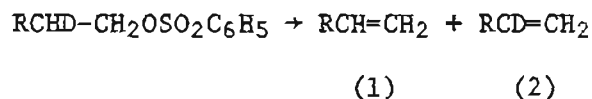
Biemann mentions several limitations. First, considerable error is introduced when a fragment ion of lower mass is present, cannot be eliminated by varying instrumental parameters, and overlaps the ion cluster of interest. Second, the emphasis on the comparison of the spectrum of the unenriched sample with that of the enriched sample neglects isotope effects in fragmentation processes thus rendering the technique invalid where considerable isotope effects are to be expected. Third, the approach is considerably more accurate when the mixture of isotopic isomers consists primarily of one species. A fourth serious limitation not mentioned by Biemann merits discussion. The success of Biemann's approach depends heavily upon the idea that the spectra of the naturally occurring and enriched samples will be comparable. It is commonly understood that experimental difficulties prevent such from being true for a good many cases. The experimental parameters of the mass spectrometer are difficult to keep constant (30) and therefore application of this

technique to fragment ion regions is limited. Also, for many applications, the natural abundance sample must be derived from a different source and therefore will contain different contaminants and not be directly comparable. The sample itself may be unstable again rendering the two spectra not comparable. However, Biemann's technique is straightforward and easily understood and has proved to be of great value for problems where a limited number of isotopically substituted sites are expected, a high degree of accuracy is not demanded, and/or the molecular ion region is the region of interest. It is the technique most commonly used in courses on mass spectral analysis.

An interesting doctoral thesis was presented in 1967 by A. C. Buchholz, a student of K. L. Rinehart, on mass spectral studies of compounds labeled with carbon-13 (41). His calculation techniques incorporated both those of Stevenson and Biemann again using the approach of isotopic isomers. Buchholz first removed the portions of his spectra due to naturally-occurring  $^{13}\text{C}$  in a manner similar to Biemann, but used simply the accepted average value for  $^{13}\text{C}$  natural abundance (0.01108) rather than that determined from an experimental spectrum of an unlabeled sample. For spectra where the molecular ion region was complicated by numerous overlapping fragment ion clusters due to loss of hydrogen (in his case those of toluene and aniline) he used the spectrum of the unlabeled sample (corrected for naturally occurring  $^{13}\text{C}$ ), the known enrichment of the starting material, and the reaction mechanism to separate the various species in a manner similar to Stevenson. His results

were of an accuracy sufficient to demonstrate the presence of the tropylium ion in the toluene spectrum.

In 1970, John Brauman presented an ingenious least squares data reduction technique which he applied primarily to the case of molecules containing heteroatoms with many and abundant naturally occurring isotopes (42). Again the spectrum is separated into the spectra of the individual isotopic isomers. The method requires prior knowledge of the spectra of the individual isomers and is, therefore, not applicable to most situations of interest in this paper; however, it does find limited application for analysis of mixtures of isotopic isomers when the individual isomers can also be produced by different mechanisms. The example given by Brauman is the mixture produced by the reaction



The Brauman technique would produce results with less error than the standard techniques because it makes use of all the data and produces a least squares solution.

In 1972, Daves, Buddenbaum and Earl recognized the need for mass spectral isotopic data reduction techniques based on a statistical picture of isotopically enriched samples rather than the traditional picture of such samples as mixtures of isotopic isomers. They described a computerized statistical approach to data reduction allowing for variation of one parameter of isotopic enrichment, i.e. degree of enrichment or number of sites of enrichment (43).

Later in 1972, Hergentobler and Lölinger presented a general

approach for calculating the isotopic composition of a labeled compound (44). They clearly demonstrated the polynomial nature of the equations relating the isotopic isomers and based their procedure on a statistical approach rather than on the method of isotopic isomers. As they pointed out, although this approach had been commonly known to practicing mass spectroscopists, formulation of this generally valid treatment was needed in a form readily understood by chemists.

Rapidly following the Hugentobler and Lölinger paper is one presented by Genty in which the statistical approach is also emphasized (45). Genty criticizes the commonly used approach of isotopic isomers as being increasingly impractical as the number of isomers grows rapidly with increasing number of enrichment sites and suggests that an isotopic ratio calculation method based on the statistical hypothesis can overcome these difficulties. The statistical hypothesis rests on the assumption that systems exhibiting chemical inertia are equilibrated at the outset and therefore theoretical equilibrium constants closely approximate the actual constants. The technique then requires only a limited number of measurements - only  $p$  ion intensity ratios - to obtain values for the relative concentrations of  $p$  isotopic isomers.

Although Genty did not extend his method to application in the case of overlapping ion clusters, it is clearly adaptable to such a case so long as the number of measurable known quantities is kept equal to the number of unknown values to be determined, e.g., in the case of overlapping ion clusters, the number of measurable ratios must be equal to the number of relative concentrations of isotopic isomers plus the number of

ion clusters. (See Part IIB3).

Genty then applied his approach to the complex theoretical case of a mixture of hydrogen-, deuterium-, and tritium-bearing propanes involving 45 different isotopic isomers!

Genty's original equations were amended in a communication by Richard W. Rozett (46). Rozett identifies an extra term in Genty's original derivation which did not cause error in this application since the use of ratios eliminated the term.

Also in 1973, Daves, et al. reported application of the previously described one parameter statistical approach to isotopic analysis of a biosynthetically  $^{13}\text{C}$  enriched sample, sepedonin (47). In addition, they described a new approach to mass spectral isotopic data reduction which fully utilized the polynomial character of the equations relating the observed spectral intensities to the isotopic content of the sample (47,48).

In December, 1974, Rozett presented what is to date the most elegant and concise discussion of data reduction techniques for isotopic mass spectral information (49). He first briefly enumerated the many and varied complications which have made the use of quantitative EIMS isotopic analysis so difficult and then gave clear and concise descriptions of three complementary methods for determining accurate isotopic abundance information: the "peak comparison method", similar to Genty's but expanded to a more general relationship based on the multinomial distribution law which included consideration of isotopic contributions other than the one of primary interest, "the graphical method" similar

to a method originally presented by R. L. Middaugh which has found general application in inorganic chemistry (50), and his own nonlinear least squares method which is more accurate, more generally applicable, but considerably more complex than the previous two. Computer programs for these three methods have been filed with the American Society for Mass Spectrometry.

Unfortunately, for the purposes of the present study, all three methods are based on the multinomial distribution law and are not directly applicable to the case of site-labeled compounds.

In 1976, Pickup and McPherson published a discussion of the theoretical equations by which calibration graphs may be determined for quantitative mass spectrometric analyses in which stable isotope enriched compounds are used as internal standards (51). They point out the neglect of such theoretical bases in previous works and present an excellent discussion of the complexity of analysis in cases where opportunity for multiple sites of isotopic enrichment exists. With this complexity in mind, their approach is based on statistical considerations.

A recent treatment of the statistical approach to mass spectral isotopic analysis was published by Yamamoto and McCloskey in 1977 (52). The derivation of the equations presented therein is tailored to treatment of samples very extensively enriched with heavy isotopes and a graphical attempt is made to illustrate the complexity of the relationships between the various factors controlling the abundance of isotopically enriched ions.

It is clear from these later publications that the picture of

an isotopic mass spectrum as a composite of spectra of various isotopic isomers is currently being replaced by a statistical picture which will allow consideration of more complex isotopic situations.

## B. Applications of Carbon-13 Labeling

### 1. Introduction

Carbon-13 labeling has been and is a technique having such widespread application that, in spite of existing analytical limitations, it has found extensive use. However, to date such use has been necessarily restricted most often to cases of limited complexity.

Experimental applications of  $^{13}\text{C}$  labeling may be generally classed at three levels of increasing complexity: (1) those involving simple detection of the presence of the artificial  $^{13}\text{C}$  enrichment, (2) those requiring location of the label at a particular atomic site within the molecule, and (3) those which involve quantitative determination of the level of artificial enrichment either (a) for the total molecule or (b), in cases of multiple sites of enrichment, at each individual site. Information at all three levels is available through mass spectrometric analysis; however, because of existing data reduction problems, most applications of mass spectrometry for  $^{13}\text{C}$  analysis have been restricted to levels (1) and (2). Quantitative determinations (level 3) have been generally restricted to case (a), total  $^{13}\text{C}$  abundance measurement. This may be done accurately and easily through use of an isotope ratio mass spectrometer following conversion of the sample to  $\text{CO}_2$  or with somewhat less accuracy by analysis of the parent ion region in a mass spectrum of the intact molecule. Examples of applications requiring quantitative

measurement of  $^{13}\text{C}$  abundance at individual sites are rarer but do exist sometimes employing innovative data reduction approaches. Although labeling with the stable isotope  $^{13}\text{C}$  should have obvious advantage over labeling with the radioactive isotope  $^{14}\text{C}$  for biological applications, such uses have been extremely limited. Interest is currently high in clinical applications of this technique.

Description of mass spectral analyses of intact,  $^{13}\text{C}$  enriched molecules follows.

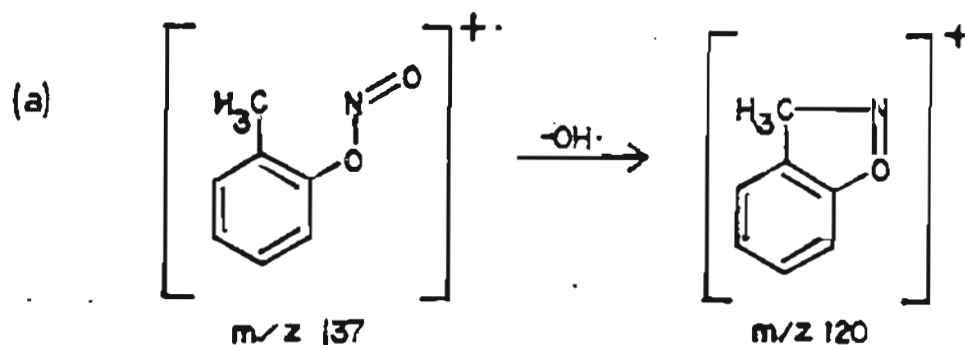
## 2. Qualitative Determinations

As previously mentioned, data reduction insufficiencies have hindered quantitative application of mass spectral analysis for  $^{13}\text{C}$  enriched samples. Experimental applications do occur, however, in which accurate quantitative determination of the isotope content is not necessary and a simple qualitative indication of the presence or absence of  $^{13}\text{C}$  in the molecule or in particular fragments will suffice. In addition, mass spectrometric results have occasionally been used in conjunction with quantitative NMR analysis.

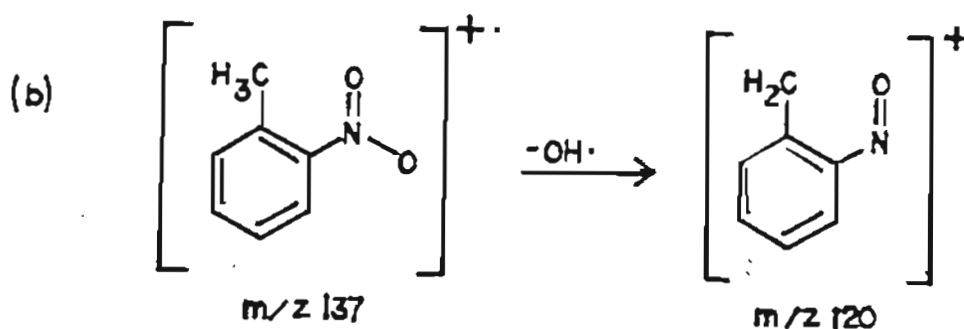
Melton and Ropp used D,  $^{13}\text{C}$  and  $^{15}\text{N}$  labeling in an investigation of one of the first negative ion-molecule reactions to be observed in the mass spectrometer (53). While using 2.3 ev. electrons to produce  $\text{HCOO}^-$  ions from formic acid and then passing these ions through a field-free space filled with the neutral molecule,  $\text{N}_2$ , negative ions of  $m/z$  26 were observed. Substitution of  $\text{DCOOH}$  for the formic acid did not effect the ion's mass; however, substitution of either  $\text{H}^{13}\text{COOH}$  for the formic acid or nitrogen- $^{15}\text{N}$  for the nitrogen increased the  $m/z$  of the ion to 27.

Use of both labeled reagents shifted the ion  $m/z$  to 28. Replacement of the formic acid by either  $\text{CO}_2$  or  $\text{CO}$  caused the ion at  $m/z$  26 to disappear.

Beynon, Saunders, Topham and Williams used high resolution data in a study of the dissociation of *o*-nitrotoluene under electron impact (54). By labeling the methyl group with  $^{13}\text{C}$ , they hoped to distinguish between the following fragmentation mechanisms:



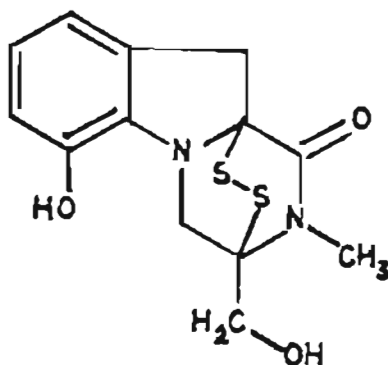
necessitating prior rearrangement of the nitrous group to the nitrite form and



which requires no such rearrangement. The ion of  $m/z$  120 further dissociates, losing  $\text{CO}$ , to form the ion  $\text{C}_6\text{H}_6\text{N}^+$  of  $m/z$  92. Discounting carbon skeleton rearrangements, when the methyl carbon is labeled

with  $^{13}\text{C}$ , loss of CO from the product of mechanism (a) would involve loss of a ring carbon and produce the ion  $^{12}\text{C}_5^{13}\text{CH}_6\text{N}^+$  of m/z 92 while loss of CO from the product of mechanism (b) would involve loss of that label and produce the ion  $^{12}\text{C}_6\text{H}_6\text{N}^+$ . High resolution spectra obtained for the region of m/z 92, 93 clearly demonstrated almost total loss of  $^{13}\text{C}$  label indicating mechanism (b) to be operative. Results were so dramatically apparent that precise quantitative calculations were not necessary.

Bose, et al. investigated the biosynthetic incorporation of  $^{15}\text{N}$ -phenylalanine,  $^{15}\text{N}$ -glycine, 2- $^{13}\text{C}$ -glycine, 1- $^{13}\text{C}$ -glycine and  $^{13}\text{C}$ -formate in gliotoxin (I-1) produced by Trichoderma viride (55).



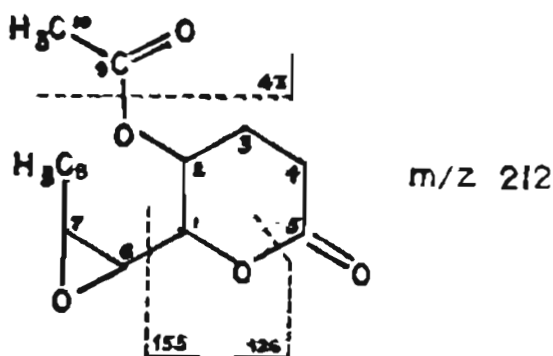
**I-1. Gliotoxin**

Suitably stable derivatives were prepared and their mass spectra examined under high resolution in the areas of interest. Results were essentially qualitative demonstrating all five precursors to be incorporated. The nitrogen of glycine seemed to be somewhat randomly distributed between both nitrogen positions of gliotoxin; however, the glycine carbons were not directly incorporated in the indole moiety. This is consistent with

a biosynthetic pathway in which the glycine releases its amino group into a pool from which phenylalanine is formed.

Another biosynthetic study utilizing high resolution mass spectra was that of Burlingame, et al.  $^{13}\text{C}$ -labeled lipids isolated from the yeast Saccharomyces cerevisiae were investigated using both  $^{13}\text{C}$  NMR and mass spectrometry (56). Although high enrichment levels were achieved ( $\sim 32\%$   $^{13}\text{C}$ ) mass spectral results obtained were purely qualitative being consistent with incorporation of the  $^{13}\text{C}$  from sodium  $[2-^{13}\text{C}]$  acetate into 8 alternate sites of the carbon chain in methyl palmitoleate. This is in agreement with the  $^{13}\text{C}$  NMR results and with accepted biosynthetic rules.

In a study of the biosynthesis of asperlin (I-2) isolated from cultures of Aspergillus nidulans grown with  $2-^{13}\text{C}$ -acetate (61%), Tanabe, et al. supplemented their primary  $^{13}\text{C}$  NMR analysis with a qualitative mass spectral isotope analysis of  $^{13}\text{C}$  presence in various fragment ions (57).



I-2. Asperlin.

Lower  $^{13}\text{C}$  enrichment in the ions of  $m/z$  155 and 126 indicated that part of the label was located in the fragment including  $\text{C}_6\text{-C}_8$ . The ion of

m/z 43 has a  $^{13}\text{C}$  content higher than natural abundance indicating label presence in carbons 9 and/or 10. Label was also observed in carbons 1-4 since ions of m/z 113 and 84 (due to loss of ketene,  $\text{CH}_2\text{CO}$ ) still demonstrated  $^{13}\text{C}$  enrichment.  $^{13}\text{CMR}$  results indicated the presence of  $^{13}\text{C}$  enrichment at the alternate carbon sites - 1,3,5,7 and 9. Mass spectrometric analysis also indicated a total  $^{13}\text{C}$  abundance corresponding to an average of 8.4% at each of the five labeled sites, a result in agreement with those obtained from  $^{13}\text{CMR}$  and proton- $^{13}\text{C}$  satellite NMR determinations.

Other examples of investigations in which the simple presence or absence of  $^{13}\text{C}$  in a parent or fragment ion yielded meaningful results will be discussed in later sections (58-64).

### 3. Quantitative Determinations

#### a. Singly-labeled compounds

Reduction of isotopic data obtained from samples with  $^{13}\text{C}$  enrichment at only one atomic site is relatively simple since the measurement of only one ion abundance ratio ( $M+1/M$ ) is involved. That is to say only two isotopic isomers will occur. The vast majority of  $^{13}\text{C}$  labeling studies observe such singly labeled species.

The pioneering study by D. P. Stevenson of  $^{13}\text{C}$  enriched propanes and butanes has already been mentioned but is of particular interest (39). Rather than discounting isotopic isomers due to naturally occurring  $^{13}\text{C}$ , Stevenson intricately calculated the abundance of all possible isomers for each sample.

Stevenson utilized this "isotopic isomer" analysis approach in at least four studies of interest here (65-68). First, a statistically

complete isomerization of propane-1- $^{13}\text{C}$  to propane-2- $^{13}\text{C}$  was observed over aluminum bromide catalyst at room temperature (65). No molecules doubly labeled with  $^{13}\text{C}$  were produced thus indicating the isomerization to be intramolecular. In addition, an isotope effect of approximately 5% was noted in the mass spectrometric dissociation of the  $^{13}\text{C}$  labeled propane.

The observation of this 5% isotope effect for mass spectrometric fragmentation led to a second study in which an isotope effect in the thermal cracking of propane-1- $^{13}\text{C}$  was expected (66). Mass spectrometric examination of the pyrolysis products demonstrated 8% more frequent rupture of the  $^{12}\text{C}$ - $^{12}\text{C}$  bonds over the  $^{12}\text{C}$ - $^{13}\text{C}$  bonds.

The third study demonstrated the statistical isomerization of n-butane-1- $^{13}\text{C}$  over aluminum bromide catalyst at room temperature (67). Mass spectrometric analysis revealed a statistical distribution of 2:3:1 for the n-butane-2- $^{13}\text{C}$ , isobutane-1- $^{13}\text{C}$ , and isobutane-2- $^{13}\text{C}$  respectively formed from the n-butane-1- $^{13}\text{C}$ . No  $^{13}\text{C}_2$  isomers were formed indicating, as in the case of the propanes, an essentially intramolecular mechanism for isomerization.

The last example involves the mechanism of propylene oxidation to acrolein over cuprous oxide catalyst (68). Propylene-3- $^{13}\text{C}$  was synthesized, oxidized with oxygen, and the resulting acrolein analyzed by mass spectrometry. The ratio of the molecular ion (m/z 56) to the fragment CHO (m/z 29) for the  $^{13}\text{C}_0$  isomer was compared to the same ratio for the  $^{13}\text{C}_1$  isomer. A 50% reduction was thus identified in the  $^{13}\text{CHO}$  intensity thus demonstrating a reaction mechanism for oxidation to be

operative in which isomerization of the double bond occurs before oxygen addition.

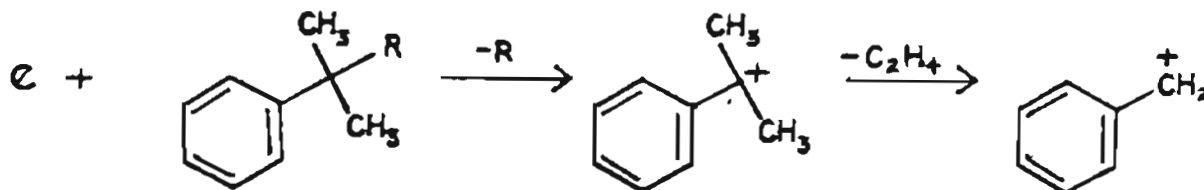
Another pioneer in the application of  $^{13}\text{C}$  labeling was R. R. Honig. Honig studied the mass spectral fragmentation of isobutane using  $^{13}\text{C}$  singly labeled species and determined the production of the "forbidden"  $\text{C}_2\text{H}_5$  from isobutane to occur via an intramolecular rearrangement followed by fragmentation (69).

A very interesting early application of  $^{13}\text{C}$ -labeling was made in 1952 by Happ and Stewart (70). They studied the mass spectrometric fragmentations of various aliphatic acids and were particularly interested in fragmentations which involved apparent ionic rearrangements. The origin of the ion of  $m/z$  60 which occurred in several of the spectra was uncertain. Since high enough resolution was not available at that time to unambiguously indicate the exact atomic composition of the ion, a way was sought to determine whether it was formed by loss of  $\text{C}_2\text{H}_4$  or  $\text{CO}$  from the original acids or their higher mass fragments. *n*-Butyric acid labeled with 51.5%  $^{13}\text{C}$  in the carboxyl group was, therefore, prepared and the effect on the abundance of the ion at  $m/z$  60 observed. After subtraction of the spectrum of the natural abundance isomers from the spectrum of the artificially enriched sample a spectrum of purely labeled *n*-butyric acid was obtained. In this spectrum the ratios of the ions at  $m/z$  74 and 89 to that at  $m/z$  61 was observed to be almost precisely the same as the ratios of the ions of  $m/z$  73 and 88 to that of  $m/z$  60 in the natural abundance spectrum thereby indicating that the labeled carboxyl carbon was retained. The commonly occurring ion of

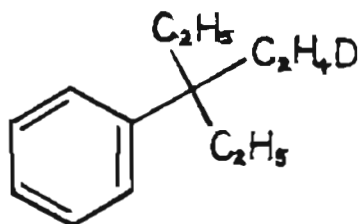
$m/z$  60 in the various aliphatic acids was thereby identified as due to loss of  $C_2H_4$ .

Meyerson and Rylander in their pioneering studies of mass spectral fragmentations and their accompanying rearrangements also used several simply labeled  $^{13}C$  compounds (58, 71-75).

They were first to suggest existence of the cationated cyclopropane ring for mass spectral interpretation (71). The observed loss of the elements of ethylene in a single step from benzyl ions could only be explained by a rearrangement:

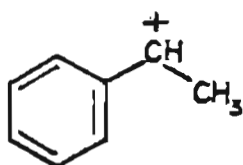


$t$ -Butylbenzene- $\alpha$ - $^{13}C$  was synthesized and its spectrum examined in the region of the resulting benzyl ions ( $m/z$  91-92). Within the limits of the expected isotope effect, a 2 to 1 distribution of unlabeled to labeled benzyl ion was observed as would be expected if all three side-chain carbons were symmetric with respect to the phenyl group. A postulated cyclopropane symmetrically placed with respect to the phenyl ring would account for such an observation. Further evidence for such a structure was obtained from the mass spectrum of 1-deutero-3-ethyl-3 phenylpentane (I-3). Statistically expected distribution of labeled (I-4 to unlabeled

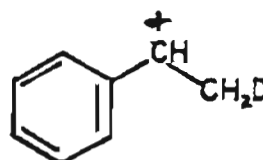


I-3. 1-Deutero-3-ethyl-3-phenylpentane

(I-5) phenylethyl ions, was observed.



I-4.

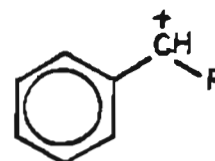


I-5.

Meyerson and Rylander with H. M. Grubb were also first to suggest the existence of the tropylium ion (I-6) in place of the commonly pictured benzyl ion (I-7) (72).

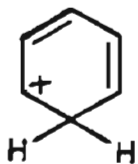


I-6. Tropylium ion



I-7. Benzyl ion

They had observed in studies of  $^{13}\text{C}$  and  $^2\text{H}$  labeled phenyl alkyl derivatives that the benzenium,  $\text{C}_6\text{H}_7^+$ , (I-8) and phenyl,  $\text{C}_6\text{H}_5^+$ , (I-9), ions were sometimes, but not always, formed by simple cleavage of the side

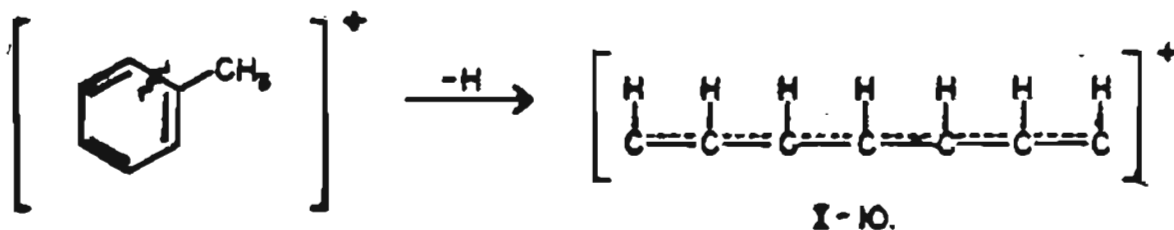


I-8. Benzenium ion



I-9. Phenyl ion

chain (58). In cases of phenyl alkyl ketones and tertiary alkylbenzenes the phenyl ring did appear to remain intact. Simple side chain cleavage produced the  $C_6$  ions. However for primary and secondary alkylbenzenes this was not the case. Deuterium substituted  $\alpha$ -chloroethylbenzene and ethylbenzene mass spectra indicated either rearrangement or ring cleavage. Investigation of the mass spectrum of toluene- $\alpha$ - $^{13}C$  produced direct confirmation of the tropylium ion (I-6) intermediate (73). If the  $C_7H_7^+$  ion is symmetrical and thus all seven carbons equivalent as in the proposed tropylium ion (I-6) structure then 5/7 or 71% of the  $^{13}C$  label should remain in the  $C_5H_5^+$  ion. Approximately 69% label retention was observed, difficulty being encountered with correction for interfering  $^{12}C$  ions of  $C_5H_6^+$  structure. If instead a linear intermediate (I-10)

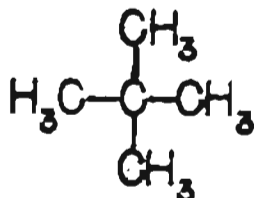


formed by rupture of the ring adjacent to the methyl group is proposed, all acetylene loss should involve end carbons and label retention would

have been only 50%, not the 69% observed. The remarkable similarity in the mass spectra of toluene and cycloheptatriene further supported the existence of a common intermediate, tropylium, and energetics derived from appearance potential measurements gave additional confirmation.

The mass spectrum of *p*-xylene- $\alpha$ - $^{13}\text{C}$  gave further evidence for the stability and, thus the preferred formation of the tropylium ion (74). It was observed that, although most alkylbenzenes cleaved a bond once removed from the ring upon mass spectral fragmentation, polymethyl benzenes such as xylene tended to cleave a ring to alkyl bond. Investigation of the spectrum of *p*-xylene- $\alpha$ - $^{13}\text{C}$  demonstrated that some carbon skeleton rearrangement occurred before or during loss of the first methyl group to form the  $\text{C}_7\text{H}_7^+$  ion but that loss of the next fragment,  $\text{C}_2\text{H}_2$ , to form  $\text{C}_5\text{H}_5^+$  followed almost complete randomization of carbons. Calculations of heats of formations for the  $\text{C}_7\text{H}_7^+$  ions from the three xylenes and ethylbenzene were in good agreement thus suggesting that all formed the tropylium ion as had been demonstrated for ethylbenzene (72).

Langer and Johnson also used mass spectrometric analysis of  $^{13}\text{C}$  labeled compounds to investigate electron-impact produced rearrangement ions (75,76). The mass spectrum of neopentane (I-11) includes



**I-11. Neopentane**

4,3, and 2-carbon fragments. In order to investigate the mechanism of

formation of these fragments, Langer and Johnson synthesized two neopentanes, one labeled in the methyl carbon (75), the other, in the central carbon (76) and observed the ratio of labeled to unlabeled ions in each fragment region. The results of the two experiments supported each other. Formation of a 4-carbon fragment by simple bond cleavage would be expected to give 75% labeled ions from the methyl- $^{13}\text{C}$  sample and 100% from the centrally labeled sample. The actual values agreed closely being 76% and 99.95%. Obviously rearrangement is not involved. The 2-carbon fragment produces a more complex situation. If a 2-carbon unit were formed by simple bond cleavage, 25% of those ions formed by the methyl labeled sample and 100% of those formed from the centrally labeled sample should contain  $^{13}\text{C}$ . The results actually obtained for the 2-carbon ions of interest are given in Table I-2

Table I-2

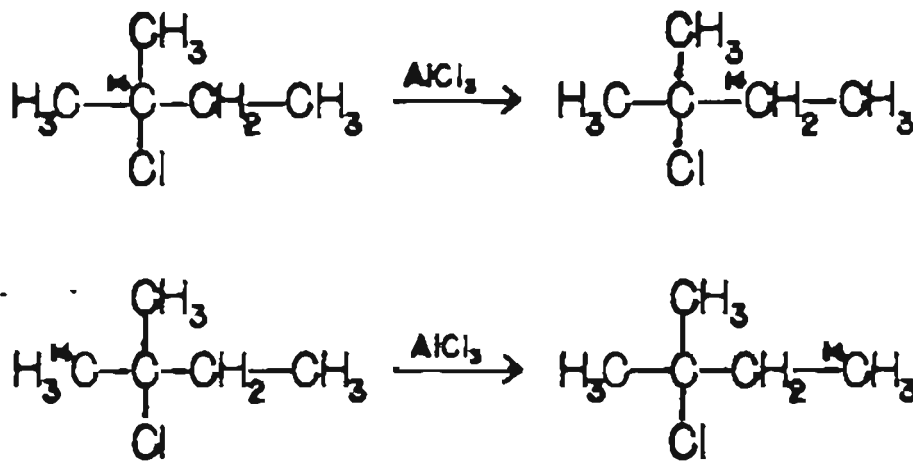
	$\text{C}_2\text{H}_3^+$	$\text{C}_2\text{H}_5^+$
methyl label	36%	38%
central label	43%	47%

To explain these results two separate mechanisms have been proposed. Langer and Johnson originally proposed a one step mechanism in which all five carbons are indistinguishable. This mechanism would anticipate 40% of the 2-carbon fragments to be labeled from either sample.

Meyerson and Rylander have also proposed a mechanism (77). It involves two steps: first, loss of methyl, followed, second, by formation of a two carbon unit from a random choice of carbons. Such a mechanism should also produce 37.5% labeled  $\text{C}_2$  fragments from the

centrally labeled sample. Neither mechanism can account for 100% of the results. Variation from anticipated results approaches the estimated error of  $\pm 2\%$ .

Meyerson continued to apply his knowledge of  $^{13}\text{C}$  labeling techniques to the study of ionic rearrangements in chemical reactions. Karabatos, Vane and Meyerson studied the isotopically labeled products of the reactions of the 2-chloro-2-methylbutanes, labeled at carbons 1 and 2, with aluminum chloride (78,79). Carbon-14 labeling of t-amyl chloride had demonstrated that the presence of  $\text{AlCl}_3$  induced rearrangements for which unimolecular mechanisms involved production of primary



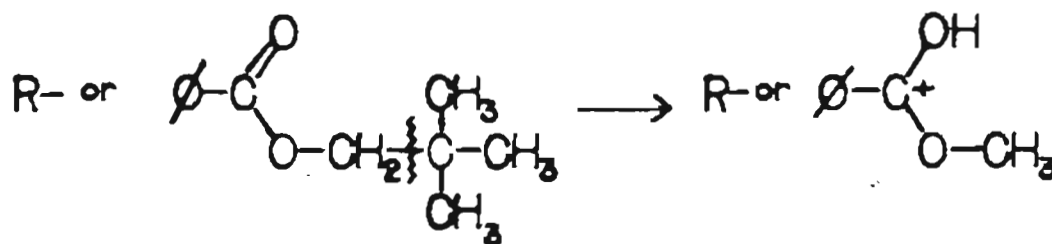
carbonium ions from secondary and tertiary ones (80). This seeming unlikely from the standpoint of energetics, a bimolecular mechanism involving  $\text{C}_{10}$  tertiary carbonium ions was proposed and tested (79,80). Production of dilabeled species and statistical distribution of various isotopic isomers gave good proof that the bimolecular reaction was indeed operative in conjunction with methyl and hydrogen shifts to produce

secondary carbonium ions from the original tertiary ones. The six methyl carbons were found to be statistically indistinguishable while the non-methyl carbons retained their identity. No need was found to postulate the existence of primary carbonium ions.

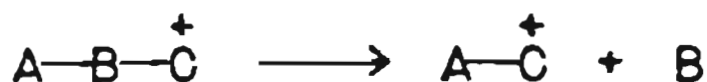
Karabatsos, Orzech and Meyerson investigated the mechanism of rearrangement of neopentyl- to 5-amyl- ions in various liquid phase reactions (81). Reactions of neopentyl- $1-^{13}\text{C}$  ions always produced t-amyl- $3-^{13}\text{C}$  indicating 1,2-methyl shifts as the preferred mechanism as opposed to proposed mechanisms involving 1,3-hydride shifts, protonated cyclopropanes, or hydrogen bridged ions. The success of this simplistic mechanism (1,2-methyl shift) was attributed to the production of a tertiary carbonium ion and to release of non-bonded interactions.

In connection with various atypical behaviors of neopentyl ions, McFadden, Stevens, Meyerson, Karabatsos and Orzech noted that the mass spectra of neopentyl esters were deficient in terms of the ion formed by cleavage of the oxygen-neopentyl bond (82). Most oxygen acid alkyl esters yield a protonated acid as the major ion of their spectrum. Such ions arise by a combination of rearrangement and dissociation in which one of the two migrating hydrogens comes from the  $\beta$ -position. Since no such  $\beta$ -hydrogens are present in the neopentyl group the abundance of the parent-less- $\text{C}_5\text{H}_9$  is sharply reduced and instead a major ion arising from the parent-less- $\text{C}_4\text{H}_7$  occurs. A mechanism had been proposed for formation of this ion analogous to that involved in formation of the protonated acid from other alkyl esters. Cleavage of the O-R bond had been visualized as usual, but with accompanying migration of hydrogen

and methyl rather than 2 hydrogens. However, mass spectra of various  $^2\text{H}$  and  $^{13}\text{C}$  labeled neopentyl esters demonstrated that this was not the case. Rather the parent- $\text{C}_4\text{H}_7$  ion arises from cleavage of the appropriate C-C bond and migration of two hydrogens:



Johnstone and Millard also used  $^{13}\text{C}$  labeling along with  $^2\text{H}$  labeling in their studies of mass spectral fragmentation phenomena (83). Their interest in fragmentations of the type



led to a study of the loss of methyl radicals from stilbene and 1,2-diphenylethyl ions. The mass spectrum of 1- $^{13}\text{C}$ -1,2-diphenylethyl chloride and the resulting isotopic ratios could be explained on the basis of the following mechanism (among others):

- (1) 84.5% equilibration involving a 1,2-hydrogen shift



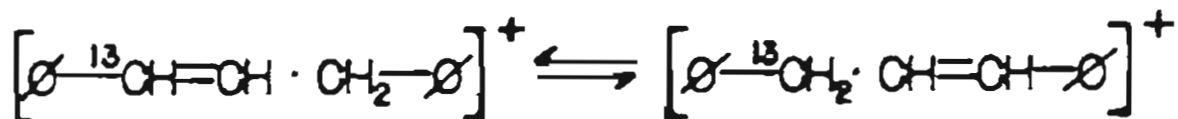
followed by (2) loss of the CH unit along with two ring hydrogens.

The spectrum of the 1-<sup>2</sup>H labeled compound sustained such a mechanism with a demonstrated equilibrium of 84.9%, excellent agreement within experimental error. The spectrum of 1-phenyl-2(2-<sup>2</sup>H-phenyl)-ethyl chloride was consistent with the same mechanism yielding an equilibrium ratio of 84.7% again in good agreement.

Other mass spectrometric reactions of the type



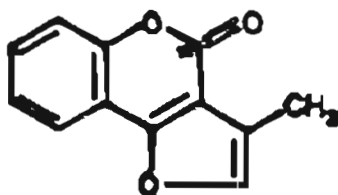
investigated by Johnstone and Millard include fragmentation of the 1,3-diphenyl-propane ion-radical to give methyl, ethyl and vinyl radicals (84). Spectra obtained of [1-<sup>13</sup>C]-1,2-diphenyl-1-chloro-propane and [3-<sup>13</sup>C]-1,2-diphenylprop-1-ene showed that the methyl radical was derived from the central carbon and that loss of the vinyl radical involved prior equilibrium of the type



followed by loss of the double bonded carbons. Loss of ethyl following equilibrium involved the singly bonded carbons. Supplementary deuterium labeling demonstrated that the additional hydrogens needed came from the aromatic rings.

Dean, Goodchild, Johnstone and Millard prepared [2-<sup>13</sup>C] furo-coumarin (I-12) to demonstrate that the first loss of CO in the mass spectrum corresponded to loss of the position 2 carbon of the coumarin

ring, i.e., the labeled carbon (59).



I-12. (2-<sup>13</sup>C)-Furocoumarin

Carl Djerassi was another of the early workers to utilize <sup>13</sup>C labeling in the study of ionic structures. Robertson, Marx and Djerassi drew qualitative evidence from metastable peak observation in the spectra of <sup>13</sup>C-labeled aromatic amines that, where the even-electron ion C<sub>6</sub>H<sub>6</sub>N<sup>+</sup> (I-13) analogous to the tropylium ion can be postulated as in the mass



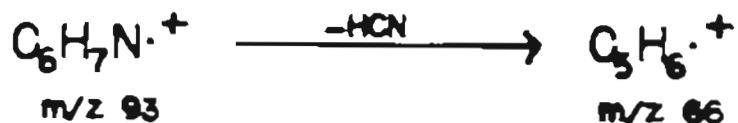
I-13.



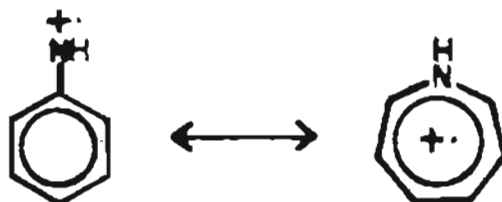
I-14.

spectrum of sulphanilamide, it will occur, but that, where the odd-electron intermediate (I-14) must be postulated, no such ring expansion intermediate will be involved (60,85,86). The complexity of the spectra produced data reduction difficulties preventing quantitative evaluation.

Rinehart, Buchholz and VanLear used <sup>13</sup>C labeling in their study of the mass spectral fragmentation of aniline (87). The primary fragmentation pathway involves loss of HCN:



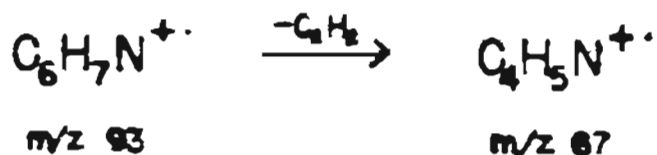
In view of the well-known tropylium ion intermediate in the rearrangement of toluene before fragmentation, an analogous azepinium ion (I-15) was proposed.



I-15. Azepinium ion

Aniline -1- $^{13}\text{C}$  was prepared and the low resolution mass spectrum examined for the presence of  $^{13}\text{C}$  in the ion  $\text{C}_5\text{H}_6^+$ . Such examination indicated that most of the  $^{13}\text{C}$  had been lost along with the nitrogen; however, some small amount, greater than that expected from naturally occurring  $^{13}\text{C}$ , appeared to remain.

In order to obtain a more quantitative evaluation of the results, a high resolution spectrum was obtained for the region of interest ( $m/z$  65-68) to separate the various isobaric ions. In particular ions from the fragmentation



and ions including additional hydrogen tended to obscure results in the low resolution spectra. It was clear from the high resolution data that, while the greatest portion of fragmentation occurred without carbon skeleton rearrangement, some rearrangement did occur particularly in cases

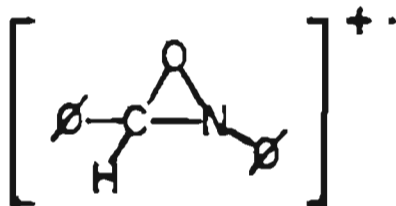
involving the  $C_6H_6N^{+\cdot}$  intermediate (aniline  $-H^{\cdot}$ ). The existence of the azepinium ion was thereby clearly suggested.

Independently, Robertson and Djerassi made a more quantitative evaluation of the existence of the azepinium ion investigating the mass spectra of  $1-^{13}C$ -aniline,  $1-^{13}C$ -acetanilide,  $1-^{13}C$ -sulfanilamide, and  $1-^{13}C$ -p-nitroaniline (86). Again the use of high resolution was necessary to separate the isobaric ions of these aromatic species. Analysis of their results clearly demonstrated that, for the fragmentation involving loss of HCN, the carbon skeleton of the odd-electron species,  $C_6H_7N^{+\cdot}$ , remained largely stable whereas the carbon skeleton of the even-electron species,  $C_6H_6N^+$ , is rearranged to a considerable extent.

From investigations of various mass spectra involving tropylium and azepinium ions, the generalization was emerging that even-electron aromatic ions rearrange while odd-electron aromatic ions do not. Woodgate and Djerassi demonstrated that such was not always the case by preparing  $1-^{13}C$  phenyl azide and observing that the odd-electron ion  $C_6H_5N^{+\cdot}$  rearranges to a considerable extent before fragmentation (88). This contrasts to the lack of rearrangement of the  $C_6H_7N^{+\cdot}$  ion of aniline.

Following the work of these pioneers,  $^{13}C$  labeling has become an accepted technique for investigation of the fate of particular atoms of interest in mass spectral fragmentation mechanisms (61,62,89-97) and other reactions involving ionic rearrangement (63,98,102,103).

Kinstle and Stam identified the oxaziridine (I-16) ion as an



I-16. Oxaziridine

intermediate in the fragmentation of nitrones by observation of the mass spectrum of  $\alpha$ -N,diphenylnitrono- $\alpha$ - $^{13}\text{C}$  (61).

Foster and Higgins observed that, in the 1-(2-thienyl)hexane-1- $^{13}\text{C}$  mass spectrum,  $\beta$ -cleavage predominates with subsequent ring expansion to a six membered ring (I-17) (62).



I-17. m/z 98

Certain similarities to aromatic systems are noted in the mass spectrum below m/z 98.

Meisels, Park and Giessner demonstrated complete carbon skeleton randomization for 1-butene-4- $^{13}\text{C}$  supporting the Rylander and Meyerson suggestion of a methylcyclopropane intermediate (90).

Berlin and Shupe studied the mass spectra of 25 triphenylmethyl substituted compounds and observed the trityl cation (m/z 243) as an ion of major importance in each (90). Analysis of the spectrum  $(\text{C}_6\text{H}_5)_3\text{C}^{13}\text{H}$  supported their proposed mechanism for fragmentation of the trityl

cation involving retention of the  $\alpha$ -carbon.

Davis, Williams and Yeo demonstrated scrambling of hydrogen and carbon atoms in butyl cations and radical-cations arising within the mass spectrometer (91). Rate constants for these randomizations were measured to be in the region  $10^5 - 10^6 \text{ sec}^{-1}$ .

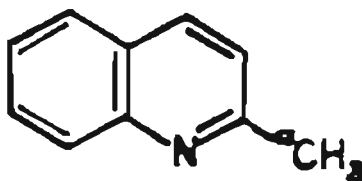
Cooks and Bernasek prepared benzothiophene-2- $^{13}\text{C}$  and, using both the  $^{13}\text{C}$  and the sulfur as labels, demonstrated carbon skeleton rearrangements (92). Use of the sulfur eliminated need for more than one  $^{13}\text{C}$  isotopic label thus simplifying calculations.

Rennekamp, Perry and Cooks demonstrated, however, that in cases where substituent migration is possible such as in 3-phenyl-thiophene and the brominated derivatives 2-bromo-3-phenylthiophene and 2-bromo-4-phenylthiophene, carbon skeleton rearrangement does not compete well and most observed rearrangements can be accounted for by substituent migration coupled with cleavage and reformation of thiophene ring bonds (93).

Henion and Kingston prepared 1- $^{13}\text{C}$ -diphenyl sulfide and observed in the mass spectrum, skeletal rearrangements whose mechanism involved expansion of either phenyl group to a 7 membered ring including sulfur (94).

In a study of  $^2\text{H}$  labeled methyl-quinolines, Draper and MacLean observed randomization of all nine hydrogens (95). They proposed ring expanded intermediates as the source of this randomization and examined the spectrum of 2-methyl-quinoline-2- $^{13}\text{C}$  (I-18) for evidence of the existence of such intermediates. Eighty five percent retention of label after

loss of HCN was observed which corresponds most closely to a mechanism

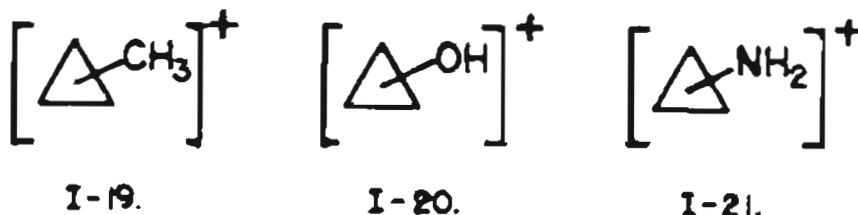


I-18. 2-Methyl-quinoline-2-<sup>13</sup>C

involving insertion of the methyl carbon into the carbon-carbon or carbon-nitrogen bond of the molecule. From such a completely random insertion, 86% label retention would be expected. However, as Draper and MacLean point out, the various bonds are not equivalent and so such random insertion might not be expected. The 85% retention could also be explained by a system of competing ring expansion mechanism. Spectra of other <sup>13</sup>C labeled methylquinolines are needed to verify the exact mechanism.

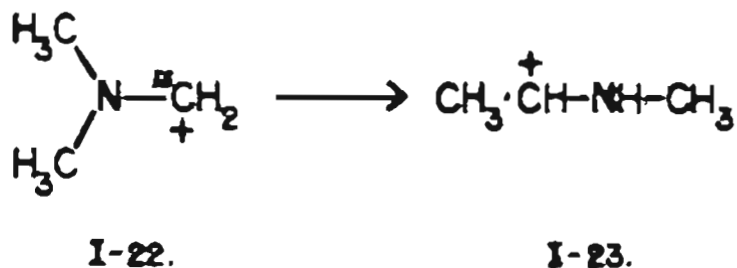
Siegel followed the work of Langer and Johnson, in which they suggested a methylated cyclopropane intermediate in the decomposition of neopentanes (75,76), with an investigation of the mass spectra of 2-methyl-2-hydroxypropane and 2-methyl-2-aminopropane (96). Such compounds containing tertiary alkyl substituents have complex, competing fragmentation pathways and high resolution techniques (1/15,000 resolution) were necessary to separate the resulting ions. By synthesizing <sup>13</sup>C enriched analogs labeled in the 1- and 2-positions and observing the mass spectra, Siegel was able to demonstrate the existence of intermediates in their fragmentation processes structurally similar to that occurring in the neopentanes. As Langer and Johnson had proposed the

methylated cyclopropane (I-19), Siegel proposed the hydroxylated and aminolated cyclopropane ions (I-20) and (I-21). Such intermediates



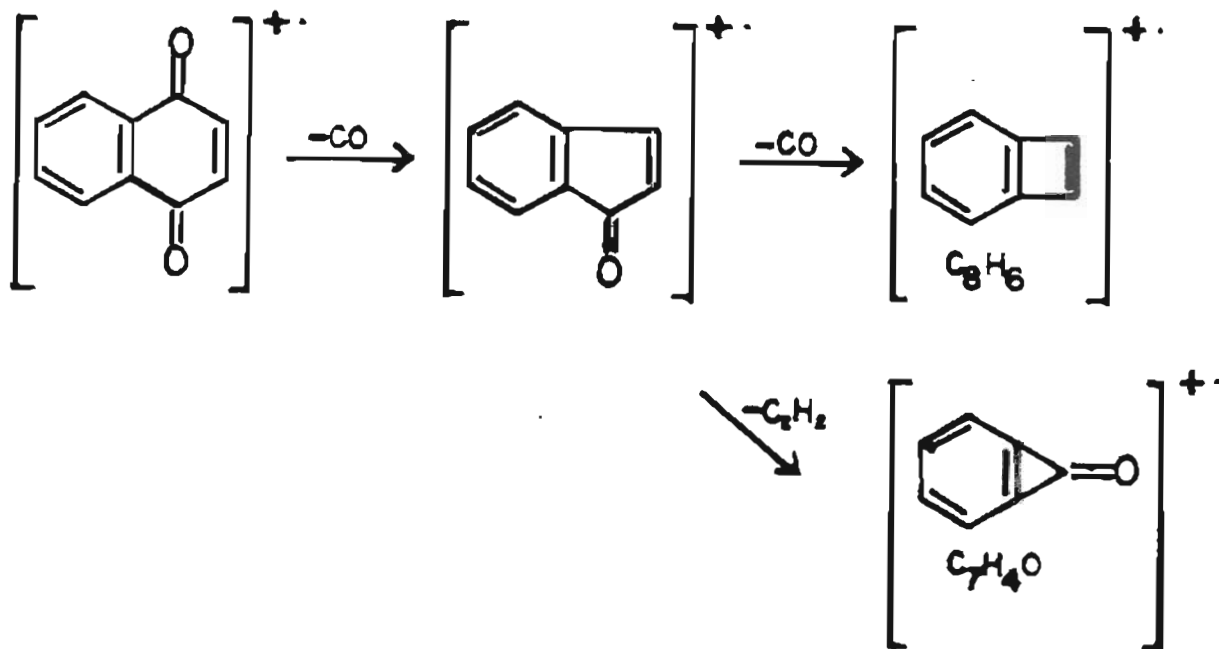
were thought to occur in all three cases after initial loss of a one carbon fragment.

Uccella, Howe and Williams used a technique similar to IKES in a study of the intermediates involved in the mass spectral fragmentation of 15 different amines and amides (97). Metastable abundance ratios, calculated kinetic energies, metastable peak shapes, and isotopic  $^2\text{H}$  labeling identified three distinct intermediates. Carbon-13 labeling was used in one instance to elucidate the rearrangement mechanism involved in formation of one intermediate. Complete statistical equivalence of carbons was demonstrated in rearrangement of the tertiary immonium ion (I-22) to the previously demonstrated intermediate (I-23):



Koptyug, Isaev and Gorfinkel used mass spectrometric methods to follow carbon skeleton rearrangement in  $^{13}\text{C}$  labeled naphthalenes

after treatment with aluminum chloride catalyst (98). Production of the 1,4-naphthoquinone derivative was carried out to take advantage of its unique fragmentation pathway. The use of the isotopic isomers data reduction technique made synthesis of both naphthalene-1- $^{13}\text{C}$  and -2- $^{13}\text{C}$  necessary. Mass spectral examination of the labeled samples before interaction with  $\text{AlCl}_3$  showed the fragmentation process of naphthoquinone to, indeed, uniquely isolate the appropriate carbon atoms and allowed

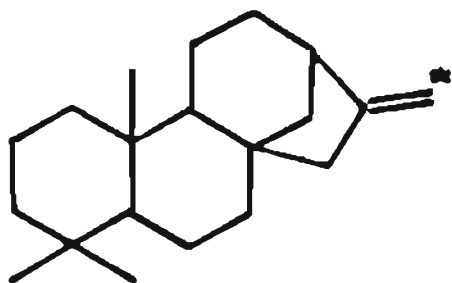


calculation of appropriate factors owing to kinetic isotope effects. Subsequent mass spectral analysis of the labeled naphthalenes after exposure to  $\text{AlCl}_3$  showed a lack of automerization disproving the work of previous authors attempting such investigation using the more tedious technique of  $^{14}\text{C}$  labeling which involves difficult chemical degradations (99). Error in the determination of isotopic isomer distribution

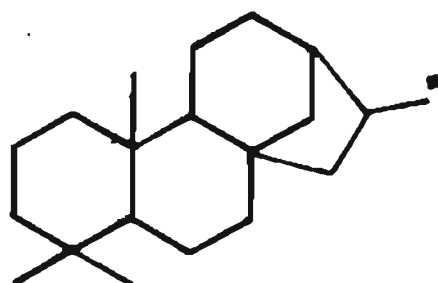
by  $^{13}\text{C}$  mass spectrometric analysis was shown to be 2-4% absolute.

Two different mechanisms had been proposed to account for the carbon skeleton rearrangements observed in n-propyl-benzene in the presence of  $\text{AlCl}_3$  catalyst. One involved a diphenylpropane intermediate (100) and the other, a diphenylhexyl cation, formed as a result of a bimolecular reaction (101). Roberts and Gibson examined the mass spectrum of n-propyl- $\alpha$ - $^{13}\text{C}$ -benzene to determine between the two intermediates and their associated mechanisms (63). The existence of the diphenylhexyl intermediate would be expected to allow formation of dilabeled and unlabeled molecules from the original monolabeled sample while a diphenylpropyl intermediate would not. No increase in unlabeled or dilabeled species was observed thus discounting the existence of a bimolecular mechanism producing diphenylhexyl intermediates. Comparison analyses were done using  $^{13}\text{C}$  NMR (Varian DP60-IL spectrometer using CAT of 2163 scans) and proton NMR (Varian HA-100 spectrometer). Results were less accurate than those obtained by mass spectrometry ( $\pm$ <5% vs.  $\pm$ <2%).

Difficulty was encountered with the use of high resolution in a study of  $^{13}\text{C}$  labeled kaurene (I-24) and kaurane (I-25) by Jimenez and Reed (102). They studied possible carbon scrambling at the molecular



I-24. Kaurene



I-25. Kaurane

level using first low resolution spectra at 70 and 14 eV. Initial results which conflicted with established Quasi-Equilibrium theory prompted utilization of high resolution in a search for competing fragmentation pathways, some involving more randomization than others. However, the extent of randomization showed dramatic change under high resolution. Although the two different AEI instruments, the low-resolution MS-12 and the high resolution MS-902, have similar source and inlet systems, the deflection path lengths necessarily differ. The path length of the high resolution instrument is approximately twice that of the low resolution instrument with the corresponding residence time being therefore approximately double. Ions with shorter mean lifetimes have reduced intensity in the high resolution MS-902.

Fajula and Gault studied the skeletal rearrangements of methylpentenes and -hexenes in the presence of the Brønsted acid, p-toluenesulfonic acid, by preparing all possible singly labeled  $^{13}\text{C}$  isomers of the compounds of interest (103). Mass spectra of the acid-exposed samples were compared with those of untreated samples for calculation of the concentrations of isomerized species.

It is interesting to note the consistent use of the isotopic isomer analytical approach throughout the work described above. The mass spectrum of an isotopically enriched sample is simply viewed as that of a mixture of isotopically related isomers.

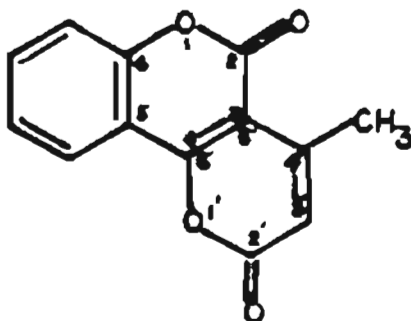
b. Multiply-labeled compounds

Although the vast majority of examples of the use of mass spectrometric analysis for  $^{13}\text{C}$ -labeled samples involve enrichment at

only one atomic site, examples do occur in which samples labeled at two or more sites have been analyzed successfully. Quantitative analysis is, then, more complex. There are three basic reasons for the appearance of these multiply-labeled compounds in research:

- (1) The synthetic method employed results in enrichment at more than the site of interest.
- (2) The problem being investigated requires such multiple labeling.
- (3) Problems of biosynthesis result in multiple incorporation of precursors.

Work done by Johnstone, Millard, Dean and Hill provides an example of the first reason (64). In an investigation of the mass spectral behavior of various coumarins and pyronocoumarin, they wished to determine the order of loss of the four distinct CO groups from the pyrono (5',6':3,4) coumarins. Carbon-13 labeling of the pyronocoumarin (I-26) provided the means for such determination. The mass spectrum of



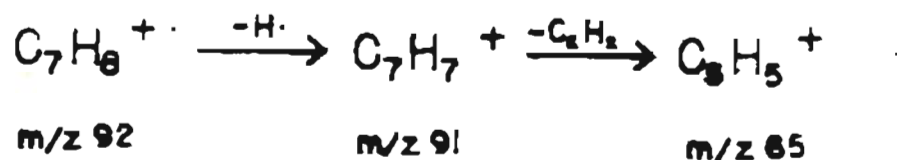
**I-26.**

[2-<sup>13</sup>C]-4'-methyl-2'-pyrone (5',6':3,4) coumarin demonstrated that the

carbon atom at the 2-position was lost second. The synthesis of a compound labeled at the 2'-carbon necessarily resulted in [2',4'-<sup>13</sup>C<sub>2</sub>]-4'-methyl-2'-pyrono (5',6':3,4) coumarin. The mass spectrum of this compound demonstrated that the 2'-carbon was lost in the first step. Metastable ion investigation showed that the second and third CO units were actually lost in a concerted process, and thus the CO group adjacent to the CO group at the 2-position was most probably involved leaving the 1'-position oxygen as the last to be expelled. Analysis was essentially qualitative and the double label presented no real difficulty.

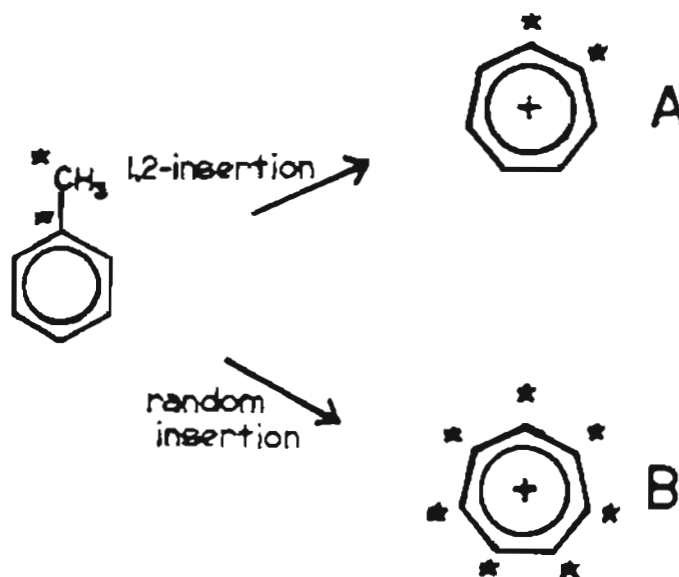
Investigation of the complex mechanisms for mass spectral decomposition of aromatic compounds provides the bulk of examples of successful multiple labeling. Carbon skeleton rearrangements are common. Elucidation of the exact mechanisms resulting in such rearrangements often requires use of compounds labeled at multiple sites.

Rinehart et al. employed high resolution mass spectral analysis in a further investigation of the tropylium ion involved in fragmentation of toluene (41,104). Carbon skeleton rearrangement before loss of



ethylene had previously been demonstrated from the spectrum toluene- $\alpha$ -<sup>13</sup>C (73); however, a question still remained regarding the formation of the tropylium ion intermediate (m/z 91). Was it formed by simple 1,2 insertion of the methyl carbon or by random insertion of the methyl carbon

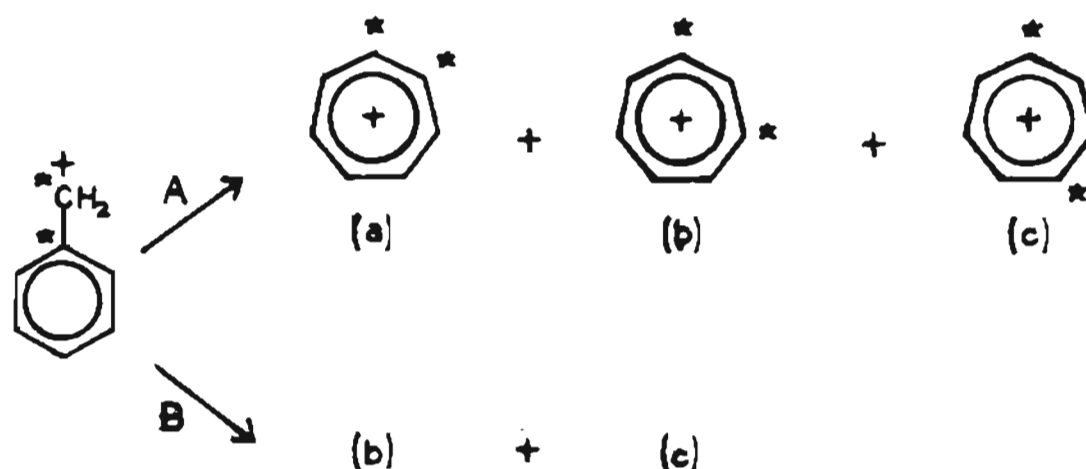
between any two ring carbons? Toluene- $\alpha,1$ - $^{13}\text{C}_2$  was prepared (I-27). Simple 1,2 insertion would obviously result in ion (A) and random insertion in ion (B). Statistical loss of  $^{13}\text{C}_2\text{H}_2$  and  $^{12}\text{C}_2\text{H}_2$  would



I-27.

therefore be greater for the tropylium ion formed by 1,2 insertion. Quantitative results were in good agreement with tropylium ion formation via random insertion (pathway b).

Further light was shed in the formation of the tropylium ion through an investigation of the mass spectral fragmentation of toluene-2,6- $^{13}\text{C}_2$  by Alan Siegel (105). While Rinehart et al. had demonstrated in their investigation of toluene- $\alpha,1$ - $^{13}\text{C}_2$  that the tropylium ion carbon skeleton was randomized (67,68), a question still remained as to the exact mechanisms of this randomization (I-28). Did it arise from a series of benzyl ion-tropylium ion isomerizations (A) or by simple and final insertion of the methyl carbon between any two carbons (B)?



### I - 26.

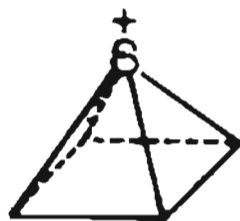
Toluene-2,6- $^{13}\text{C}_2$  could not produce a tropylium ion of structure (a) if randomization occurred via benzyl ion-tropylium ion isomerizations.

Quantitative isotope abundance measurements obtained from high resolution data in the region  $m/z$  65-67 demonstrated that the tropylium ion is completely randomized as expected from pathway (A). If pathway (B) is operative then pathway (A) also exists completing the randomization. Siegel also employed high resolution in later work with the complex spectra of tertiary hydroxy- and amino-methyl propanes (96).

Two examples exist which clearly illustrate the difficulty inherent in the isotopic isomer approach to mass spectral interpretation (106,107). With such an approach each spectrum, considered as a mixture, must be separated into the spectra of the individual isotopic components. Information for effecting these separations must be gleaned from spectra of individually synthesized isomers ( $^{13}\text{C}_0$ ,  $^{13}\text{C}_\alpha$ ,  $^{13}\text{C}_\beta$ , etc.), from fragmentations specific to individually labeled carbons, from established average natural abundance ratios, and/or from the isotopic composition

of the reagents.

In the first example, de Jong, Sinnige and Janssen investigated the mass spectral behavior of thiophene (106). They synthesized six different  $^2\text{H}$  and  $^{13}\text{C}$  labeled isomers including 2,5- $^{13}\text{C}_2$ -thiophene and 2- $^{13}\text{C}$ -thiophene. Each spectrum was corrected to represent 100% of the isomer of interest. Resulting  $^{13}\text{C}$  and  $^{13}\text{C}_2$  fragment ratios were then observed to demonstrate partial carbon skeleton rearrangement through the proposed pyramidal intermediate of  $\text{C}_{4v}$  symmetry (I-29).



I-29.

Deuterium labeling demonstrated independent hydrogen scrambling to be concurrent.

In the second example, Venema, Nibbering and de Boer also used the isotopic isomer approach in their investigation of the mass spectral behavior of styrene and 1-phenylethylbromide (107). The mass spectra of the  $\alpha$ - $^{13}\text{C}$ ,  $\beta$ - $^{13}\text{C}$ , and  $\alpha,\beta$ - $^{13}\text{C}$  analogues of 1-phenyl-ethylbromide and the  $\alpha$ - $^{13}\text{C}$  and  $\alpha,\beta$ - $^{13}\text{C}$  derivatives of styrene were examined. Carbon skeleton rearrangement, presumably via a cyclooctatetraene intermediate, were shown to occur, independent of hydrogen randomization whenever the internal energy of the parent ion was low enough to allow time for such a process. High internal energy resulted in more rapid fragmentation and retention

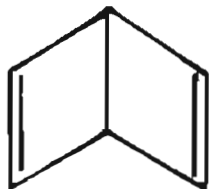
of carbon individuality. Again spectra of samples were corrected for the presence of individual isomers before quantitative analysis was attempted. The difficulties inherent in extension of such a technique to cases involving enrichment at a greater number of sites and thus "mixtures" involving greater numbers of isotopic isomers is obvious. (See Table I-1 for the geometric increase in total isomer number with increase in enriched sites.)

The extent to which this view of isotopic mass spectra as the spectra of mixtures invaded the thinking of early workers in the field is demonstrated by the words of Horman, Yeo and Williams (108): They refer to a sample of 1,3,5- $^{13}\text{C}_3$ -benzene as "contaminated by  $^{13}\text{C}_0$ -,  $^{13}\text{C}_1$ -, and  $^{13}\text{C}_2$ -benzenes". The scrambling of carbons in benzene before loss of acetylene is demonstrated with excellent quantitative results by inspection of the metastable peak ratios arising from decompositions in the first field-free region of a double focusing mass spectrometer. This technique relieves the analysis of correction for overlapping ion intensities due to "contaminants". Predicted ratios for loss of  $\text{C}_2\text{H}_2$ : $^{13}\text{CCH}_2$ : $^{13}\text{C}_2\text{H}_2$  following complete randomization of carbons are calculated at 20:60:20. Experimental results yield the ratios  $21.4 \pm 3.8\%$ : $60.8 \pm 3.8\%$ : $17.8 \pm 1.8\%$ .

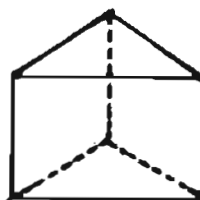
Complimentary work done by Meyerson, et al. (109) and by Davidson and Skell (110) further elucidated the mechanism of hydrogen and carbon scrambling occurring prior to electron impact decomposition of benzene.

Meyerson et al. used mass spectrometry in an investigation of the observed randomization of both hydrogen and carbon in benzene

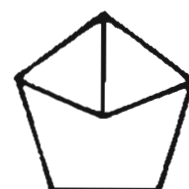
decomposition under electron impact (109). They prepared benzene- $1,2^{13}\text{C}_2-3,4,5,6^2\text{H}_4$ . Difficulty was encountered because complete separation of all isobaric ions in the region of interest would have required resolution of 1/55,000 while only 1/20,000 was obtainable. Estimates were made based on shapes of incompletely resolved doublets. Expected isotopic compositions were calculated for isotopic isomers of  $\text{C}_4\text{H}_4^+$  and  $\text{C}_3\text{H}_3^+$  ions for three pathways to randomization each involving a different intermediate - Dewar benzene (I-30, prismane (I-31) and benzvalene (I-32).



I-30. Dewar benzene



I-31. Prismane



I-32. Benzvalene

Observed ion intensities were compared with those calculated giving evidence that at least intermediates, I-30, and I-32, were involved in carbon scrambling and did not rule out contribution from I-31. Additional scrambling of hydrogens beyond carbon scrambling was observed.

Davidson and Skell reported on the electron impact fragmentations of cycloheptatriene, cyclopentadiene, and norbornadiene, all doubly labeled with vicinal  $^{13}\text{C}$  atoms (110). Total loss of positional identity was reported for acetylene extrusion from the positive  $\text{C}_5\text{H}_6^+$  and  $\text{C}_5\text{H}_5^+$  ions produced within the mass spectrometer from cyclopentadiene and for the  $\text{C}_7\text{H}_7^+$  positive ion similarly produced from cycloheptatriene. However, little, if any, randomization of carbons was observed in the comparable

decomposition of norbornadiene.

Analytical problems involved in biosynthetic enrichment studies are frequently more complex than any of the above situations. In many cases labeled precursors are incorporated at multiple sites within the complex biosynthetic product, often at differing enrichment levels. Individual researchers have handled these complexities in different ways. These biologically oriented studies will be discussed in the following section.

C. Applications of  $^{13}\text{C}$  mass spectral analysis to problems of biological significance

Mass spectrometric stable isotope analysis is a tool having several significant attributes of particular importance for biosynthetic and metabolic applications: First, the use of stable rather than radioactive isotopes is involved which thereby eliminates many of the complications associated with radiation. Radiation damage to living systems may result from the primary ionizing radiation and/or the recoil kinetic energy which can disrupt chromosomes and create harmful free radicals (111). Radioactive decay introduces new chemical species, the daughter decay products, which may produce biological response and are potentially toxic (111). Radioactive isotope tracers are, therefore, contraindicated in human studies, particularly those involving children or pregnant women (112). Biological effects of stable isotopes have proven minimal even at extremely high concentrations (113-115).

Second, radioactive chemicals have, by their very natures,

finite lifetimes. Therefore, the reagents have definite "shelf lives", the products want immediate analysis, and such tracers are not amenable to use in extended studies. Mass spectrometric analysis permits the use of stable isotopes with essentially infinite life spans.

Third, use of stable isotopes opens new opportunities for double labeling experiments (116,117). Double labeling experiments using radioactive isotopes have involved, in most instances, simultaneous use of  $^{14}\text{C}$  and  $^3\text{H}$  or use of two atoms of  $^{14}\text{C}$ . Use of  $^2\text{H}$  presents many problems in that hydrogen frequently exchanges with the environment and is subject to extensive isotope effects. Double  $^{14}\text{C}$  label experiments require extensive specific chemical degradations which are, at best, time-consuming or even impossible. Use of the stable isotopes  $^{13}\text{C}$ ,  $^{14}\text{N}$ ,  $^{18}\text{O}$  greatly simplifies double labeling experiments.

Fourth, many elements do not have radioactive isotopes of sufficiently long half-life to be useful in biosynthetic or metabolic studies (112). Nitrogen and oxygen, two elements commonly occurring in biochemicals, are examples. Trace nutrient studies as well as studies of metal toxicity are two specific fields where convenient radioactive labels are rarely available (111). Stable isotopes present the alternative.

Fifth, mass spectrometry as a detection tool has proven extremely sensitive. This is important in biological experiments in which the sample taken may be necessarily small or where dilution effects limit the isotope incorporation (118).

And sixth, in favorable cases, sensitivity and accuracy in measurement of stable isotope enrichment with some mass spectrometric

techniques may exceed that obtainable for radioactivity levels (111,112, 118,119).

With so much in its favor it is not surprising that mass spectrometric stable isotope analysis has found application in biological studies in spite of the practical difficulties previously discussed. Such analysis has been used on all three previously mentioned levels of application - qualitative identification of isotope presence or absence, quantitative determination of enrichment levels, and specific location of enrichment sites within a molecule. However, although interest in the use of this technique has been and is currently high (8,9,14,18,111, 112,118-120), the actual number of successful applications to biological problems has been quite limited. Use of the stable isotope  $^{13}\text{C}$  with mass spectrometric analysis has been especially limited although importance of the element carbon is obvious.

Biological fractionation of naturally occurring isotopes has been clearly demonstrated for carbon as well as other elements (3-6). Such fractionation has been used to elucidate biosynthetic and metabolic pathways (121-123). In these studies the samples are reduced to  $\text{CO}_2$  and the simple  $^{13}\text{C}/^{12}\text{C}$  measured with an isotope ratio mass spectrometer. Perhaps one of the most interesting applications of this technique is its use in medical diagnosis. In 1970 Jacobson, Smith, Epstein and Laties showed that the increase in the respiration rate of potatoes after slicing was due the increase in carbohydrate metabolism relative to that of lipids. Potato lipids were shown to have considerably lower  $^{13}\text{C}/^{12}\text{C}$  ratios than potato carbohydrates (123). The initial or basal  $^{13}\text{C}/^{12}\text{C}$  ratio of

respired  $\text{CO}_2$  most nearly approximated that of tissue lipids. However, as the respiration rate increased 3-5 fold in the period immediately after slicing, the  $^{13}\text{C}/^{12}\text{C}$  ratio of the respired  $\text{CO}_2$  approached that of tissue carbohydrates.

Following this work, Jacobson, Smith and Jacobson applied these principles to rat metabolism in diagnosing diabetes (124). Rat lipids were also shown to have lower  $^{13}\text{C}/^{12}\text{C}$  ratios than rat carbohydrates. Respired  $\text{CO}_2$  from alloxan-induced diabetic rats was shown to have a significantly lower  $^{13}\text{C}/^{12}\text{C}$  ratio than that respired by untreated rats. Diabetes is associated with a change in lipid metabolism. Such work which does not require dosing the patient with any foreign element (radioactive or otherwise) shows promise as a rapid, inexpensive diagnostic aid in human diabetes as isotope ratio mass spectrometers become available in medical laboratories.

Independently, Shreeve, et al. developed a test for the glucose intolerance associated with diabetes in humans (125). Patients were fed uniformly labeled glucose- $^{13}\text{C}$ . Diabetic patients exhibited sub-normal rates of expired  $^{13}\text{CO}_2$ .

The isotope ratio mass spectrometer which has brought a significant increase in the precision of mass spectrometric isotope measurements is now being used in studies of the effect of artificial enrichment on living tissues. Flaumenhaft, Uphaus and Katz have published a particularly intricate study detailing the cellular level effects on the algae chlorella vulgaris of high (~90%) artificial isotopic enrichment (113). Levels of  $^{13}\text{C}$  and  $^2\text{H}$  were artificially increased individually and in

combination and relative growth rates, cell size distribution, and cytochemical changes were investigated. Deuterium substitution was responsible for the most pronounced abnormalities. Carbon-13 produced some limited cellular disturbance. But the most remarkable result was that introduction of  $^{13}\text{C}$  tended to diminish the adverse effects of  $^2\text{H}$  enrichment. The study concluded that incorporation of high concentration of  $^{13}\text{C}$  into many living organisms will not produce special difficulties.

In this regard, Los Alamos Scientific Laboratories has conducted a series of experiments culminating in ~60% replacement of body carbon with  $^{13}\text{C}$  in two rats, male and female (114,115,126). Various waste and tissue samples were taken before and after sacrifice, burned in the presence of  $\text{O}_2$  to  $\text{CO}_2$ , and the  $^{13}\text{C}/^{12}\text{C}$  ratio measured with an isotope ratio mass spectrometer as well as by proton bombardment. The mass spectrometric measurements were found to have much higher precision. No adverse physiological effects directly attributable to this high incorporation of  $^{13}\text{C}$  were noted except an area of necrosis in the adrenal cortex. Reproductive processes appeared to function normally at high  $^{13}\text{C}$  levels; however, no live offspring were obtainable through two pregnancies. This was felt to be most probably due to well documented, normal mouse behavior in stress situations. The  $^{13}\text{C}$  enriched mice were, of necessity, kept in confining metabolism chambers.

Klein, Haumann, and Eisler have used a combined gas chromatograph-mass spectrometer equipped with accelerating voltage alternation to measure stable isotope ratios and have suggested its use for measuring  $^{13}\text{CO}_2/^{12}\text{CO}_2$  ratios of metabolic compounds after administration of a

labeled precursor (127).

Perhaps the ultimate system for application of  $^{13}\text{CO}_2/^{12}\text{CO}_2$  measurement has been developed by Sano, et al. (120). They incorporate the latest techniques, combined GC-MS mass fragmentography, and computer aids, along with an inline pyrolyzer for converting the sample to  $\text{CO}_2$ . Carbon-13 labeled aspirin metabolites are identified using this system.

However, prior combustion of the sample destroys much potentially useful information and, therefore,  $^{13}\text{C}$  abundance measurements on intact biological products have also been accomplished. The works of Bose, et al. (55), Tanabe, et al. (57) and Burlingame, Balogh, et al. (56) have previously been mentioned. All obtained essentially qualitative results. In the Tanabe study of the biosynthesis of asperlin, mass spectrometric analysis supported NMR analysis demonstrating acetate incorporation in various parts of the asperlin molecule (57). Burlingame, Balogh, et al. also demonstrated mass spectrometric results to be in qualitative agreement with NMR results showing acetate incorporation, head to tail, in eight sites of methyl palmitoleate, a fatty acid ester (56). Bose, et al. in their study of the biosynthesis of gliotoxin, used mass spectrometry as the primary analytical tool (55,128). However, the use of a crude data reduction technique, subtraction of  $M+1/M$  ratios of the natural abundance and labeled compounds, reduced the results for the labeled gliotoxin to essentially qualitative levels. Mass spectrometry was especially important as an analytical tool in their study because it allowed investigation of the nitrogen precursor as well as specific carbon precursors.

The gliotoxin analysis was rediscussed by a student of Bose, R. F. Tavares in his doctoral dissertation (116). Tavares derives a more sophisticated formula for easy calculation of the percent enrichment of a singly labeled species:

$$X = \frac{R-Q}{1 + (R-Q)-RS} \quad 100\% \quad (I-1)$$

where X = percent enrichment

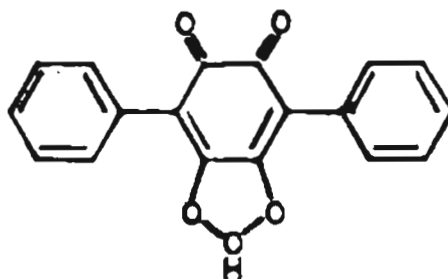
$$R = I_{L(k+1)} / I_{Lk}$$

$$Q = I_{U(k+1)} / I_{Uk}$$

$$S = I_{U(k-1)} / I_{Uk}$$

and I refers to the intensity of a mass spectral peak at mass  $k+i$ ,  $i = -1, 0, +1$ , and L and U refer to the spectra of the labeled and unlabeled samples respectively. Gliotoxin data reduced using equation (I-1) is qualitatively similar but quantitatively more accurate than the originally reported results. Tavares discusses the difference between the two methods explaining that (I-1) is accurate for compounds labeled at only one site. This Tavares considers to be the "normal situation in all biosynthetic problems in which either  $^{15}\text{N}$  or  $^{13}\text{C}$  are used" (116). This opinion is questionable in the light of other biosynthetic studies discussed herein (56, 57, 129-131) but certainly such simple cases do frequently exist.

In later work, Bose and coworkers obtained more quantitative results (117). An interesting double labeling experiment was conducted investigating the biosynthesis of phlebiarbrone (I-33):

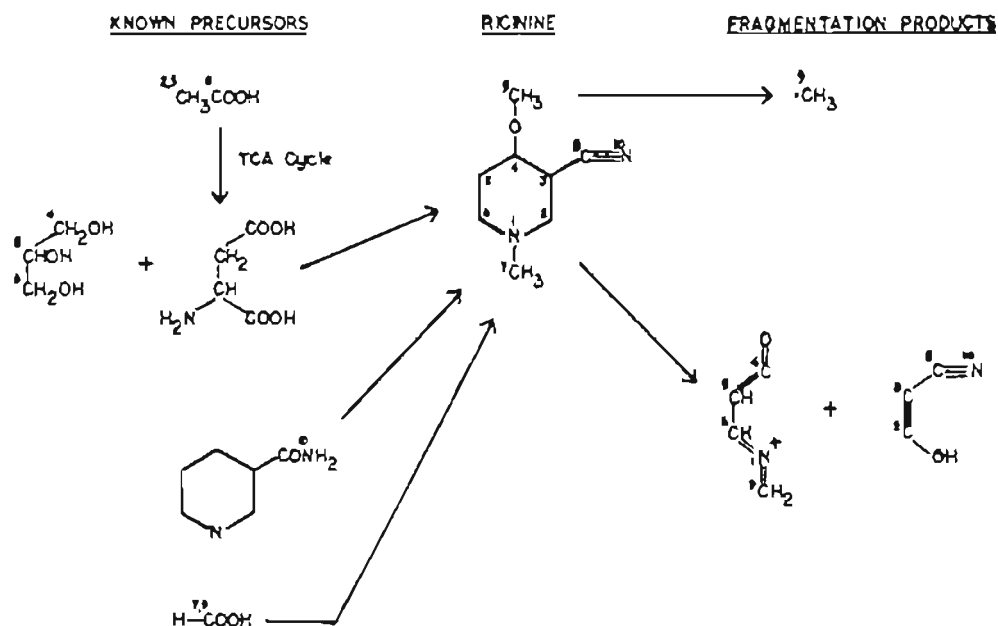


I-33. Phiebiarbrone

( $\pm$ )-[3- $^{13}\text{C}$ ]Phenylalanine and ( $\pm$ )-[1- $^{14}\text{C}$ ]phenylalanine were administered simultaneously. The relative proportions of the  $^{14}\text{C}$  to  $^{13}\text{C}$  in the precursor and product were found to be similar thus indicating that the three carbon atoms of the phenylalanine side chain remain intact during biosynthesis.

In an exhaustive pioneering study, Waller, Ryhage and Meyerson used stable isotopes to elucidate the mass spectral fragmentation pattern of biosynthesized ricinine and then applied this knowledge of the fragmentation pattern to obtain further information regarding ricinine biosynthesis (129). Figure I-34 shows the ricinine structure, its precursors, and fragmentation products. The numbers indicate the positions of specific carbons with respect to reagents and products. Previous carbon-14 and nitrogen-15 experiments followed by chemical degradation had shown the incorporation of certain precursors in specific positions. Using this information ricinine was produced labeled at known sites with  $^{13}\text{C}$  and  $^{15}\text{N}$ . Observing the distribution of these labels in the mass spectral fragments identified the fragment origins as summarized in Figure I-34.

FIGURE I-34.  
Biosynthesis and EIMS Fragmentation of Ricinine.



Walker, Ryhage, Meyerson, *Anal Biochem.* **16**, 277 (1966).

The fragmentation study results were then used to allow further investigation of the ricinine biosynthesis. Nitrogen-15 was administered as aspartate, the ricinine bioproduct degraded by the mass spectrometer, and the labeled site thereby located. The nitrogen-15 appeared in the  $C_4H_4NO$  ion showing that the aspartate nitrogen is incorporated as the ring nitrogen of ricinine.

Vandenhoeval and Cohen attempted a quantitative analysis of the most advanced type, determination of enrichment levels at multiple sites, in their investigation of  $^{13}C$  enriched amino acids (130,131). The data reduction method employed yielded a measure of the average  $^{13}C$  content of all carbons remaining within a particular fragment. Results were

sufficiently accurate to demonstrate the existence of an isotope effect of the appropriate magnitude in biosynthesis of the amino acids by algae from  $\text{CO}_2$  enriched 15% with  $^{13}\text{C}$ . The data presented is extensive, unique, and extremely interesting. Therefore, a reevaluation was done in the light of more accurate data reduction techniques. This reevaluation is presented in Part IV herein.

The advantages of the use of stable isotopes over radioactive isotopes make them of particular interest for clinical application. Mass spectrometric analysis techniques have advanced to the point where such clinical application is becoming practical. Two papers suggesting such clinical application have already been discussed (118,124). Sweetman, Nyhan, Klein and Szczypanik have reported a clinical application and have carefully compared results obtainable with the stable isotope  $^{13}\text{C}$  to those obtainable with the commonly used radioactive isotope  $^{14}\text{C}$  (119). They used both glycine-1,2- $^{13}\text{C}$  (93 atom % excess) and glycine-10 $^{14}\text{C}$  (7.65 mCi/mMole) to study glycine metabolism in three children with in-born errors of metabolism. Carbon-14 specific activity in the respiratory  $\text{CO}_2$  was determined by manometry and liquid scintillation counting and in recovered uric acid by liquid scintillation counting and specific enzymatic spectrophotometric analysis. Carbon-13 enrichment was determined in both metabolic products by AVA-MS. For uric acid, determination included measurement of three ratios, (M+1), (M+2), and (M+3) to M, corrected for natural abundance, in order to evaluate the enrichment at three carbon sites. Results indicated that stable isotope labeling could, indeed, provide information similar to that provided by radioactive

isotope labeling thus eliminating the need for exposing the patient to radioisotope hazards. In addition, the  $^{13}\text{C}$  offered an advantage in that information was obtainable about incorporation of more than one atom of tracer per molecule without specific chemical degradation. Thus additional clues about the metabolism of the tracer molecule were obtained. The 95% excess  $^{13}\text{C}$  used was found to be higher than necessary to produce results of accuracy comparable to  $^{14}\text{C}$  results.

#### D. Conclusion

In conclusion, review of the literature pertaining to mass spectral analysis of compounds enriched with the stable isotope,  $^{13}\text{C}$ , reveals that most applications of this technique have employed simplistic data reduction techniques. The use of such techniques has, in the past, severely limited the complexity of problems which might be approached with  $^{13}\text{C}$  labeling. Biological applications of mass spectral  $^{13}\text{C}$  analysis of complex molecules have been particularly limited. However, current research is developing increasingly useful theoretical approaches to reduction of more complex mass spectral isotopic data. When such data reduction techniques are fully employed, mass spectrometry can be expected to be an even more useful tool for isotopic analysis.

This current study, therefore, undertakes to develop a generally applicable data reduction technique for isotopic mass spectral analysis and applies that technique to extensive examination of biosynthetically produced,  $^{13}\text{C}$  enriched samples.

## PART II

## DEVELOPMENT OF THE POLYNOMIAL DATA REDUCTION TECHNIQUE

## A. Introduction

## 1. Generality of mass spectral theory

The mass spectrometer is an analytical tool which is capable of accepting a molecule, degrading it into fragments by application of energy in some or several forms, and then sorting those fragments according to mass and electronic charge. The mass of the fragment is dependent upon its empirical formula and the number and identity of the atomic isotopes present. The charge is dependent upon the type and amount of energy applied.

Experimental considerations have limited the application of mass spectrometric isotopic analysis, but, in fact, little in the theory of mass spectrometric analytical procedure seems to be extremely limiting. In contrast, analytical methods which depend upon nuclear spin and magnetic moment are inherently applicable only to select samples (16).

Traditional analyses of isotopically labeled molecules have employed radioactive isotopes and manual chemical degradation. Of course, this approach is restricted only to atoms which have radioactive analogs. In addition the degradation procedures may be inordinately time consuming and laborious (17).

Beside these other techniques mass spectrometry may appear to be an approach of more general application and "ultimate automation" (18). It is dependent upon mass differences rather than magnetic moment ;

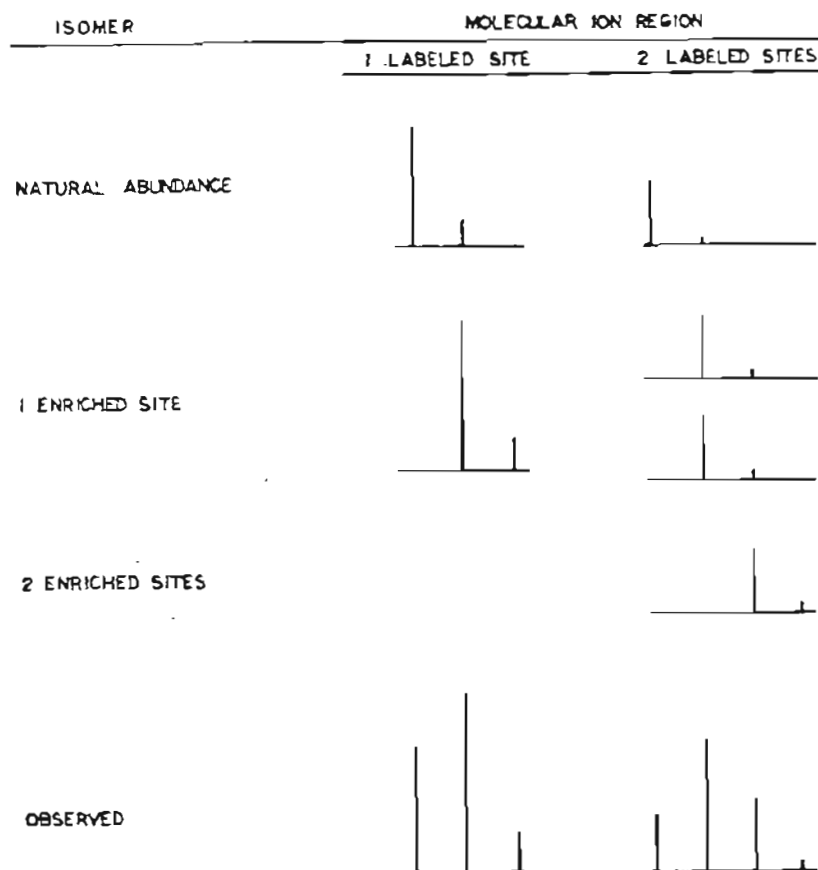
it is applicable to stable and radioactive isotopes alike (132); and its major result is the rapid degradation of the molecule. The data obtained yield information about the exact mass, and thus the empirical formula, and about certain energetics which may sometimes be interpreted as clues to structure (18). Traditional electron impact mass spectrometric (EIMS) data reduction techniques have, unfortunately, degraded the generality of its approach to isotopic analysis (7).

## 2. Traditional approach - a model of isotopic isomers

Pure isotopic compounds have not been and are not now readily available; therefore, isotopically enriched samples have been traditionally viewed as mixtures of isotopically related isomers or "isotopic isomers" (39). The mass spectra of enriched samples, then, have been viewed as the composite mass spectra of mixtures necessitating the removal of "contaminants" to clearly view the "isomer of interest". Figure II graphically illustrates this point of view.

The left hand column pictures the molecular ion region of the mass spectrum of a compound in which a label has been selectively introduced at one particular site. In the traditional view, the observed spectrum (bottom) is viewed as a composite of the spectra of two isotopic isomers: first, a set of isotopically enriched molecules always containing  $^{13}\text{C}$  at the enriched site (center) and second, a set of molecules containing  $^{13}\text{C}$  distributed randomly across all carbon sites at natural abundance (top). The spectrum of the natural abundance isomer does contain a small peak at  $M+2$ ; however, it is invisible at the scale used.

FIGURE II.  
Observed Mass Spectra Can Be Viewed As Composites



Clearly, the use of the "natural abundance isomer" is, in itself, a simplification, for it can be viewed as a mixture of molecules identical to the desired labeled ones, molecules containing no  $^{13}\text{C}$  atoms, and still other isomers containing  $^{13}\text{C}$  atoms at any or all of the other carbon sites. The original work in  $^{13}\text{C}$  analysis did view spectra of enriched compounds in this complex way (39); however, the simplification resulting from consideration of a "natural abundance isomer" was soon introduced (71,133). Therefore, a compound selectively labeled at one

site is pictured as a mixture of two isomers as it is in Figure II.

The right hand column pictures the spectrum of a compound selectively labeled at two sites as a composite of the spectra of four isotopic isomers: a natural abundance isomer, a set of molecules actually containing  $^{13}\text{C}$  atoms at both sites at which the label was to be introduced, and two sets of molecules each with  $^{13}\text{C}$  atoms at only one of the selected sites. The spectra of these latter two sets are identical in the molecular ion regions illustrated. The intent to label two different carbon sites, therefore, results in a mixture of four isomers.

Unfortunately the number of isomers continues to increase exponentially with the number of labeled sites. Table I-1, p. 7 tabulated this uncomfortable progression revealing a possible 32,768 isomers for 15 labeled sites! Remember, of those 32,768 isomers only one is desired. Obviously, such an approach becomes unreasonably complex.

Mass spectra of isotopically labeled molecules need not be viewed in this manner, as though it were possible to simply take each molecule and paint the carbon of interest with red paint. Rather labeling may be viewed as a process of "statistical enrichment" in which a sample consists of a set of molecules containing more  $^{13}\text{C}$  atoms than would occur naturally and with this additional  $^{13}\text{C}$  selectively concentrated at the sites of interest. This approach is readily amenable to mathematical treatment using standard probability equations (7,133,134).

### 3. General approach - statistical model

Any alteration of the naturally occurring isotopic composition will produce a predictable shift of the EIMS spectrum. For example, if

all  $^{12}\text{C}$  at a particular site is replaced by  $^{13}\text{C}$ , the mass of the molecular ion will be increased by one and the molecular ion intensity along with the intensities of its associated naturally occurring isotopic ions will appear one  $m/z$  unit higher in the spectrum as will the  $m/z$  of all fragments containing that particular carbon along with their associated isotopic ions (See Figure II). Replacement of more than one  $^{12}\text{C}$  with  $^{13}\text{C}$  will result in similar shifts in  $m/z$  equal to the number of isotopic substitutions. Replacement of a common isotope with another differing by weight will always cause a shift in  $m/z$  equal to that difference, e.g., replacement of  $^{16}\text{O}$  by  $^{18}\text{O}$  will shift ionic masses by 2 amu;  $^{12}\text{C}$  by  $^{13}\text{C}$ , 1 amu;  $^{12}\text{C}$  by  $^{14}\text{C}$ , 2 amu, etc.

Complexities in interpretation of isotopic spectra arise when some, but not all, of the common isotope at a particular site is replaced with another, i.e., the concentration of molecules containing the isotope of interest is less than 100%. In general, any enrichment by a heavy isotope will shift a portion of the spectrum to higher  $m/z$ ; however, at low enrichment levels such a shift may be nearly imperceptible without sensitive measurement. The shift will not apply to a particular total ion intensity, but will involve only that portion of the ion intensity due to molecules containing the heavy isotope. If enrichment at more than one site is involved, distribution of the isotopic mass increase will occur statistically across an entire "ion cluster," a particular ion with its associated, naturally occurring isotopic forms. (See Part III C.)

## B. Considerations for general application of mass spectral carbon isotopic analysis

### 1. Preliminary Remarks

The statistical approach to mass spectral isotopic analysis is not new; however, in the past, its general application has been severely limited by several considerations. These considerations have been discussed in great detail by Biemann and include sources of possible error due to both theoretical and experimental factors (133). The data reduction approach described herein in which reference spectra of known isotopic concentration are not necessary and in which results are obtained from several separate spectra and then averaged for error reduction effectively obviates many of these considerations particularly for information obtained from the molecular ion region alone. However, at least three deserve special mention. They are (1) kinetic isotope effects, (2) ion region complexity, and (3) carbon skeleton ambiguity.

### 2. Kinetic isotope effects alter isotopic content of fragment ion regions

Kinetic isotope effects are a theoretically controlled source of ambiguity in results and are of special significance when analysis involves use of data from fragment ion regions of the spectrum (134,135). Their effect can only be eliminated by introduction of carefully determined correction factors which have not been included in this work. They are of importance because of their influence upon the fragmentation processes themselves.

A difference in the reactivity of isotopic ions occurs as a

direct result of the difference in mass (134,136). Essentially, the activation energy for the fragmentation process is a function of the difference in ground state and transition state energies for the reacting entity. These energies are, of course, functions of the critical stretching frequencies of the bonds under consideration which are, in turn, related to the masses of the bonded moieties. Whenever the breaking of a bond to an isotopic atom is the rate determining step in production of a particular fragment, the isotope effect involved is termed primary and will have its maximum value. If the isotopic atom is located in a position more distant to the fracturing bond or when the bond cleavage is not rate limiting, the isotope effects will be less pronounced. Factors which increase the magnitude of the isotope effect  $k_A/k_B$ , where  $k$  equals the rate constant for a given reaction and A and B are indices of particular isotopes, will decrease the abundance of heavy isotopes in fragment regions. As examples,  $k_H/k_D$  will be greater than  $k_{12C}/k_{13C}$ ,  $k_{16O}/k_{18O}$  will be greater than  $k_{12C}/k_{13C}$ , and multiple isotopic substitutions will exhibit greater effects than single substitutions (133,137, 138).

As methods for obtaining quantitative measurements of isotopic content from mass spectral fragment ion regions become more precise, accurate values will require that corrections be included to deal with the kinetic isotope effects. The magnitude of these effects on certain mass spectral fragmentation reactions is being investigated (39,134-142).<sup>8</sup>

---

<sup>8</sup>For a determination involving the effect of <sup>13</sup>C substitution see Beynon, Brothers, & Cooke (139).

### 3. Complex regions contain overlapping ion clusters

Another aspect of mass spectral behavior which has complicated data interpretation is the complexity of the ion region (43,49,133). Rarely does a single region contain simply a particular ion and its associated isotopic forms, but instead, is composed of two or more overlapping ion clusters. Since these clusters result from ions of differing empirical formulas then a spectrum of high enough resolution will separate them. Separation of clusters differing by  $^{13}\text{C}$  and  $^{12}\text{CH}$  requires a very high resolution of  $\sim 45,000$  at  $m/z$  200. An increase in instrumental resolving power has been accompanied by a decrease in instrumental accuracy of intensity measurement (30). This is, indeed, an unfortunate circumstance for the presence in a region of ions differing by number of hydrogen atoms is common, often unavoidable, and often irreproducible (49,133).

Such apparent complexity is, however, amenable to solution within a possible set of polynomial equations. Each additional overlapping ion cluster simply adds an additional unknown to the equations and thus requires observation of an additional ion intensity. The approach applied herein treats the problem of overlapping ion clusters (See Part II C 3).

### 4. Complexity of spectral processes results in carbon skeleton ambiguity

A final difficulty presented by common mass spectral behavior is the complexity of molecular fragmentation. In many cases the major fragments may be easily rationalized; however, the chemistry of the actual mass spectrometric reactions may be more complex so that such

rationalizations may be oversimplifications (7,143-145). Loss of a particular fragment may be possible from more than one portion of the original ion, resulting in ions of identical formulas but with atoms derived from different portions of the parent molecule. Such loss may be either sequential in the simple case or may involve competing reactions. Difficulty exists then for unique isolation of a labeled segment. Similar situations, of course, arise in traditional chemical degradation schemes. In favorable situations, the polynomial nature of the data reduction technique used in this present investigation allows determination of, at least, the number of enriched sites and the isotopic content of each from the parent ion region alone via the distinctive ion intensity pattern. (See Part III D.) Of course, molecular fragmentation is still necessary to pinpoint the location of those enriched sites.

### C. Mathematical formulation

TABLE II  
INDEX OF VARIABLES

$n$	=	number of carbon atoms
$p$	=	number of hydrogen atoms
$s$	=	number of nitrogen atoms
$q$	=	number of oxygen atoms
$F_m$	=	isotopic generating function for cluster beginning at $m/z = M$
$M$	=	lowest $m/z$ value in given region
$X_{M+j}$	=	mole fraction of ion appearing at $m/z = M+j$
$j$	=	incremental addition to $M - j + 1 =$ number of different isotopic isomers
$Z$	=	$n + p + s + 2q - 1 + 1 =$ number of $X_{M+j}$ in ion cluster
$a$	=	abundance of light isotope
$b$	=	abundance of heavy isotope (one mass unit heavier than isotope signified by "a")
$c$	=	abundance of heavy isotope (two mass units heavier than isotope signified by "a")
$R$	=	constant representing the contribution of hydrogen, nitrogen, and oxygen to a particular expression.
$C_i$	=	a particular carbon isotopic abundance
$m$	=	maximum number of different carbon isotopic abundance values.
$Q$	=	contribution to a given expression resulting from the contribution of carbon sites containing the natural abundance of isotopes
$I_t$	=	total ionic intensity of a given region
$I_{M+j}$	=	ionic intensity of the ion cluster originating at $m/z = M + j$ .
$t$	=	index of ions in a given region - $t + 1 = m/z$ of highest mass ion in that region
$A_{M+j}$	=	relative abundance for ion cluster originating at $m/z = M + j$ .
$P_{M+L}$	=	polynomial describing ionic intensity of a given cluster, $M + L$ .
$L$	=	number of carbons in the molecule responsible for cluster $M + L$ .
$x$	=	number of atoms of $^{12}\text{C}$ in a given isotopic isomer
$y$	=	number of atoms of $^{13}\text{C}$ in a given isotopic isomer
$k$	=	number of unknown abundance values
$a_x, b_x$	=	trial abundance values for light and heavy isotope
$\lambda$	=	$b_x/a_x$
$P_{M+L}(\lambda)$	=	polynomial representing the difference between $P_{M+L}$ for the true isotopic abundance values and $P_{M+L}$ for the trial abundance values.
$T$	=	order of the derivative of $P_{M+L}(\lambda)$

### 1. Ion cluster - general

The theory of the mass spectra of isotopic molecules has been discussed in detail by Beynon (146), Biemann (133) and Brauman (42) and several procedures have been described for generating from elementary statistics the isotope peak patterns for ion clusters of known elemental composition at both natural and enriched levels of isotopic abundance (13,21,22,26,28) or for evaluating the isotopic abundances from such statistical considerations (7,29,33,44,49). According to mass spectral theory, the isotope peak pattern of an ion cluster, e.g.,  $C_n H_p N_s O_q$  is given by its isotopic generating function  $F_M$ , which is the sum of the mole fractions,  $X_{Mj}$ , of the ions originating at each  $m/z$ ,  $M + j$  (47).

$$F_M = \sum_{j=0}^{\ell} X_{Mj} \quad (\text{II-1})$$

where  $\ell + 1 =$  number of these  $X_{Mj}$ 's ( $\ell = n+p+s+2q$ ). The relative values for the  $X_{Mj}$  are statistically determined and may be described as a multinomial distribution.

$$F_M = (a_C + b_C)^n (a_H + b_H)^p (a_N + b_N)^s (a_O + b_O + c_O)^q \quad (\text{II-2})$$

where  $M = m/z$  of the lightest isotopic ion and  $a, b, c =$  abundances of the isotopic forms of the indicated element.

Inasmuch as the values to be determined are related only to the carbon abundances, equation (II-2) may be simplified to

$$F_M = R(a_C + b_C)^n \quad (\text{II-3})$$

where  $R$  is a constant for a particular ion cluster representing that portion contributed by the hydrogen, nitrogen, and oxygen.

## 2. Ion cluster - isotopically enriched sample

Whenever carbon isotope abundance is identical for all carbon sites within the compound, equation (II-3) will be the proper expression. This occurs, for example, in the case of natural abundance samples. However, when carbon isotope abundance values vary across the several carbon sites as in the case of  $^{13}\text{C}$  enriched compounds, the term  $a$  and  $b$  may be divided into the appropriate number of terms, i.e.

$$F_M = R \prod_{i=1}^m (a_{\text{Ci}} + b_{\text{Ci}})^{n_i} \quad (\text{II-4})$$

In some cases the number of sites containing only natural abundances of carbon isotopes will be known. For these cases

$$\begin{aligned} F_M &= (a_{\text{C1}} + b_{\text{C1}})^{n_1} R \prod_{i=2}^m (a_{\text{Ci}} + b_{\text{Ci}})^{n_i} \\ &= QR \prod_{i=2}^m (a_{\text{Ci}} + b_{\text{Ci}})^{n_i} \end{aligned} \quad (\text{II-5})$$

where  $Q$  is a constant contributed by the portion of the sample at natural abundance and multiple terms still exist equal to the number of different abundance values.

Then since,

$$a_{\text{C}} + b_{\text{C}} = 1 \quad (\text{II-6})$$

when  $i$  and  $n$  are known, the values  $a_C$  and  $b_C$  may be calculated in a straight-forward manner from the simple set of linear equations. When  $i$  or any  $n_i$  is known that unknown value may be systematically varied, various possible peak patterns calculated, and comparison made against the experimental data being interpreted. The variation of the one parameter,  $b_{Ci}$ , for assumed models (values of  $n_i$ ) followed by manual comparison with observed intensities, constitutes the "one parameter approach" described herein. (See Appendix A 2.)

### 3. Complex ion regions - overlapping clusters

When a particular ion region is composed of overlapping ion clusters, its peak pattern may still be described but by a more extensive set of linear equations. The total ion intensity of the region,  $I_T$ , will be equal to the sum over the ion intensities of the individual ion clusters,  $I_{M+j}$ , originating at mass  $M+j$ , that is

$$I_T = \sum_{j=0}^t I_{M+j} \quad (\text{II-7})$$

where  $t+1$  equal the number of observed peaks in the region. The individual ion cluster intensities,  $I_{M+j}$ , may be expressed in terms of their relative abundance,  $A_{M+j}$ , and their isotopic generating function  $F_{M+j}$ , so that

$$I_T = \sum_{j=0}^t A_{M+j} F_{M+j} \quad (\text{II-8})$$

Therefore, when the number of observable ion intensity ratios is equal to the number of values to be determined, i.e., the number of labeled sites,  $m_1$ , plus the number of individual ion cluster abundance values, exact solutions may be expected. Systematic variation of the parameters involved and comparison of the calculated values with experimental data constitutes a curve-fitting technique which allows identification of the isotopic enrichment and the labeling pattern (number of enriched sites).

This approach using binomial expansions and sets of linear equations was felt to require the fewest prior assumptions and thus to be the most generally applicable for analysis of isotopically enriched molecules (See Appendix A 2).

#### 4. Residual ion intensities as monitoring parameters - the factor method

Obviously this one parameter approach has at least three very serious restrictions: (1) Only one unknown isotopic abundance value at a time may be determined exactly; (2) manual comparison of results with observed values is time consuming and inexact; (3) the number of observable ion abundance ratios must be equal to the number of unknowns. Therefore, a more generally useful approach was sought.

From the intensity data generated by equation II-11, a polynomial,  $P_{M+L}$ , where L equal the number of carbons in the molecule of interest, may be constructed in terms of the relative abundance values  $a_{Ci}$  and  $b_{Ci}$ .

$$P_{M+L} = \sum_{i=0}^k a_{Ci}^x b_{Ci}^y \quad (\text{II-9})$$

where  $k =$  the number of unknown abundance values and  $x+y=m$ ; the number of sites of unknown isotopic content (44).

Defining a quantity,  $\lambda$  equal to  $b_x/a_x$  where  $b_x$  is the trial abundance value for iterative calculations and  $a_x + b_x = 1$ , a more general polynomial,  $P_{M+L}(\lambda)$ , may be written (47)

$$P_{M+L}(\lambda) = \sum_{j=0}^L I_{M+j} (-\lambda)^{L-j} \quad (\text{II-10})$$

expressing the difference between the observed intensity and that calculated from the trial abundance value.

Its factors may be extracted

$$P_{M+L}(\lambda) = \left( \frac{b_C}{a_C} - \lambda \right)^n \left( \frac{b_H}{a_H} - \lambda \right)^p \left( \frac{b_N}{a_N} - \lambda \right)^s \left[ (-\lambda)^2 + \frac{b_O}{a_O}(-\lambda) + \frac{c_O}{a_O} \right]^q \quad (\text{II-11})$$

For cases where carbon isotope abundance is of interest, the hydrogen, nitrogen, and oxygen terms are calculable constants for a given cluster and the polynomial of interest reduces to

$$P_{M+L}(\lambda) = R \left( \frac{b_C}{a_C} - \lambda \right)^n \quad (\text{II-12})$$

This equation will be valid whenever all carbon sites contain equal isotopic abundance as in the case of natural abundance samples. However, in the case of  $^{13}\text{C}$  enriched samples any number of different abundance values may occur up to the total number of carbons. Therefore

$$P_{M+L}(\lambda) = R \prod_{i=1}^m \left( \frac{b_{Ci}}{a_{Ci}} - \lambda \right)^{n_i} \quad (\text{II-13})$$

It is obvious from expressions (II-12) and (II-13) that, when  $\lambda$  is equal to an accurate isotope abundance ratio, one term will be equal to zero and thus the entire expression will be equal to zero. If, therefore, the value of  $P_{M+L}(\lambda)$ , called the residual ion intensity at  $M+L$ , is used as a monitoring parameter correct isotopic abundance values may be easily obtained.

One final but serious limitation exists in this approach: The number of observable ion abundance ratios must be equal to the number of carbon isotope abundance values plus the number of ion clusters present in the region. In practice this is rarely possible. The dynamic range of observable intensity is limited by experimental considerations. It, therefore, becomes necessary to use a value of  $P_{M+L}$  which corresponds to other than the ion abundance of highest mass in the region. This may be accomplished by construction of the derivatives,  $P_{M+L}^{(T)}(\lambda)$ , where  $T$  equals the order of the derivative (48). As examples, if

$$P_{M+L}(\lambda) = \left( \frac{b_C}{a_C} - \lambda \right)^n \left( \frac{b_1}{a_1} - \lambda \right)^p \quad (\text{II-14})$$

then

$$P_{M+L}^{(1)}(\lambda) = (-1) \left( \frac{b_C}{a_C} - \lambda \right)^{n-1} \left( \frac{b_1}{a_1} - \lambda \right)^{p-1} \left( \frac{b_C}{a_C} + \frac{b_1}{a_1} - L\lambda \right) \quad (\text{II-15})$$

$$P_{M+L}^{(L-1)}(\lambda) = | (-1)^{L-1} (L-1)! \left| \left( \frac{b_C}{a_C} + \frac{b_1}{a_1} - L\lambda \right) \right. \quad (\text{II-16})$$

By this means, the order of the polynomial is progressively decreased.

This approach featuring the extraction of factors of the polynomial,  $P_{M+L}^{(T)}(\lambda)$ , is termed the "factor approach". It lends itself readily to graphical display of  $b_x$  vs.  $P_{M+L}^{(T)}(\lambda)$  in which case intersections on the  $P_{M+L}^{(T)}(\lambda)$  axis will occur for  $b_x = b_{C_1}$ , the real  $^{13}\text{C}$  isotope abundance values. The most promising aspect of this approach is its capacity for the treatment of the common complex experimental situations in which more than one unknown occurs and the number of observables falls short of the number of such unknowns.

## PART III

MODEL CALCULATIONS DESCRIBING THE UTILITY OF THE POLYNOMIAL  
DATA REDUCTION TECHNIQUE

## A. Introduction - a rationale for model calculations

The initial application of any analytical technique should ideally involve carefully chosen cases with specifically structured problems whose answers are obtainable independently by other techniques. Analysis of isotopic molecules is a multidimensional problem of huge proportion involving numerous interrelated variables. Real, experimentally obtained mass spectra of isotopically enriched molecules are notably complex (40). However, the use of artificially constructed spectra provides for easily obtainable data, selective control of the complexity of the investigation, systematic introduction of variables and absolute foreknowledge of correct solutions. Therefore, model spectra were constructed from chosen isotopic models for initial application of the developed technique. Such model calculations may serve to elucidate the difficulties involved, to investigate the interrelationship of the multiple variables, to establish guidelines to experimental design, and to illustrate the use of the developed method.

## B. A discussion of some difficulties involved in the interpretation of isotopic mass spectra

## 1. Carbon-13 content - a quantity in need of definition

a. Four models containing "20%  $^{13}\text{C}$ "

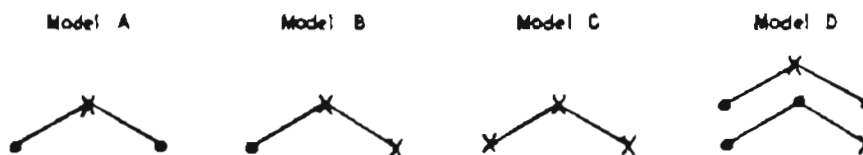
Interpretation of the mass spectra of isotopically enriched

samples must be laid on a sound mathematical basis for the change in relative ion abundance ratios is not as readily predictable as it is in the case of the spectra of pure isotopic isomers. The spectrum of an individual isomer exhibits a simple mass shift of the ion equal to the change in ionic weight. However, the observed spectrum of the "mixture" or enriched sample will show only a shift in the percentage of the total ionic intensity to higher  $m/z$ . (See Figure II, p. 61) The actual peak pattern will be dependent on several factors in addition to the degree of isotopic enrichment within the molecule, such as the distribution of that enrichment, the size of the molecule, and the dynamic range of measurement.

Figures III-1 and III-2 illustrate this interrelationship of variables for a  $C_3$  sample. Figure III-1 diagrams four model samples of different isotopic composition.

FIGURE III-1.

FOUR 3-CARBON SAMPLES WITH ISOTOPICALLY ENRICHED SITES



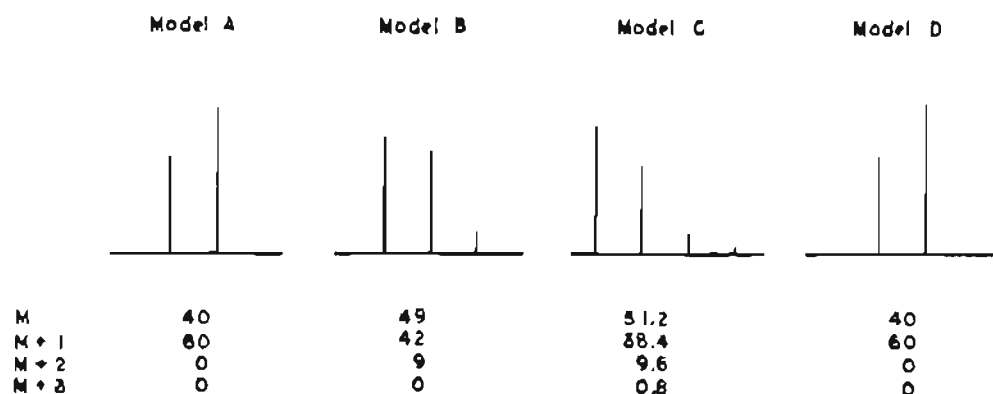
● Indicates presence of isotopes at natural abundance.

X Indicates presence of isotopically enriched sites.

Figure III-2 pictures the molecular ion region of the mass spectra of these four different, three carbon,  $^{13}\text{C}$  enriched models.

FIGURE III-2.

MOLECULAR ION MASS SPECTRA OF MODELS A-D (FIGURE III-1)



They are identical in structure and if converted to  $\text{CO}_2$  and then analyzed for carbon-13 content all four would be found to contain 20%  $^{13}\text{C}$ , i.e. 20% of the carbon atoms are  $^{13}\text{C}$ . However, the difference lies in the distribution of that  $^{13}\text{C}$  among the three carbons of each molecule.

In model A, with one isotopically labeled site, 40% of the molecules contain no  $^{13}\text{C}$  and 60% contain  $^{13}\text{C}$  at one particular site.

In model B with two labeled sites 30% of the molecules contain  $^{13}\text{C}$  at one site and 30% contain  $^{13}\text{C}$  at another site. Since there is no restriction requiring molecules included in the first 30% not to be also included in the second 30%, some molecules will contain two atoms of  $^{13}\text{C}$  and, therefore, the fraction of molecules containing no  $^{13}\text{C}$  will be greater than 40%.

In model C the entire sample is enriched so that 20% of the

molecules contain  $^{13}\text{C}$  at one site, 20% at a second site, and 20% at a third site. Again, sets may be overlapping; therefore, any individual molecule may contain from 0-3  $^{13}\text{C}$  atoms.

Model D is a mixture of two isotopic isomers each labeled at a different single site. Each isomer is only partially labeled to the extent of 60%. An inspection of the sample would reveal that 30% of the total mixture contains molecules with  $^{13}\text{C}$  atoms at one given labeled site. Another 30% of the mixture contains molecules with  $^{13}\text{C}$  atoms only at a second given labeled site. The remaining 40%, half arising from each component, contains no  $^{13}\text{C}$ .

These models represent four different examples in which 20% of all carbon atoms are  $^{13}\text{C}$ . However, commonly used terminology would describe them each quite differently. Exact phraseology varies considerably. Model A might be termed "60%  $^{13}\text{C}$  labeled"; model B, "30%  $^{13}\text{C}$  double labeled"; model C, "18.9% (20% minus 1.1% natural abundance)  $^{13}\text{C}$  enriched"; and model D, "a mixture of two 60%  $^{13}\text{C}$  labeled isomers". Unfortunately no uniform descriptive format has yet been adopted. A possible format used in this investigation is the formula followed by a listing of the individual  $^{13}\text{C}$  contents for enriched sites. In this case each of these four models would be described as follows:

$$A = {}^{13}\text{C} {}^{12}\text{C}_2 \quad (60)$$

$$B = {}^{13}\text{C}_2 {}^{12}\text{C} \quad (30,30)$$

$$C = {}^{13}\text{C}_3 \quad (20,20,20)$$

$$D = {}^{13}\text{C}^1 {}^{12}\text{C}_2 (60) + {}^{13}\text{C}^2 {}^{12}\text{C}_2 (60)$$

Model D has righthanded superscripts which indicate the label position

in order to differentiate between the two singly labeled components of the mixture. Models A-C might also include this notation when desired.

b. Model D - a true isomeric mixture

Model D is similar to model B in that both are composed of two sets of molecules containing one  $^{13}\text{C}$ . In both cases, each set comprises 30% of the total, and in both cases, 20% of all carbon is  $^{13}\text{C}$ . However, in model B, a doubly labeled sample, these sets are overlapping; in model D, the true mixtures, they are not. The spectra as viewed in Figure III-2 are markedly dissimilar. In fact, the spectrum of model D is indistinguishable from that of model A in the molecular ion regions illustrated. In neither models A nor D do any molecules contain more than one label.<sup>9</sup> Model B contains a set of doubly labeled molecules. Models A and D may be differentiated in the fragment ion regions provided that the decomposition pattern is such that fragments occur containing only one of the two labeled carbons in model D.

2. M+1/M ratio measurements for determination of isotopic content - a potential for abuse

a. A mathematical expression of the relationship between the isotopic abundance and M+1/M

A common technique for obtaining isotopic abundance measurements

---

<sup>9</sup>In the real case naturally occurring  $^{13}\text{C}$  would be present at all carbon sites and thus molecules containing more than one  $^{13}\text{C}$  would be present in both samples. However, spectra due only to the  $^{13}\text{C}$  of the label may be obtained in some cases by subtraction of natural abundance spectra. [See Part III-B-2b(2).]

primarily involves use of the M+1/M ratio. A derivation of the exact mathematical expressions involved will yield an understanding of the assumptions and limitations implicit.

Expressions for the relative intensities of each mass spectral peak in an isotopic ion cluster may be obtained by expansion of the binomial sums of isotopic abundance values. The resultant terms are then grouped by isotopic composition to obtain the desired relative ion abundance values. As an example, the expression for a three carbon ion originally involves three sums:

$$(a_1 + b_1) (a_2 + b_2) (a_3 + b_3) \quad (\text{III-1})$$

where  $a_i$  equals the abundance of  $^{12}\text{C}$  at each given site and  $b_i$ , the abundance of  $^{13}\text{C}$ . Expansion of this expression yields eight terms:

$$a_1 a_2 a_3 + a_1 a_2 b_3 + a_1 a_3 b_2 + a_2 a_3 b_1 + a_1 b_2 b_3 + a_2 b_1 b_3 + a_3 b_1 b_2 + b_1 b_2 b_3 \quad (\text{III-2})$$

Grouping these by isotopic composition, the following relative intensities are obtained:

$$M = a_1 a_2 a_3 \quad (\text{III-3})$$

$$M+1 = a_1 a_2 b_3 + a_1 a_3 b_2 + a_2 a_3 b_1 \quad (\text{III-4})$$

$$M+2 = a_1 b_2 b_3 + a_2 b_1 b_3 + a_3 b_1 b_2 \quad (\text{III-5})$$

$$M+3 = b_1 b_2 b_3 \quad (\text{III-6})$$

Formation of the ratio of expression III-4 to III-3 and simplification yields

$$\frac{M+1}{M} = \frac{b_1}{a_1} + \frac{b_2}{a_2} + \frac{b_3}{a_3} \quad (\text{III-7})$$

A general expression for this M+1/M ratio, may then be written

$$\frac{M+1}{M} = \sum_{i=1}^n \frac{b_i}{a_i} \quad (\text{III-8})$$

where  $n$  equal the number of carbon atoms in the molecule. Of course, expressions analogous to (III-8) may also be derived for real molecules which obviously would include atoms other than carbon. The original sums of expression (III-1) may represent the isotopic abundance value for any element present and sums comprised of any appropriate number of terms may be included.

- b. Solutions to the equations relating isotopic abundance and mass spectral ion intensity

(1) Overview

Equation (III-7) may be viewed as an equation in three unknowns since the sum of the isotopic abundance values for each site will equal 1.

$$a_i + b_i = 1$$

Obviously no exact solution for equation (III-7) may be obtained without observation of more than the usual one ion intensity ratio. Observation of additional relative ion intensities above  $M+1$  will provide the needed relationships.

It is important to remember that derivation of equation III-7 from equation III-8 requires a known value of  $n = 3$ . When  $n$  is unknown another observable will be required for exact solution, since the number of observables must be equal to the number of unknowns. Within the scope of this common data reduction technique, the observables are the ion intensity ratios.

Assumptions may be made to suit the individual case in order

to simplify equation (III-8).

- (2) Assumption 1 - Natural abundance and isotopically enriched samples yield comparable spectra.

The most common simplification involves use of natural abundance standard spectra in order to reduce the number of terms in equation III-1. It is assumed that spectra of natural abundance and isotopically enriched samples are comparable.<sup>10</sup> When this assumption is justified, subtraction of the two spectra after necessary normalization removes terms arising from unenriched sites in the ion (40). If the example described by equation (III-7) contained one carbon site at natural abundance, the ion intensity remaining after subtraction would be due only to the enriched carbons and the appropriate equation would read

$$\frac{M + 1_e}{M_e} = \frac{b_1}{a_1} + \frac{b_2}{a_2} \quad (\text{III-9})$$

---

<sup>10</sup>In actuality this comparison requires a number of assumptions which are discussed extensively by other authors (40,147). Perhaps the least justified are

1. The electron energy is identical for recording of both spectra.
2. The frequency of ion-molecule collisions remains constant.
3. Background due to impurities and instrument noise does not change.

4. The natural abundance of the isotopes is the same in each case. Assumption 4 will generally be justified when the samples are both obtained from the same source. The natural abundance of isotopes is known to vary across various animal, vegetable and mineral origins. For examples, see refs. (3-6). It is generally agreed that, while assumptions 1-3 are not entirely justified, errors thereby introduced will be small (40). Unfortunately, this is not always true and great difficulty has been encountered in this and other work in reproducing results even for multiple spectra of the same sample (129).

and equation (III-8) would become

$$\frac{M + 1_e}{M_e} = \sum_{i=1}^m \frac{b_i}{a_i} \quad (\text{III-10})$$

where  $m$  equals the number of enriched carbon sites.

- (3) Assumption 2 - All enriched sites are equally enriched

A second common simplification arises with the assumption that all enriched carbons are equally enriched. Whether this is a justified assumption depends on the method of synthesis and/or the molecular fragmentation.<sup>11</sup> However, when equality is the case, the example given in equation III-9 will be reduced to

$$\frac{M + 1_e}{M_e} = 2 \frac{b}{a} \quad (\text{III-11})$$

and the general case described

$$\frac{M + 1_e}{M_e} = m \frac{b}{a} \quad (\text{III-12})$$

- (4) Determination of the number of enriched sites

Equation (III-11) is one equation in one unknown; however, equation (III-12) still contains an additional unknown,  $m$ , the number of enriched carbon sites. The value for  $m$  may sometimes be assumed from experimental considerations. When  $m$  is truly unknown the most obvious

---

<sup>11</sup>Isotopic labeling is frequently used in experiments for which the result is dependent upon determination of the relative enrichment levels at two or more sites. Such experiments may involve investigations of isotope effects, biosynthetic or metabolic pathways, mass spectral fragmentation processes, and ionic structure.

method for its determination is observation of the number of intensities in the ion cluster which arise from  $^{13}\text{C}$  isotopes since the one of highest  $m/z$  will represent the case where all carbons are  $^{13}\text{C}$ . Failing this an additional ratio may be measured comparing a previously measured ion intensity to one of greater  $m/z$  arising from addition of an isotope of another element. In the real case these solutions are often not possible.<sup>12</sup> Simplifying assumptions must be made based on the known ion structure and the number of visible ion intensities.

Returning to the example and equations III-3 through III-6, a possible means of solution is

$$\frac{M + 2}{M} = \frac{b_2 b_3}{a_2 a_3} + \frac{b_1 b_3}{a_1 a_3} + \frac{b_1 b_2}{a_1 a_2} \quad (\text{III-13})$$

Removing the contribution of the natural abundance carbon and assuming the remaining two carbons to be equally enriched

$$\frac{M + 2}{M_e} = \frac{M + 1}{M_e} + \frac{b^2}{a^2} \quad (\text{III-15})$$

Equation (III-11) may be introduced

$$\frac{M + 2}{M_e} = 2 \frac{b}{a} + \frac{b^2}{a^2} \quad (\text{III-16})$$

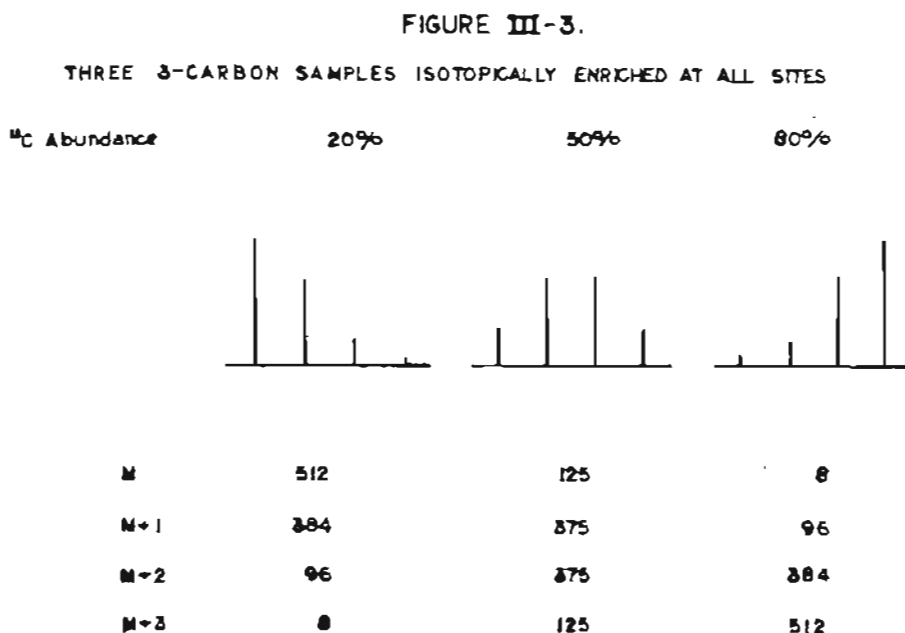
to produce one equation in one unknown.<sup>13</sup>

<sup>12</sup>The true value for the number of intensities in a cluster may not be observed for two reasons: (1) Overlapping ion clusters of a region may add to the number of intensities observed (147). (See Part II-B-3) At lower enrichments the magnitude of intensities at higher  $m/z$  may be too small to permit observation.

<sup>13</sup>For this particular case, after the natural abundance spectrum has been subtracted,  $M + 2$  corresponds to the intensity of highest  $m/z$ . This will not be the case, of course, for molecules with a larger number of enriched carbons.

c. Ion intensity ratios in spectra of highly enriched compounds

When the previously described assumptions are justified and measurement of only one or two ratios is necessary, use of the lower  $m/z$  intensities will produce good results at lower enrichments, for in that case these intensities will contain the greatest percentage of the total ion intensity. Figure III-3 illustrates isotopic ion clusters for three-carbon molecules at three different  $^{13}\text{C}$  abundance levels. As higher abundance levels are involved, ion intensity will progressively be transferred to higher  $m/z$  presenting a different set of analytical considerations in which use of the  $M+1/M$  ratio is clearly not the method of choice (52).



d. The potential for abuse of data reduction procedures

A word of caution is perhaps warranted with regard to the potential which exists for abuse of data reduction procedures based on

limited sets of ion intensity ratios. It is extremely important that the exact mathematical expressions which relate isotopic abundance and mass spectral ion intensity be considered at all times. When necessary simplifying assumptions are employed the limitations imposed thereby should never be discounted. Serious error may be introduced when either researcher or reader develops conclusions beyond these limitations. Quantitative results obtained from samples with numerous sites of enrichment seem particularly susceptible to such misjudgments.<sup>14</sup>

C. An investigation of the interrelationship of variables relating isotopic content and ion cluster appearance

1. The ion cluster contour

a. A concept of uniqueness

The exact appearance of the mass spectral isotopic ion cluster is unique to each individual ion. This appearance is dependent upon variables, both theoretical and experimental, which describe the specific enrichment level and pattern and determine the visibility of the spectrum. Thus, each ion containing isotopic elements may be viewed as possessing a uniquely identifying "ion cluster contour" much as each sample is viewed as possessing an uniquely identifying mass spectrum.

---

<sup>14</sup> As an example of the magnitude of errors which may be introduced by disregard of the use of assumption 2, see Part IV.

b. Interrelationship of variables in predicting ion cluster contour

Isotopic enrichment of a sample does not necessarily result in a straightforward, linear change in any given isotopic intensity. Table III-1 clearly illustrates that it is the complex interrelationship of variables which determines the exact isotopic ratios and thus, the cluster contour. It contains relative ion intensity values for eight different model ion clusters.

Compare spectra A and D, the natural abundance compounds, with spectra B and E, the respective isotopically enriched analogs. The shift of ion intensity to higher mass is clearly visible in both although the change is twice as marked in the three carbon ions (A to B) as in the ten carbon ions (D to E). In both cases one carbon site is enriched to a value of 8.4%  $^{13}\text{C}$ .

Compare spectra B and C with their natural abundance isomer A. All are three carbon ions. Each enriched sample contains 3.53%  $^{13}\text{C}$  atoms. However, sample B has all enrichment concentrated at one atomic site while sample C has the enrichment equally divided among the three carbon sites. Sample B shows the larger increase in the size of the  $M + 1$ ; sample C, the larger increase in  $M + 2$ .

A second example illustrating the same point is seen in a comparison of the spectra of samples E and F with that of their natural abundance isomer, D. These are ions of higher  $m/z$  containing ten carbons, a nitrogen, and an oxygen. In sample E the  $^{13}\text{C}$  enrichment is concentrated at one site. In sample F it is evenly divided among the ten carbons.

TABLE III-1

RELATIVE EIMS ION INTENSITY VALUES FOR EIGHT MODEL ION CLUSTERS

Model	Isotopic Distribution	Spectrum	M+1/M
A	$^{12}\text{C}_3$	96.6	.035
		3.4	
		0.1	
B	$^{13}\text{C}^{12}\text{C}_2(8.4)$	89.5	.115
		10.3	
		0.2	
C	$^{13}\text{C}_3(3.53 \times 3)$	89.7	.111
		9.9	
		0.4	
D	$^{12}\text{C}_{10}$	88.7	.118
		10.4	
		0.7	
		0.1	
E	$^{13}\text{C}^{12}\text{C}_9(8.4)$	82.2	.199
		16.3	
		1.4	
		0.1	
F	$^{13}\text{C}_{10}(1.84 \times 10)$	82.4	.193
		15.9	
		1.6	
		0.1	
G	$^{13}\text{C}_3^{12}\text{C}_3(7.3 \times 3)$	77.0	.270
		20.8	
		2.1	
H	$^{13}\text{C}_4^{12}\text{C}_2(5.8 \times 4)$	77.0	.269
		20.7	
		2.2	
		0.1	

Although again the sample with one enriched site, E, does exhibit a larger increase in the  $M + 1$  and a smaller increase on  $M + 2$ , for these ions, this difference is much less marked than in the previous set of smaller ions. Thus, not only isotopic enrichment but also isotopic distribution and molecular size are important in predicting spectral changes.

Samples G and H are both six carbon ions containing a total of 4.2%  $^{13}\text{C}$  carbon. Sample G has the enrichment distributed among three carbons. Sample H has the enrichment distributed among four carbons. One must examine the ion abundance values to three significant figures in order to observe a difference between these two samples. In practice dynamic range of measurement may obscure such small variations in isotopic distribution.

In conclusion, mass spectrometric analysis of isotopically enriched samples is a multidimensional problem involving a complex interrelationship of variables. Four which affect the appearance of the ion cluster contour are (1) the degree of enrichment, (2) the distribution of that enrichment within the molecule, (3) the size of the molecule, and (4) the dynamic range of measurement.

The interrelationship of these variables has greatly complicated data reduction. In fact, the difficulties encountered have been so extreme that, in general, only the most simple cases have yielded satisfactory results. Current techniques have suggested use of extremely high  $^{13}\text{C}$  levels for simplification of the mass spectral data (52). Many applications of isotope enrichment may be visualized particularly for biochemical or medical problems in which such high enrichment is either impossible,

impractical, or unwise. It, therefore, seems desirable to examine the exact relationships of the various factors.

The relationship between any two of these four variables may be examined graphically with a simple two-dimensional plot and a third variable may be included with the use of multiple graphs drawn on a common scale. Figure III-4 through III-12 illustrate examples of such an approach. Yamamoto and McCloskey have included other examples in their investigation of isotopic distribution relationships (52).

2. Four variables important to the ion cluster contour

a. Total isotopic content

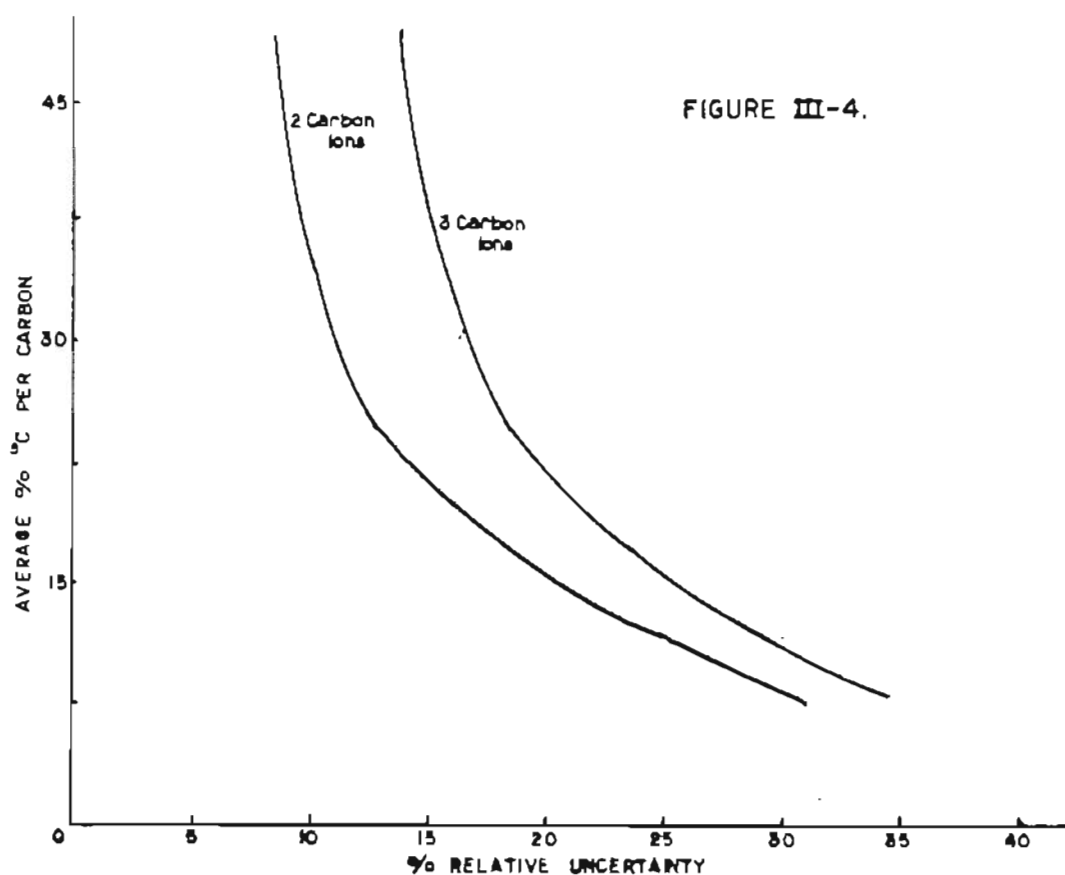
The total isotopic content may be defined in several ways. Most basically one might consider reducing the enriched molecule to simple one carbon units and measuring the ratio of  $^{12}\text{C}$  to  $^{13}\text{C}$  such as is done in the case of  $\text{CO}_2$  analysis with an isotope ratio mass spectrometer. This isotopic abundance measurement may be defined in units of total  $^{13}\text{C}$  content or of the average  $^{13}\text{C}$  per carbon.

Figure III-4 illustrates the relationship between the average %  $^{13}\text{C}$  per carbon and the relative uncertainty in the calculated value for isotopic abundance due to error limits defined in the data.<sup>15</sup> As

---

<sup>15</sup>The effect of experimentally induced uncertainty is to produce uncertainty in the result. Simple manual measurement of potentiometrically-recorded mass spectral ion intensity peak height resulting in an uncertainty of at least  $\pm 1$  unit was included in all model calculations described herein unless otherwise noted.

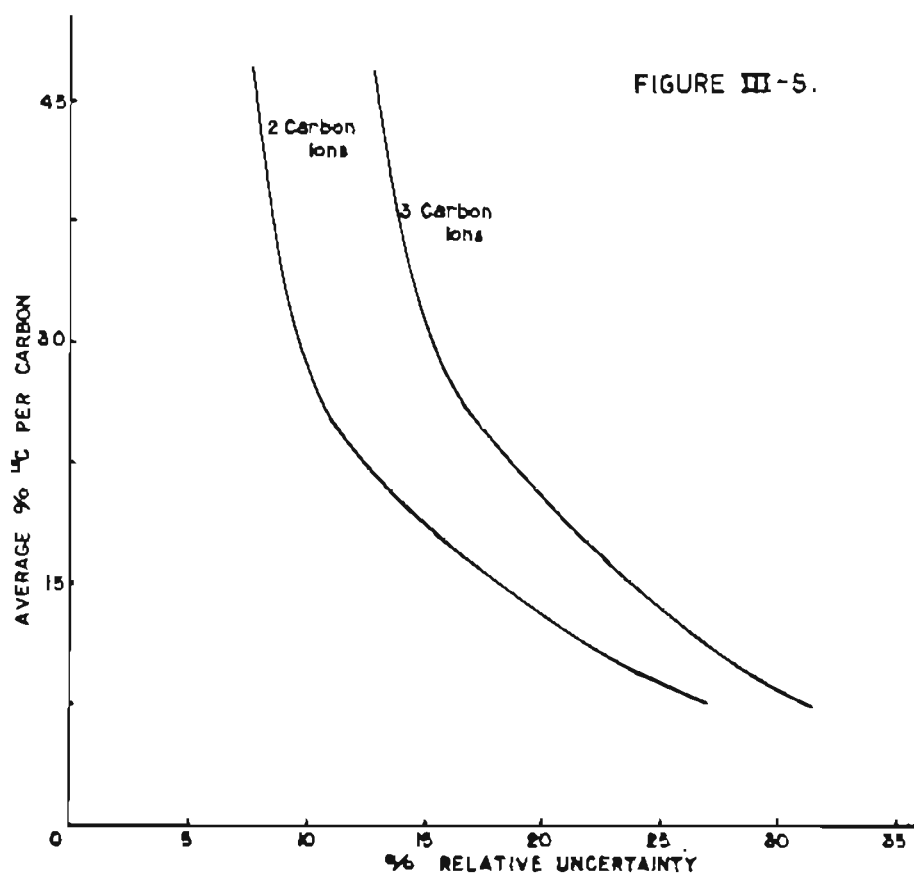
would be expected the greater the  $^{13}\text{C}$  abundance, the smaller the relative uncertainty no matter what the size of the molecule. Data for 2-carbon and 3-carbon molecules are plotted. Comparison of the two curves demonstrates the effect of molecular size: The larger the ion, the greater the uncertainty.



b. Distribution of enrichment

In the case of labeled molecules, however, this total isotopic abundance value is often of limited interest. It is the distribution of that abundance within the molecule that is of importance. Figure III-4

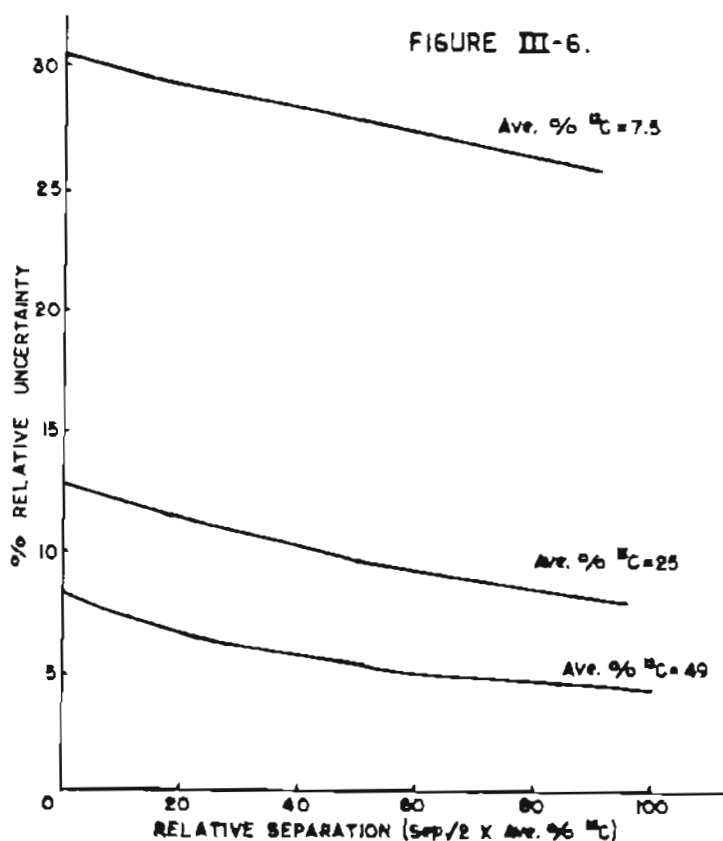
used data for 2- and 3-carbon molecules in which the  $^{13}\text{C}$  was evenly distributed. That is, each carbon actually had a  $^{13}\text{C}$  abundance equal to the average value. Figure III-5 illustrates a similar plot for molecules in which the  $^{13}\text{C}$  is unevenly distributed. In Figure III-5, data



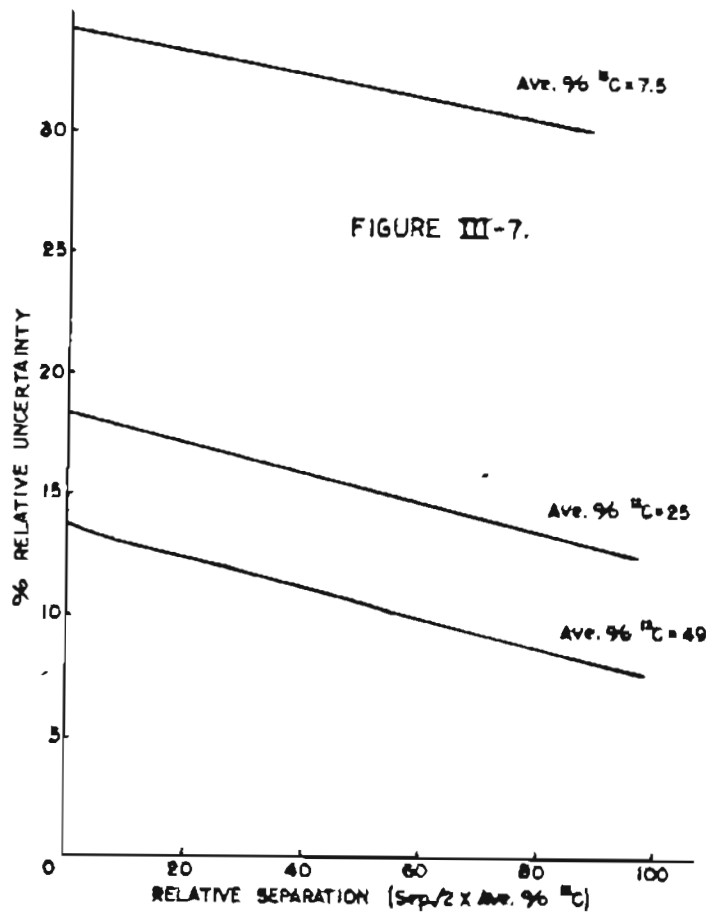
are plotted for molecules in which there is a difference of ten percentage points between the high and low  $^{13}\text{C}$  values. As an example, for a 2-carbon molecule with an average abundance of 7.5%/carbon, one carbon will actually contain only 2.5%  $^{13}\text{C}$  while the other contains 12.5%  $^{13}\text{C}$  [ $^{13}\text{C}_2(2.5, 12.5)$ ]. For a 3-carbon molecule with the same average enrichment (7.5%/carbon), one carbon would contain 2.5%  $^{13}\text{C}$ , another 7.5%

$^{13}\text{C}$ , and the third  $12.5\%^{13}\text{C}$  [ $^{13}\text{C}_3(2.5,7.5,12.5)$ ]. Superposition of Figures III-4 and III-5 would illustrate a shift to lower uncertainty for the molecules with non-identical carbon sites.

This effect of isotope distribution is more clearly demonstrated in Figure III-6. Here the effect of increasing relative separation in extreme values is plotted against the relative uncertainty in



the calculated isotopic abundance for various levels. All data are for two carbon molecules. Clearly the greater the separation the lower the uncertainty. Figure III-7 employs similar data for three carbon molecules. The parallel nature of the curves is apparent here where relative



separation values are used. This parallel character disappears when absolute separation values are plotted as in Figure III-8.

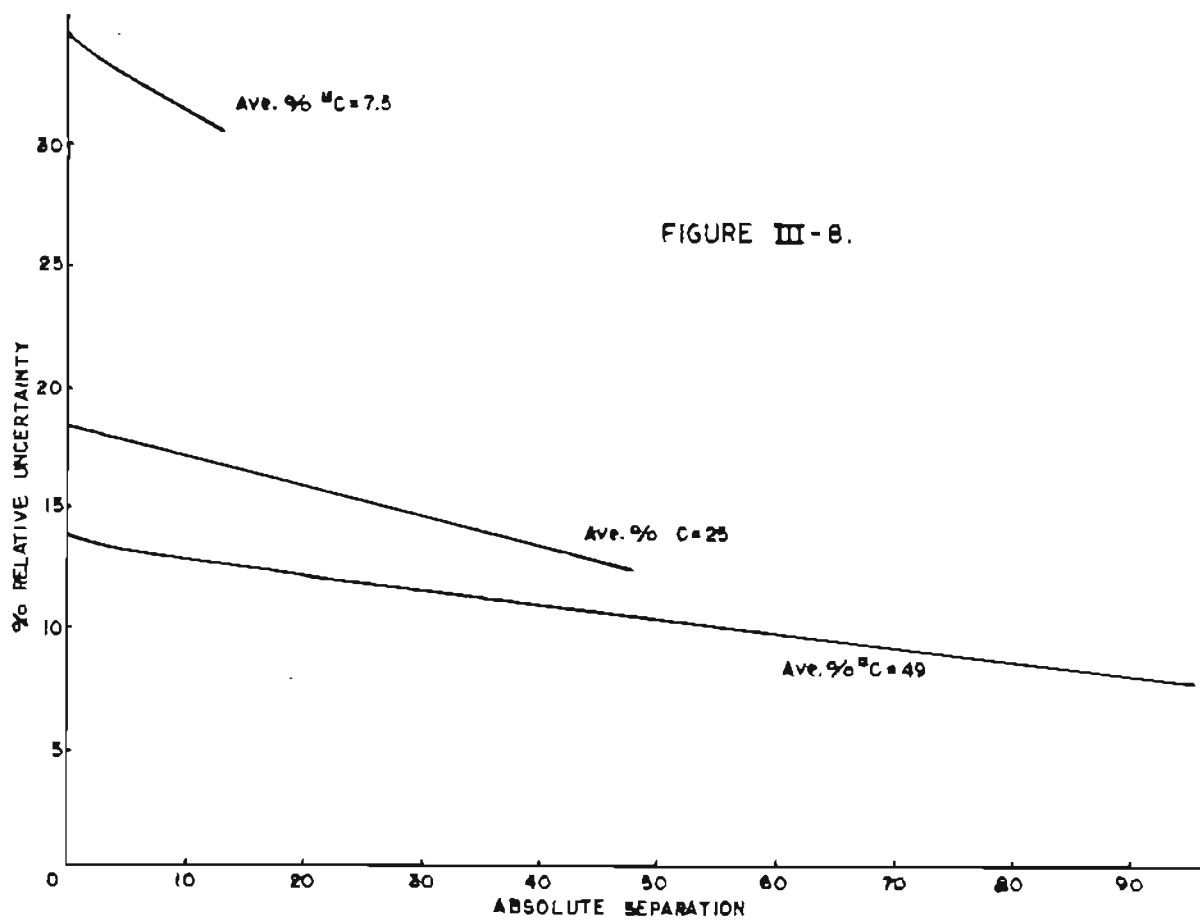
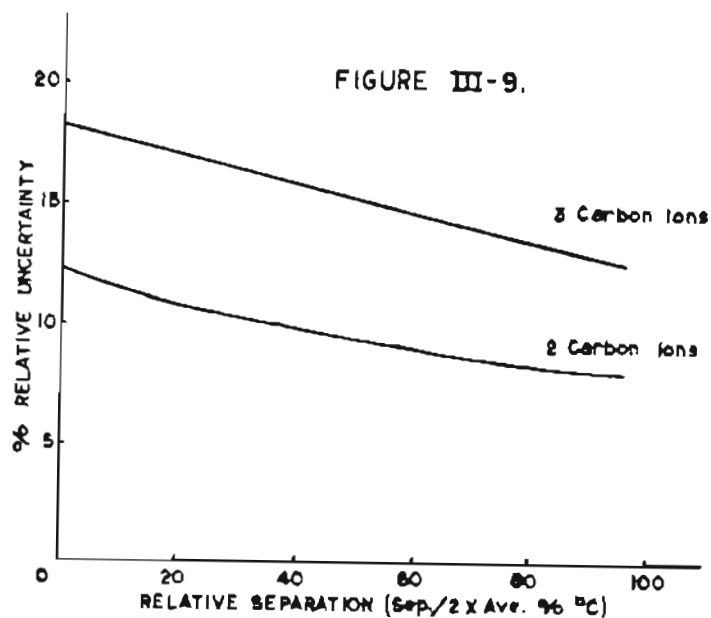
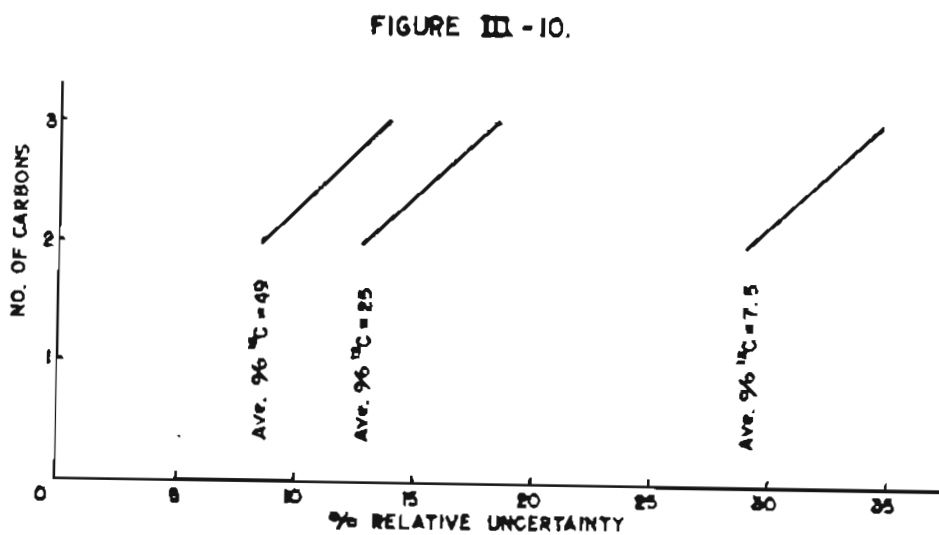


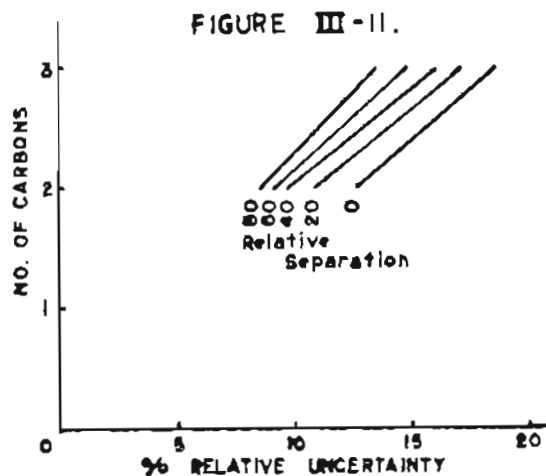
Figure III-9 summarizes data from Figures III-6 and III-7 for molecules with an average  $^{13}\text{C}$  content of 25%/carbon. The effect of molecular size is here apparent. Again, the larger the ion, the greater the uncertainty.



c. Molecular size

Figures III-10 and III-11 summarize the effect of the third variable molecular size on the degree of uncertainty. In general, as previously

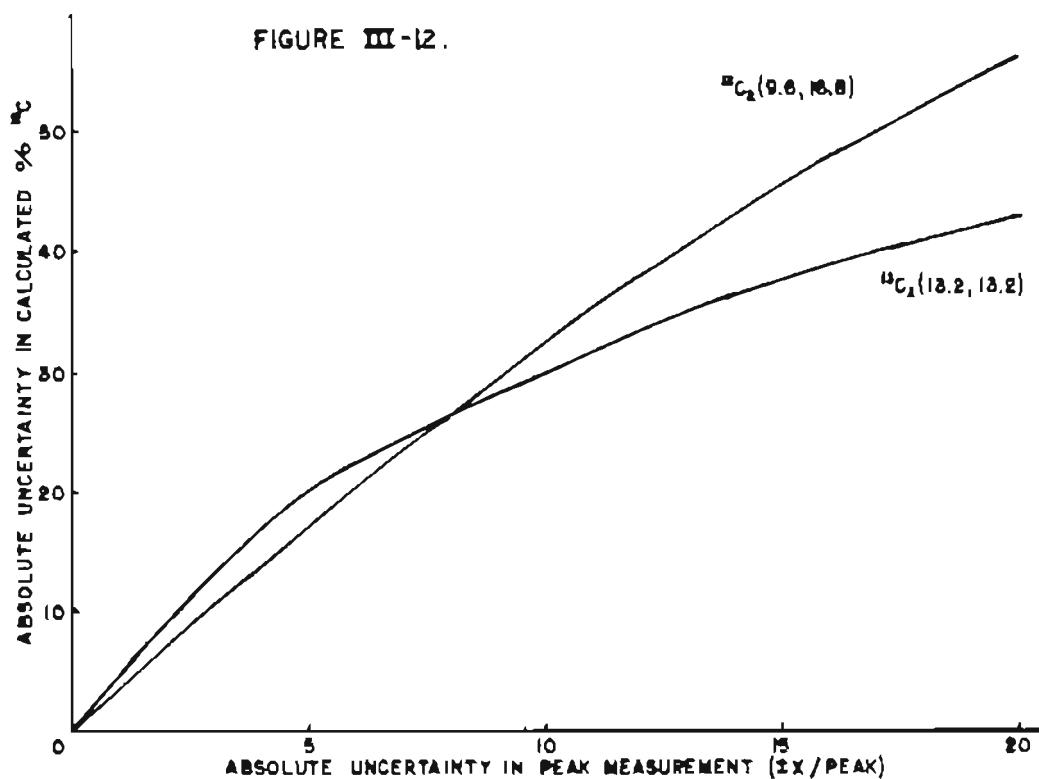




observed, the larger the molecule the greater the uncertainty. Figure III-10 illustrates data for various total isotopic abundance levels with even distribution and Figure III-11 illustrates data for various relative separation values at a constant value of 25%  $^{13}\text{C}$ /carbon.

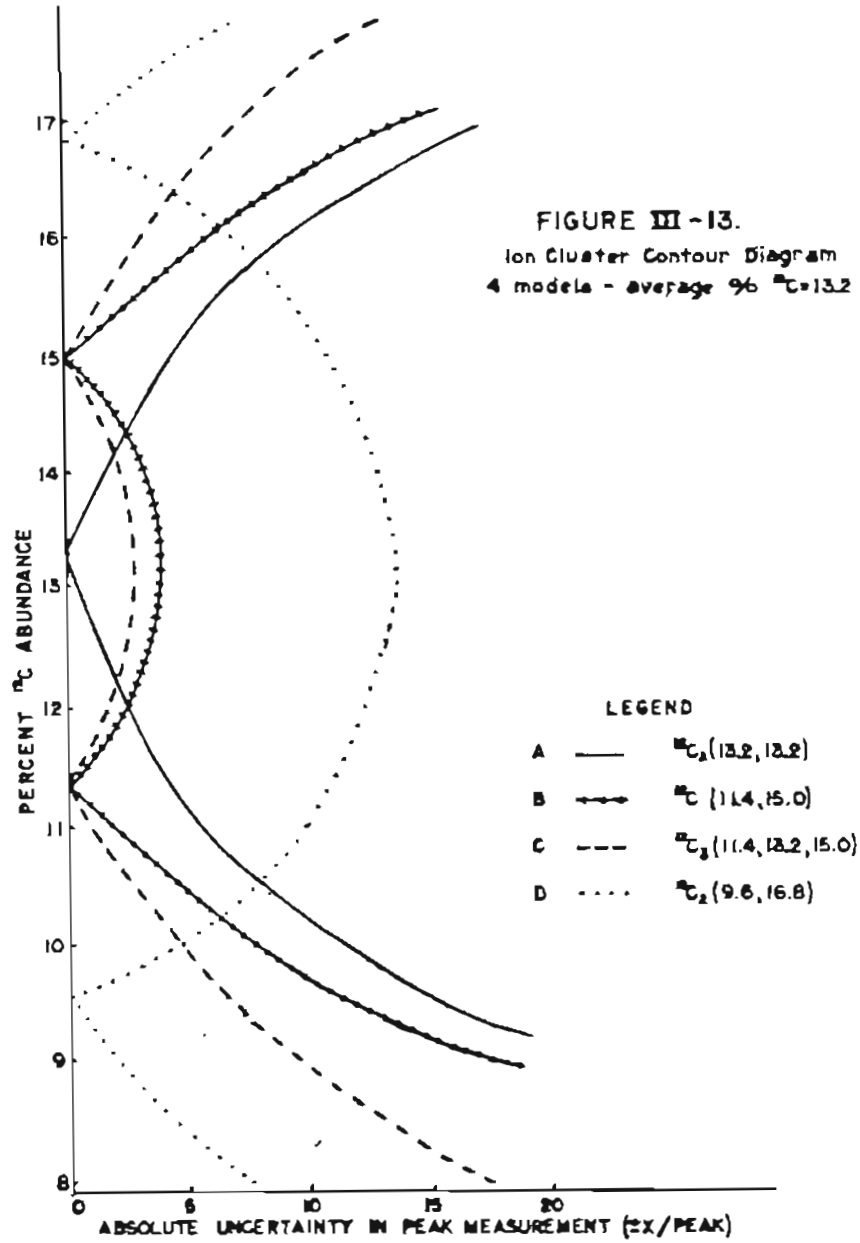
d. Dynamic range of measurement

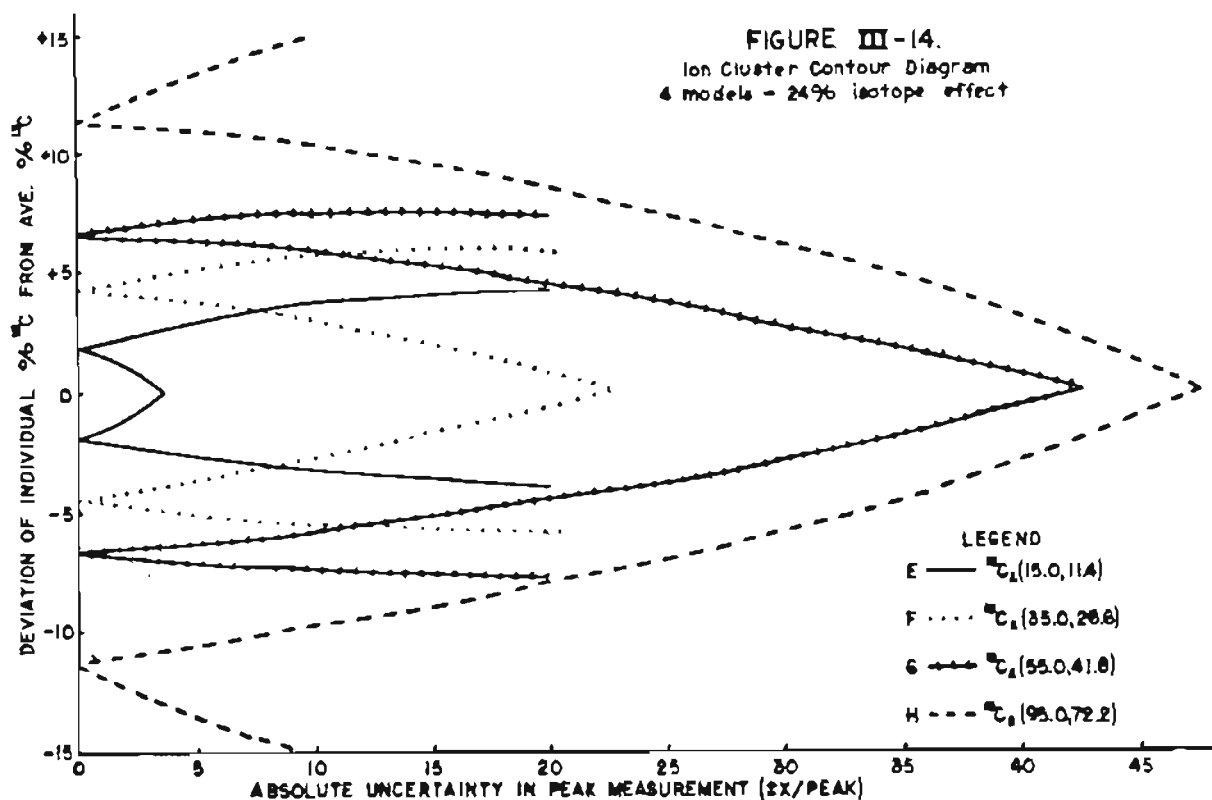
The effect of the fourth variable, dynamic range of measurement, is obvious - the larger the uncertainty in measurement of ion intensities, the poorer the result. Figure III-12 illustrates this effect for two different molecules both with an average  $^{13}\text{C}$  enrichment of 13.2%. (The intersection of the two curves results from the use of absolute rather than relative uncertainties in the mass spectrometric peak measurements.)



### 3. Experimental guidelines through Ion Cluster Contour Diagrams

A convenient method for summarizing these complex inter-relationships is via diagrams of the type illustrated in Figures III-13 and III-14. These "Ion Cluster Contour Diagrams" or "ICCDs" are extremely useful in experimental design and for evaluation of data interpretation. The most valuable feature of these ICCDs is their ability to display the relationship of these numerous variables within a single diagram.





An ICCD is a plot of the set of acceptable model solutions against given experimental uncertainty in mass spectral ion intensity measurements (a measure of dynamic range). Figure III-13 shows an ICCD for a set of models each with an average of 13.2% <sup>13</sup>C/carbon site. Figure III-14 is an ICCD for a set of models of varying total abundance levels but with a constant separation equal to 24% of the highest abundance value. The legend describes each individual model. To obtain such a diagram a mass spectrum is calculated for each model from statistical probability equations. These data are then assigned sample experimental error values dependent upon the dynamic range of measurement, the data returned and treated as the mass spectrum of an unknown sample, and the

set of acceptable solutions determined.

For example, the two carbon model with each carbon site enriched to 13.2%  $^{13}\text{C}$  gives a spectrum as follows:

$$M = 7534$$

$$M + 1 = 2292$$

$$M + 2 = 174$$

If this spectrum is introduced without any uncertainty in these ion intensity values, the only correct solution will be a molecule as described, two carbon sites each containing 13.2%  $^{13}\text{C}$ . However, if the spectrum is introduced with an uncertainty of  $\pm 5$  units/ion intensity any two carbon model whose values lie within the appropriate section of the ellipse, A, on Figure III-13, will fit as long as the two carbons average the 13.2% each.

The previously observed generalizations are all visible on these two ICCD, Figures III-13,14: (1) Higher total isotopic abundance produces results with less uncertainty, (Compare E, F, G and H); (2) greater difference in abundance values between individual carbon sites also results in less uncertainty, (Compare B and D); (3) increase in molecular size at constant average abundance results in greater uncertainty, (Compare B and C); (4) increased experimental error yields increased uncertainty in results.

Once constructed, the ICCD may be used in reverse to answer questions of experimental design regarding preferred or necessary values for these variables. For example, the dynamic range of measurement necessary to view a particular separation of extreme abundance values may easily be ascertained. [See Parts IV E2, V B 2d (1), V C 2e (1), and V C 2f (1).]

The mathematically constructed ICCD is thus seen as a valuable aid to experimental design since the influence of the four most important variables may be visually evaluated. The ICCD is also an aid to evaluation of results since it identifies sets of possible solutions.

D. Two illustrations of the use of the polynomial data reduction techniques

1. One parameter approach

The one parameter approach finds its basic utility in experimental design. It provides an easily understood method for study of individual parameters controlling the mass spectral pattern and, thus, through construction of ICCDs, ascertaining those experimental conditions which make possible optimum utilization of isotopic mass spectral data. However, it may also be profitably used for isotopic analysis in some situations.

As an example of the use of this approach, a model mass spectrum was constructed for a  $C_3$  molecule with each carbon enriched at a different level,  $^{13}C_3(15.0, 14.1, 11.4)$  (See Table III-2). The data for this model were then treated as experimental data with uncertainties  $\pm 1$  unit/peak measurement. An attempt was made to determine the individual isotopic abundance values.

In Table III-2, models 1-3 indicate an average  $^{13}C$  abundance equal to 13.5% since models 1 and 3 give no fit and model 2 yields a low cumulative error ( $\pm .0039$ ). Models 4-9 are attempts to specify the particular value for the carbon site with lowest abundance. The  $b_x$  values

TABLE III-2  
EIMS ISOTOPIC ANALYSIS OF A MODEL SYSTEM

$^{13}\text{C}_3(15.0,14.1,11.4)^a$   
Isotopic Generating Function<sup>b</sup> -  $(a_x+b_x)^m(a_1+b_1)^{m_{a_1}}(a_2+b_2)^{m_{a_2}}$

Model No.	$m_{a_1}$	$b_1$	$m_{a_2}$	$b_2$	$m$	$b_x$	Error <sup>c</sup>
1	2	1.11			1	d	
2	0	-			3	13.5	.0039
3	1	1.11			2	d	
4	1	12.5			2	d	
5	1	11.5			2	14.5	-.0078
6	1	10.5			2	d	
7	1	11.4			2	14.55	-.0156
8	1	11.6			2	14.45	+.0059
9	1	11.55			2	14.47	+.0039
10	1	11.52			2	14.49	.0000
11	1	11.3			2	14.60	.0000
12	1	11.2			2	14.65	.0059
13	1	11.0			2	14.74	.0059
14	1	10.9			2	d	
15	1	12.0			2	d	
16	1	11.8			2	14.35	.0000
17	1	11.9			2	d	
18	1	14.0			2	d	
19	1	14.5			2	d	
20	1	15.0			2	d	
21	1	13.5	1	10.9	1	d	
22	1	13.5	1	11.0	1	d	
23	2	13.5			1	d	
24	1	11.4	1	15.0	1	14.10	.0100

<sup>a</sup>Model mass spectral intensity data: 646.0, 303.6, 47.1, 2.4

<sup>b</sup>Binomial expression the expansion of which gives the mass spectrum of each model

Symbols:  $a_x$  =  $^{12}\text{C}$  abundance being calculated

$b_x$  =  $^{13}\text{C}$  abundance being calculated

$a_i$  = assumed  $^{12}\text{C}$  abundance

$b_i$  = assumed  $^{13}\text{C}$  abundance

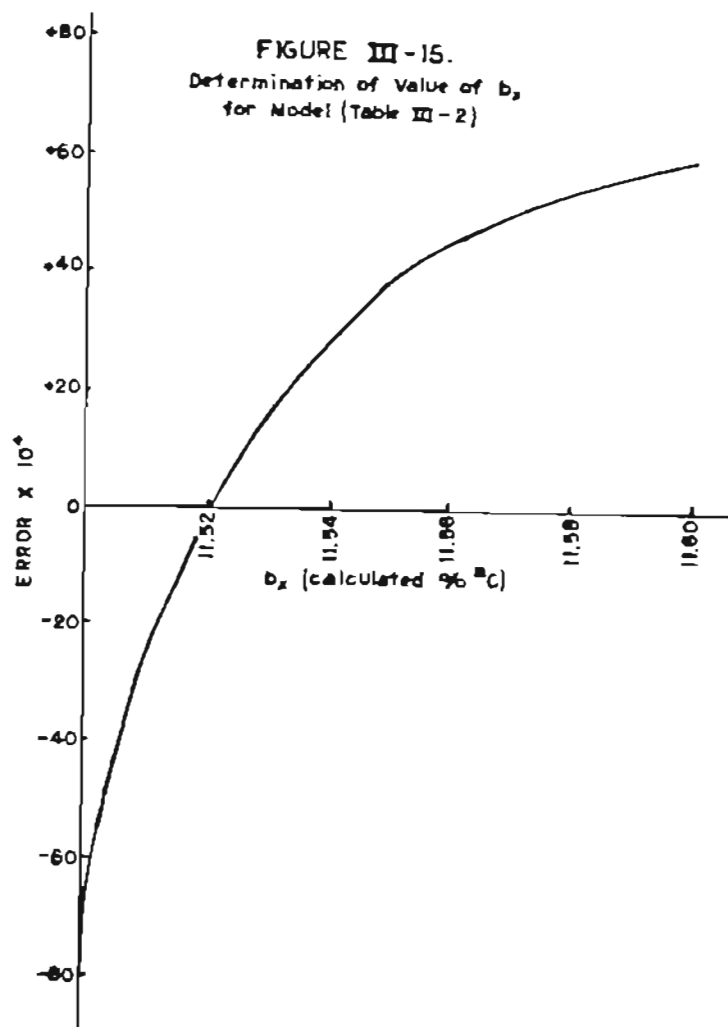
$m$  = number of carbons for which isotopic abundance is to be calculated

$m_{a_i}$  = number of carbons of assumed isotopic abundance

<sup>c</sup>Cumulative error resulting from subtraction of the spectrum calculated for model (1-24) from that given in note a above

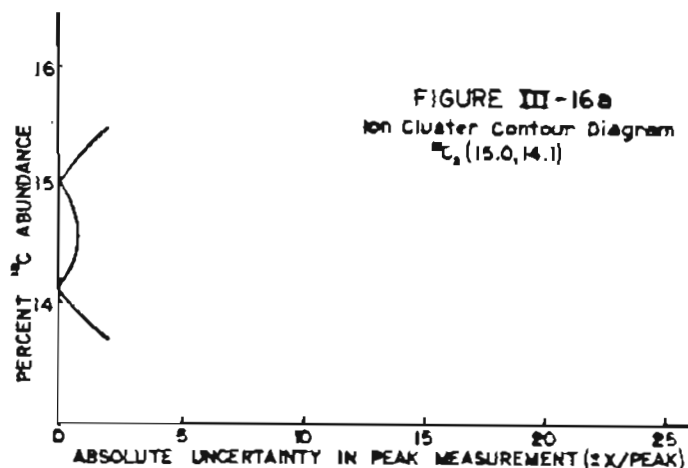
<sup>d</sup>No fit possible

obtained in these determinations are plotted against the errors (E) in Figure III-15. The value  $b_x = 11.52$  occurs at the intersection on the  $b_x$



axis. This value is then reintroduced as model 10 giving a fit with  $E = .0000$ . The assumption that carbons 1 and 2 are equally enriched introduces the error observed. Models 11-14 establish a minimum value for this particular carbon of 11.0%  $^{13}\text{C}$ . Models 15-17 establish a maximum of 11.8%  $^{13}\text{C}$ . The carbon site with the lowest enrichment level then contains  $11.5 + .3$  or  $-.5\%$   $^{13}\text{C}$  which compares well with the actual

value of 11.4%  $^{13}\text{C}$ . The error margin is introduced by the assigned experimental error of  $\pm 1$  unit and the skew is the result of the assumption that the other two carbons are equally enriched. Models 18-24 illustrate the indistinguishability of carbon 2 and 3 (15.0 and 14.1%  $^{13}\text{C}$ ) as clearly indicated by the appropriate ICCD (See Figure III-16a. Values 15.0



and 14.1 are there indistinguishable at an uncertainty of  $\pm 1$  unit/peak measurement.)

A second example is illustrated in Table III-3 for  $^{13}\text{C}$  (15.0, 12.3, 11.4). Model 1 establishes the average value of 12.9%  $^{13}\text{C}$ . Models 2 and 3 illustrate that one value is above the average and two are below. Models 4-8 establish that high value to be  $15.0 \pm .2\%$   $^{13}\text{C}$ . Again, from the ICCD (Figure III-16b), carbons 2 and 3 (12.3 and 11.4%  $^{13}\text{C}$ ) are indistinguishable at given error levels.

TABLE III-3  
 EIMS ISOTOPIC ANALYSIS OF A MODEL SYSTEM  
 $^{13}\text{C}_3$  (15.0, 12.3, 11.4)<sup>a</sup>  
 Isotopic Generating Function<sup>b</sup> -  $(a_x + b_x)^m (a + b)^{m_a}$

Model No.	$m_a$	b	m	$b_x$	Error <sup>c</sup>
1	0	--	3	12.9	.01
2	1	11.4	2	11.85	.97
3	1	14.5	2	13.66	.65
4	1	14.6	2	d	
5	1	14.6	2	d	
6	1	14.8	2	11.95	.90
7	1	15.2	2	11.75	.81
8	1	15.3	2	d	

<sup>a</sup>Model mass spectral intensity data: 660.5, 294.2, 43.3, 2.1

<sup>b</sup>Binomial expression the expansion of which gives the mass spectrum of each model

Symbols:  $a_x$  =  $^{12}\text{C}$  abundance being calculated

$b_x$  =  $^{13}\text{C}$  abundance being calculated

a = assumed  $^{12}\text{C}$  abundance

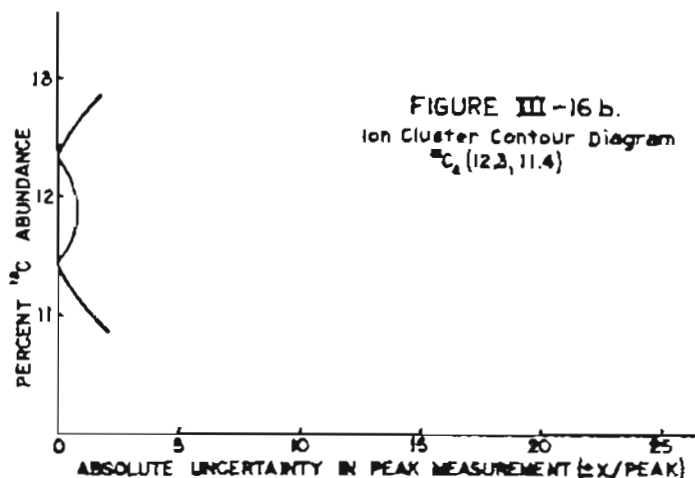
b = assumed  $^{13}\text{C}$  abundance

m = number of carbons for which isotopic abundance is being calculated

$m_a$  = number of carbons of assumed isotopic abundance

<sup>c</sup>Cumulative error resulting from subtraction of spectrum calculated for model (1-8) from that given in note a above

<sup>d</sup>No fit possible



Thus, the one parameter approach is an aid to study of individual parameters which affect the accuracy of results obtained from isotopic mass spectra. Through the construction of ICCDs, this approach serves as a valuable aid to experimental design. As illustrated in the above examples, the use of the ICCD allows recognition of the complete set of possible answers to which a particular result may belong.

## 2. Factor approach

The factor approach holds promise as an easily applied, general approach for detailed isotopic analysis from mass spectral data. It has the advantage that it assumes little about the isotopic content of the sample and makes maximum use of the polynomial character of the isotopic generating functions for the mass spectral ion intensities. It also is readily adaptable to graphic display of results. The program applied herein utilizes this graphic display.

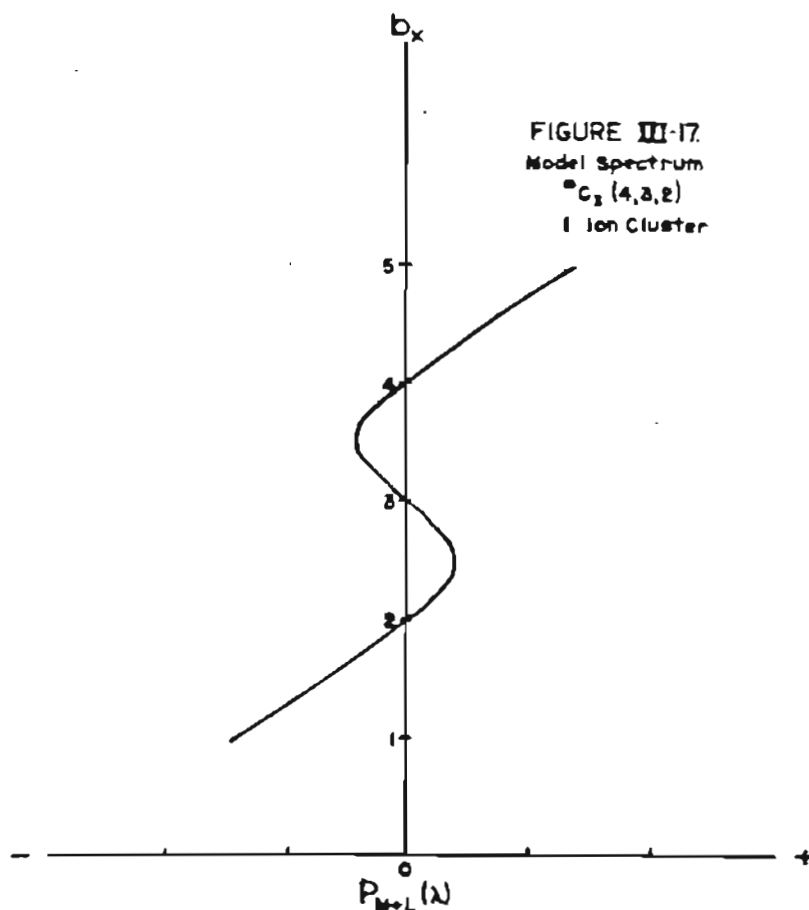
The key concept of this approach is that the roots of the polynomials which describe the observed spectral intensities and their derivatives are analytically related to the isotopic content and distribution of the ions which give rise to those intensities. (See Part II C 4.)

For this reason factors of the polynomial may be extracted by observation of the residual ion intensity at a particular  $m/z$ .

As a simple illustration of the application of this factor approach, consider a  $^{13}\text{C}_3(2,3,4)$  model system. A model spectrum may be constructed involving only a single ion cluster. The roots 2, 3, and 4 factors of the polynomial which results from the expansion of

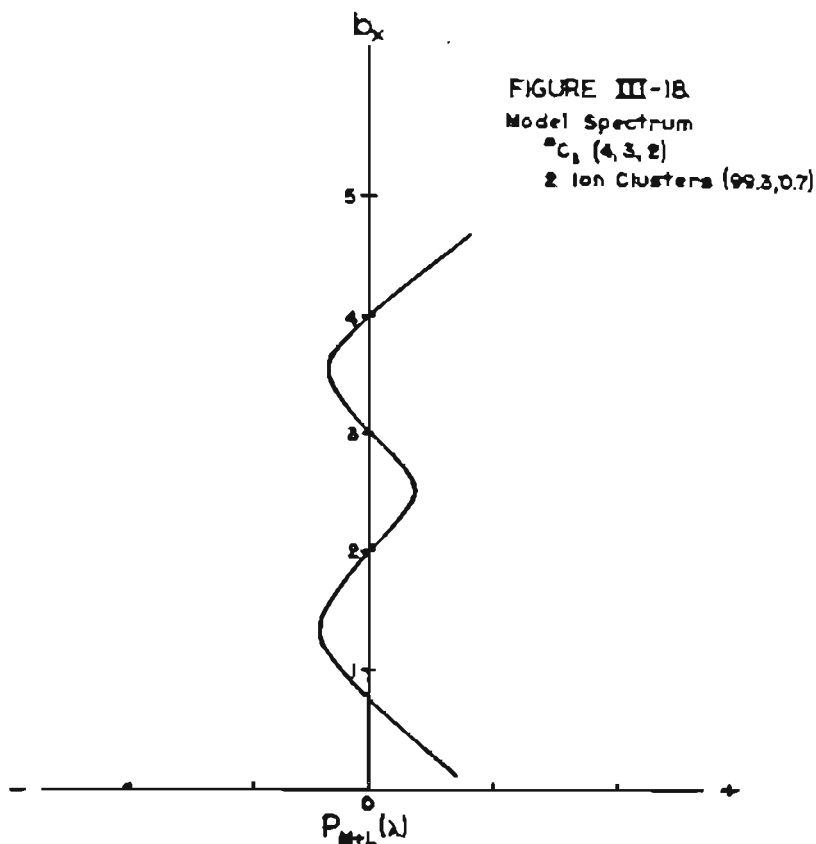
$$(a_1 + b_1)(a_2 + b_2)(a_3 + b_3)$$

may then be extracted by observation of the change in the fourth ion intensity as shown in the graphic display in Figure III-17, the intersections occurring at the roots. (Note that four observed intensities



result in three ratios. In other words, three observables are necessary to determine three unknowns.)

A second model spectrum may be constructed containing two overlapping ion clusters of identical isotopic composition but originating at  $m/z$  differing by one unit. If the intensity of this additional ion cluster is constructed to comprise 0.7% of the region intensity, analysis with the factor approach will yield four roots - 2, 3, 4 and 0.7 - by observation of the residual at the fifth ion intensity. (See Figure III-18.) This is to be expected since the polynomial describing this

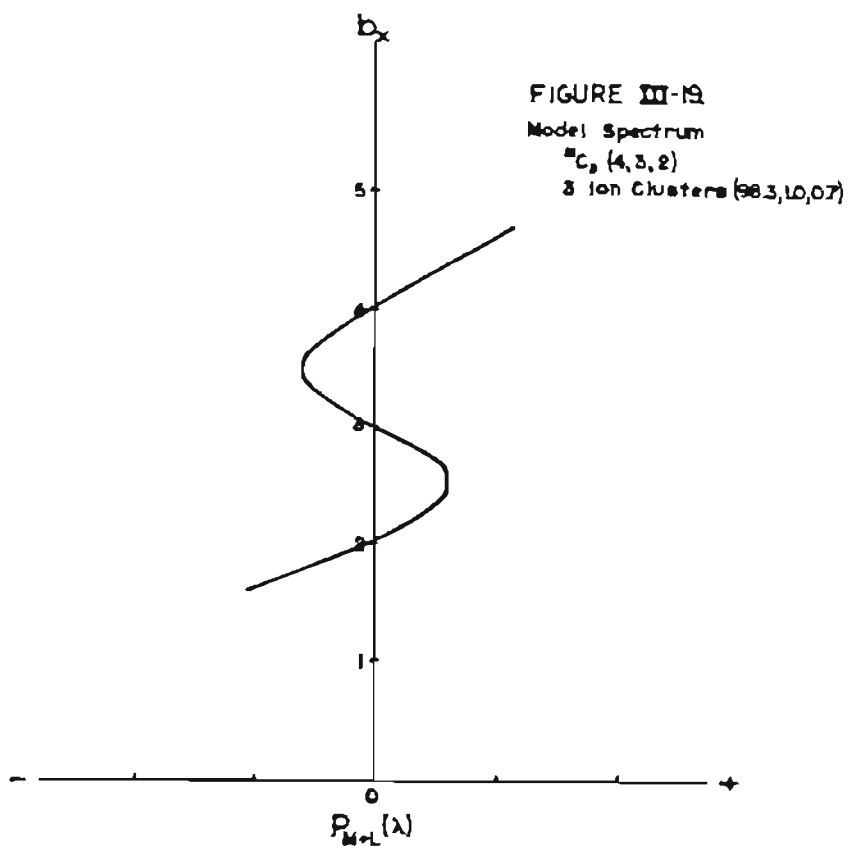


complex region results from the expansion

$$(a_1 + b_1)(a_2 + b_2)(a_3 + b_3)(I_M + I_{M+1})$$

where  $I_{M+j}$  represents the portion of the region intensity due to the cluster originating at  $m/z M+j$ .

Inclusion of a third ion cluster originating at  $m/z M+2$  introduces a quadratic factor,  $(I_M + I_{M+1} + I_{M+2})$  into the polynomial and observation of the sixth ion intensity residual yields only the common linear factors of each ion cluster resulting from the isotopic concentrations - 2, 3, and 4. (See Figure III-19.)



Experimental data obtained from complex molecules most commonly contain numerous overlapping ion clusters of identical isotopic composition which result from addition or subtraction of H from the ion of

primary interest. In the past this complex nature of experimental mass spectral data has been very detrimental to data reduction attempts (40, 128). Various techniques have been employed, often unsuccessfully, to eliminate this complexity (40). However, the factor approach has thus been shown to take maximum advantage of this experimental idiosyncrasy by readily extracting only the linear factors most often resulting from the isotopic composition alone.

The full potential of this factor approach has yet to be determined. Current investigation involves use of the derivatives of the primary polynomial for extraction of the quadratic factors and for extraction of  $n$  linear roots where  $n + 1$  ion intensities are not visible.

Utilization of the polynomial nature of the generating functions of isotopic ion intensities is thus demonstrated through model spectra analysis to provide a new and general approach to mass spectral isotopic analysis. The computer programs developed in Appendix A have provided a simple and useful format to accomplish the necessary data reduction.

PART IV  
APPLICATION OF THE POLYNOMIAL DATA REDUCTION  
TECHNIQUE TO DATA PREVIOUSLY ANALYZED BY OTHER METHODS

A. Introduction

1. A rationale for this investigation

The polynomial data reduction technique developed herein and described in Part II offers distinct advantages over more traditional techniques. One way of illustrating these advantages is through comparison with another specifically described and applied methodology. For this reason, an example was sought in the literature to which the polynomial approach might be applied. The greatest strength of the polynomial approach lies in its ability to analyze data obtained from molecules with multiple sites of isotopic enrichment. Unfortunately examples of such multiple enrichment are rare in the literature. (See Part I.) However, one good example of such a situation is the work published in 1970 by W. J. A. Vandenheuvél and J. S. Cohen in which isotopic mass spectral analysis was approached using amino acids biosynthetically produced by growth in a 15%  $^{13}\text{C}_2$  environment (130,131).

2. Scope of this investigation

Vandenheuvél and Cohen developed a simply applied data reduction technique useful for their particular situation. They applied it in a well designed investigation of biological isotope effects. Three areas of discussion will be developed for comparison of their technique with the polynomial data reduction approach developed herein: First, the

Vandenheuvel and Cohen method will be compared to other available methodology. Second, application of their technique to situations other than those of their particular investigation will be discussed. And third, results obtainable by the polynomial data reduction technique will be illustrated. The first two of these discussions will be designed to give a measure of the accuracy to be expected using the equations derived by Vandenheuvel and Cohen. The third will demonstrate the improved accuracy to be expected from the polynomial approach.

B. The data reduction technique of Vandenheuvel and Cohen

1. Derivation of data reduction equation

Vandenheuvel and Cohen intend to demonstrate the presence of a biological isotope effect in the production of a group of amino acids by certain algae. To do this they suggest obtaining the average  $^{13}\text{C}$  content of various amino acid fragments. Inasmuch as larger fragments can be shown to contain a relatively lower average  $^{13}\text{C}$  content than smaller fragments, the preference of the algae biosynthetic system for  $^{12}\text{C}$  is demonstrated.

A simple equation is derived for determination of the  $^{13}\text{C}$  content based on the ratio of the M+1/M ion intensity ratio where M represents the  $^{12}\text{C}_x$  isomer and M+1, its  $^{13}\text{C}^{12}\text{C}_{x-1}$  analog:

$$C = \frac{100 r_{c_0}^2}{r_{c_0} + m} \quad (\text{IV-1})$$

Here C is the  $^{13}\text{C}$  content expressed as "excess atom percent", i.e. C plus the natural abundance of  $^{13}\text{C}$  (1.11) equals the total  $^{13}\text{C}$  content.

The natural abundance of  $^{12}\text{C}$  is  $c_o$ , the number of carbons is  $m$ , and  $r$  is equal to  $\Delta I/100$  where  $\Delta I$  is the difference between the  $M+1$  ion intensities from the spectra of the natural abundance and enriched samples, both  $M$  intensities being normalized to 100.

A derivation of this equation reveals the assumptions inherent therein:

The value for the ratio  $M+1/M$  may be obtained from statistical considerations by summing the ratios  $b_i/a_i$  for the individual carbons of the ion where  $a$  equals the  $^{12}\text{C}$  content and  $b$ , the  $^{13}\text{C}$  content and  $a + b = 1$ . That is

$$\frac{M+1}{M} = \sum_{i=1}^m \frac{b_i}{a_i} \quad (\text{IV-2})$$

(See Part III-B-2).

In terms defined by Vandenhoevel and Cohen,  $c_o$  equals the natural abundance of  $^{12}\text{C}$  or  $a$  for the unenriched species and  $C$  equals the  $^{13}\text{C}$  enrichment. Therefore, for the natural abundance compound,

$$\frac{M+1}{M} = m \frac{1-c_o}{c_o} \quad (\text{IV-3})$$

and for the enriched species,

$$\frac{M+1_e}{M_e} = \sum_{i=1}^m \frac{C+1-c_o}{c_o-C} \quad (\text{IV-4})$$

When the  $M$  intensities for both species are set equal to each other,  $\Delta I$  may be calculated by a direct subtraction of these ratios and so, when

$$M = M_e = 100 \quad (\text{IV-5})$$

then

$$r = \frac{1}{100} \left[ \sum_{i=1}^m \frac{C+1-c_o}{c_o-C} - m \left( \frac{1-c_o}{c_o} \right) \right] \quad (\text{IV-6})$$

Assuming all carbons in a given ion to be equally enriched

$$r = \frac{m}{100} \left( \frac{C+1-c_o}{c_o-C} - \frac{1-c_o}{c_o} \right) \quad (\text{IV-7})$$

Making the necessary algebraic manipulations results in the simplification

$$r = \frac{mC}{100(c_o^2 - cC_o)} \quad (\text{IV-8})$$

Solving for C

$$C = \frac{100 rc_o^2}{rc_o + m} \quad (\text{IV-9})$$

the equation employed in the amino acid investigation.

## 2. Discussion of assumptions and limitations

As clearly illustrated above, the derivation of equation (IV-9) rests on the assumption that all carbon sites contain equal amounts of  $^{13}\text{C}$ . On the other hand, the proof of the hypothesis, that a biological isotope effect is operative, clearly requires that the opposite is true, that each additional carbon added by the algae in production of the amino acid have a lower  $^{13}\text{C}$  abundance. It is, therefore, apparent at the outset that error has been introduced and that the accuracy of quantitative measurements of that isotope effect will be impaired. The more the individual  $^{13}\text{C}$  abundance values differ from one another, the greater will be the error introduced by equation (IV-9). The amino acids analyzed by Vandenhuevel and Cohen are expected from experimental design to contain  $^{13}\text{C}$  abundances of about 15%. At such low enrichment levels the absolute variation in  $\%^{13}\text{C}$  values is not expected to be great. Therefore, errors

introduced by equation (IV-9) will be small. This technique then will yield a close approximation of the average  $^{13}\text{C}$  content of each clearly observable ion in the amino acid spectra and differences in these averages will demonstrate the presence of an isotope effect.

### C. Use of other current methodology

#### 1. Overview

Use of equation (IV-9) provides a technique for isotopic mass spectral data reduction which may be generally applied for all of the amino acids in the series regardless of molecular size and regardless of fragmentations observed. This generality is of importance since results obtained from numerous ions are to be compared. However, more exact isotopic abundance values may be obtained for a certain few select carbon sites by simple arithmetic subtraction of the  $M+1/M$  values.

#### 2. Derivation of exact analytical expressions

As previously derived (Part III-B-2) expressions for  $M+1/M$  values may be obtained from statistical considerations. These ion intensity ratios will be simple functions of the  $^{13}\text{C}/^{12}\text{C}$  abundance ratios. For the most general case, where each carbon site abundance value is considered separately, the correct expression is given in equation (IV-2) above. To repeat:

$$\frac{M+1}{M} = \sum_{i=1}^m \frac{b_i}{a_i}$$

It is therefore obvious that for two ions which differ only by one carbon as may be the case in parent and daughter of a particular fragmentation, the  $^{13}\text{C}$  abundance for that one carbon may be determined by simple

subtraction of the two  $M+1/M$  ratios. For example, equation (IV-2) for a three carbon ion becomes

$$\left(\frac{M+1}{M}\right)_P = \frac{b_1}{a_1} + \frac{b_2}{a_2} + \frac{b_3}{a_3} \quad (\text{IV-10})$$

and for its two carbon daughter, A, from which carbon 3 has been lost

$$\left(\frac{M+1}{M}\right)_{D_A} = \frac{b_1}{a_1} + \frac{b_2}{a_2} \quad (\text{IV-11})$$

Therefore

$$\frac{b_3}{a_3} = \left(\frac{M+1}{M}\right)_P - \left(\frac{M+1}{M}\right)_{D_A} \quad (\text{IV-12})$$

If a second daughter, B, is observed from which carbon 1 is missing then

$$\left(\frac{M+1}{M}\right)_{D_B} = \frac{b_2}{a_2} + \frac{b_3}{a_3} \quad (\text{IV-13})$$

and subtracting equation (IV-13) from (IV-10)

$$\frac{b_1}{a_1} = \left(\frac{M+1}{M}\right)_P - \left(\frac{M+1}{M}\right)_{D_B} \quad (\text{IV-14})$$

Substitution of values obtained from equations (IV-12) and (IV-14) into equation (IV-10) will yield a value of  $b_2/a_2$ .

### 3. Application to amino acid analysis

Within the framework of the amino acid investigation, the above approach might have been used to obtain exact values for serine since both appropriate daughter ions were observed for this three carbon

amino acid.<sup>16</sup> (See Figure IV-1)

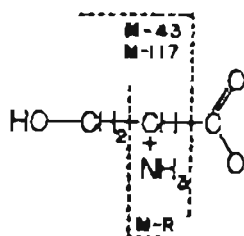


FIGURE IV-1  
Serine Fragmentation

TABLE IV-1  
RESULTS OF EIMS ISOTOPIC ANALYSIS OF VARIOUS  
AMINO ACID FRAGMENT IONS<sup>a</sup>

Number of amino acid C atoms	Total <sup>13</sup> C (%)	Number of values used
1,2	14.2 ± 0.4	13
3,4	13.7 ± 0.4	12
5,6	13.3 ± 0.4	15
8,9	12.6 ± 0.2	6

<sup>a</sup>W.J.A. Vandenhoevel and J. S. Cohen, *Biochim. Biophys. Acta*, 208, 231 (1970).

<sup>16</sup>Table IV-1, taken directly from the literature, shows the decrease in the calculated average <sup>13</sup>C abundance value with the increase in the number of carbons per ion (130). Values have been listed with ion sizes grouped by twos. That is, one and two carbon units are averaged, three and four carbon units, etc. Thus grouped a smooth curve of average <sup>13</sup>C content vs. ion size is obtained. However, were each ion size to be plotted separately a plateau would be observed. This plateau results because the fragmentation pattern is neglected and, in the case of serine, both two carbon daughter ions are included. Inclusion of the M-R ion composed of carbons one and two is clearly not justified considering the hypothesis. Its removal removes the plateau.

This approach may also be used to obtain individual values for the carbons of glycine, a two carbon amino acid. Alanine, another three carbon amino acid, unfortunately does not exhibit both necessary daughter ions. In cases where some but not all of the necessary fragmentations are observed, exact values may still be obtained for those isolated carbon sites and average values be calculated similarly for the rest. Table IV-2 presents values obtained in this manner for glycine, serine, tyrosine and phenylalanine and compares the averages thus obtained with values obtained from equation (IV-9). An interesting alternating pattern in the magnitude of the  $^{13}\text{C}$  abundance values begins to be visible. Such a trend would bear further investigation for its obvious implications to biosynthetic mechanism.

TABLE IV-2  
Values for  $^{13}\text{C}$  Abundance Obtained from Subtraction  
of M+1/M Ratios

	Glycine	Serine	Tyrosine	Phenylalanine	
Carbon No. 1	12.3	11.4	11.7	<sup>a</sup> 12.2	<sup>b</sup> 15.3
2	15.0	14.5	15.5	15.0	11.9
3		11.4	10.7 <sup>c</sup>	11.2 <sup>c</sup>	11.2 <sup>c</sup>
Average	13.7	12.7	11.3	11.7	11.7
Ave. from M+1/M	14.5	13.1	12.4	12.7	12.7

<sup>a</sup>Values obtained using M-43 ion intensities.

<sup>b</sup>Values obtained using M-117 ion intensities.

<sup>c</sup>Values reflect an estimate of average  $^{13}\text{C}$  abundance for all 7 remaining carbons.

D. Application of the method of Vandenhoevel and Cohen to model data

1. Overview

As previously discussed, errors introduced by application of equation (IV-9) will be greater as the differences in individual carbon  $^{13}\text{C}$  abundance values become greater. When these differences are introduced by an isotope effect such as is apparent in the amino acid production, the absolute difference in the individual values will become greater as the magnitude of the  $^{13}\text{C}$  abundance increases. For example, a 24% isotope effect at the 15%  $^{13}\text{C}$  level will result in formation of a two carbon unit,  $^{13}\text{C}$  (15.0, 11.4), whereas at the 95%  $^{13}\text{C}$  level the two carbon unit produced would be  $^{13}\text{C}$  (95.0, 72.2).

Inasmuch as higher  $^{13}\text{C}$  enrichment levels are now possible and popular, it is interesting to construct model compounds at these levels and investigate the utility of equation (IV-9) in these circumstances (126,148). Unfortunately, the errors inherent become clearly unacceptable.<sup>17</sup>

2. Variables for consideration

At least three variables should be considered in judging the acceptability of equation (IV-9) for application in similar experiments under other experimental conditions. They are (1) the isotopic enrich-

---

<sup>17</sup>Part III-B-2c discussed spectral changes with regard to very highly enriched compounds. It is not unexpected that data reduction methods based on M+1/M ratios are not satisfactory when a majority of carbon atoms are  $^{13}\text{C}$ . Part III-C-2 described four variables which influence the ion cluster contour. The change in the M+1/M is not linear with respect to these variables; therefore M+1/M is by itself insufficient for total analysis.

ment level, (2) the magnitude of the isotope effect, and (3) the size of the molecule. The effect of these three variables is illustrated in Figures IV-2,3 and 4.

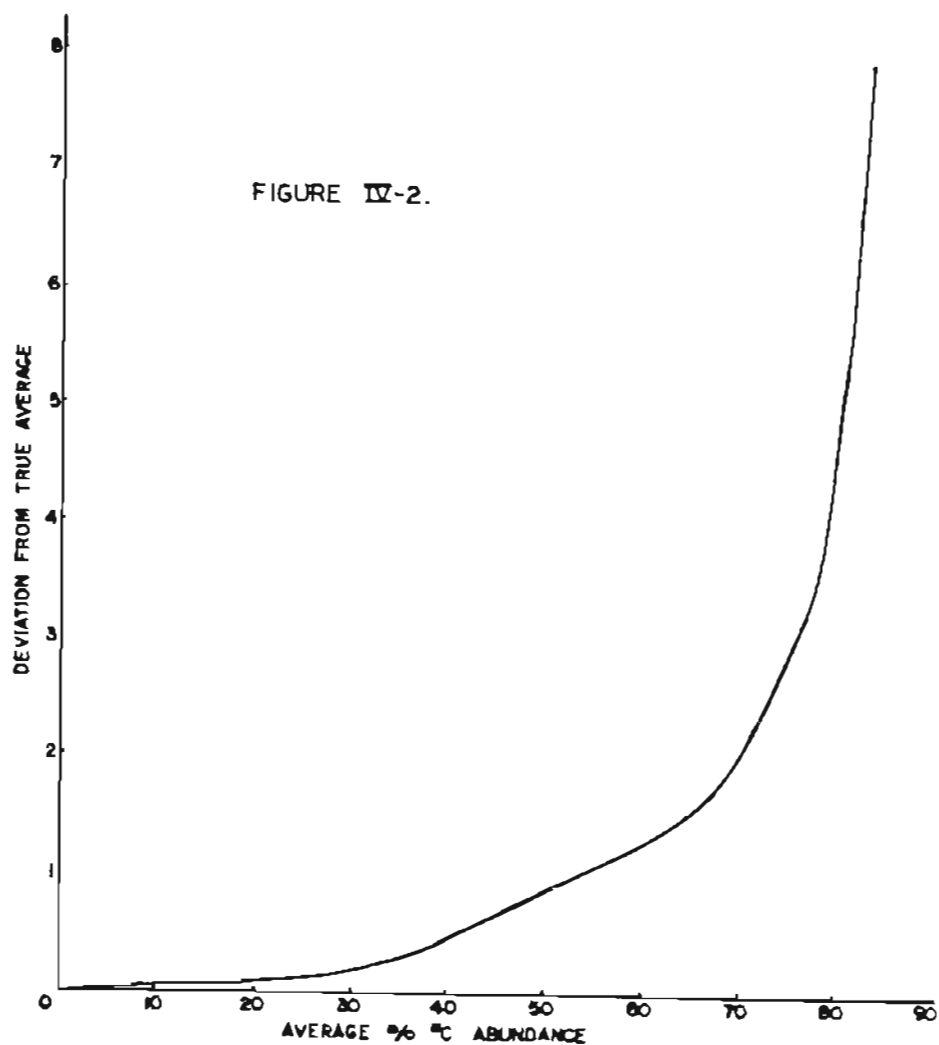


Figure IV-2 plots the difference between the true average  $^{13}\text{C}$  content and that obtained from equation (IV-9), hereafter called the deviation, versus increasing average  $^{13}\text{C}$  abundance. All data is for  $\text{C}_2$  ions with a 24% isotope effect. A rapid rise in the curve is observed, particularly at high enrichment levels.

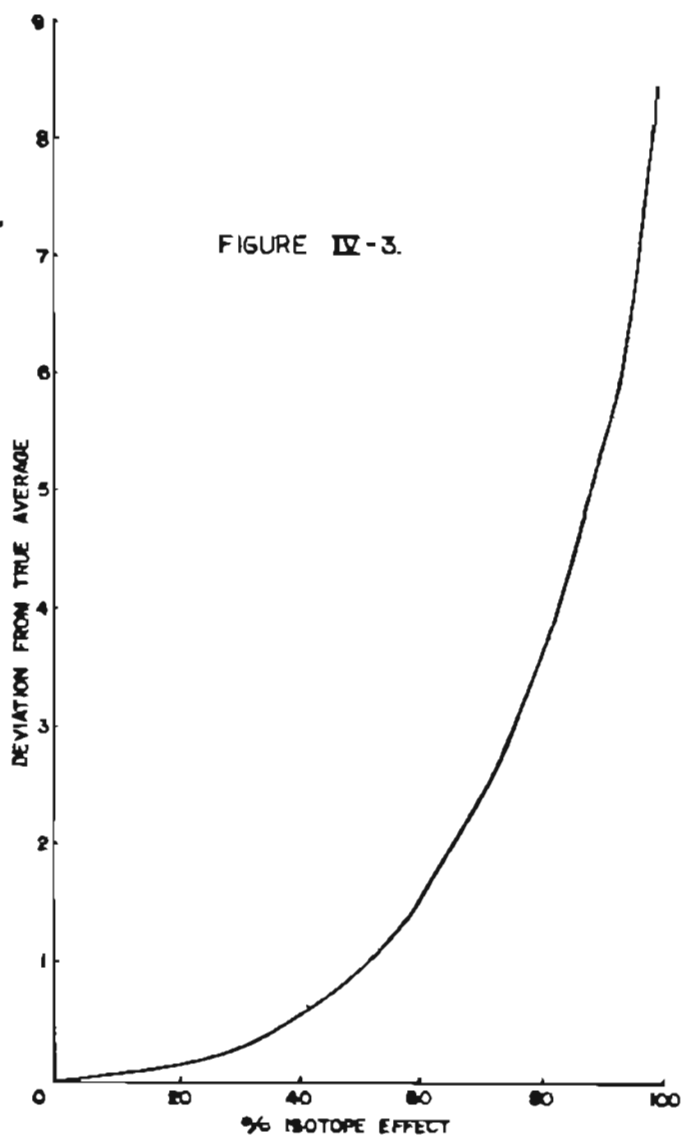
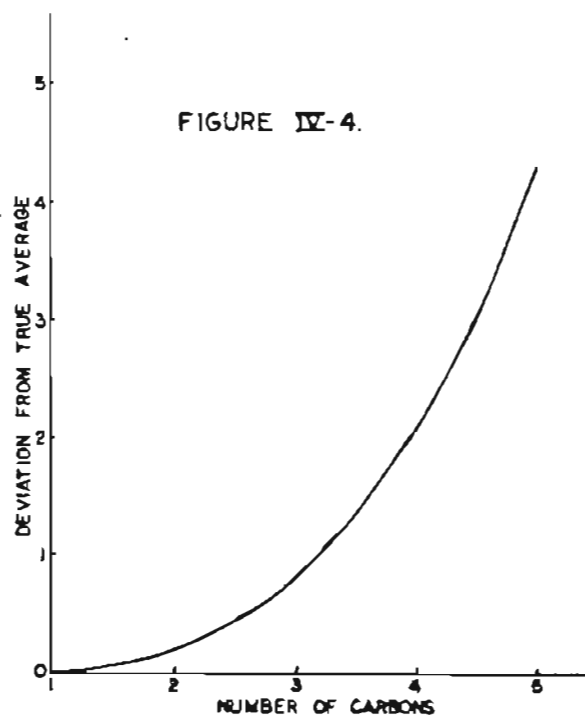


Figure IV-3 illustrates the relationship between the same deviation and the magnitude of the isotope effect. Data is for  $C_2$  ions now at a constant average  $^{13}C$  abundance of 25%. Here a rapid rise in the curve occurs particularly with higher isotope effects.

Figure IV-4 pictures the effect on this deviation on increasing carbon number at a constant average  $^{13}C$  content of 25%. Each ion



is constructed so that individual  $^{13}\text{C}$  abundance values differ from each other by 24% of the highest value. Equation (IV-9) is least applicable to larger ions.

### 3. Conclusion

Clearly application of equation (IV-9) requires carefully selected experimental conditions such as those under which the isotope effect operative in the amino acid biosynthesis was determined. At an average  $^{13}\text{C}$  abundance of less than 15% with an isotope effect in the range of 24%, errors incurred with use of equation (IV-9) will be small.

The trend exhibited in Figure IV-3 warrants special consideration in light of the approach taken in the amino acid analysis. It would appear that deviations of the true average from the value obtained using equation (IV-9) would be greater for the larger ions analyzed. Deviations

will all be in a positive direction producing high results. Inasmuch as larger amino acid ions were shown to have lower "average"  $^{13}\text{C}$  contents, the quantitative measure of the isotope effect might be expected to be smaller than reality. Results of calculations previously presented in Table IV-2 seem to support this expectation. Vandenneuvel and Cohen observed a maximum isotope effect of 19% whereas the limited calculations presented in Table IV-2 exhibit a maximum isotope effect of 24%.

E. Application of the polynomial approach to observation of biological isotope effects.

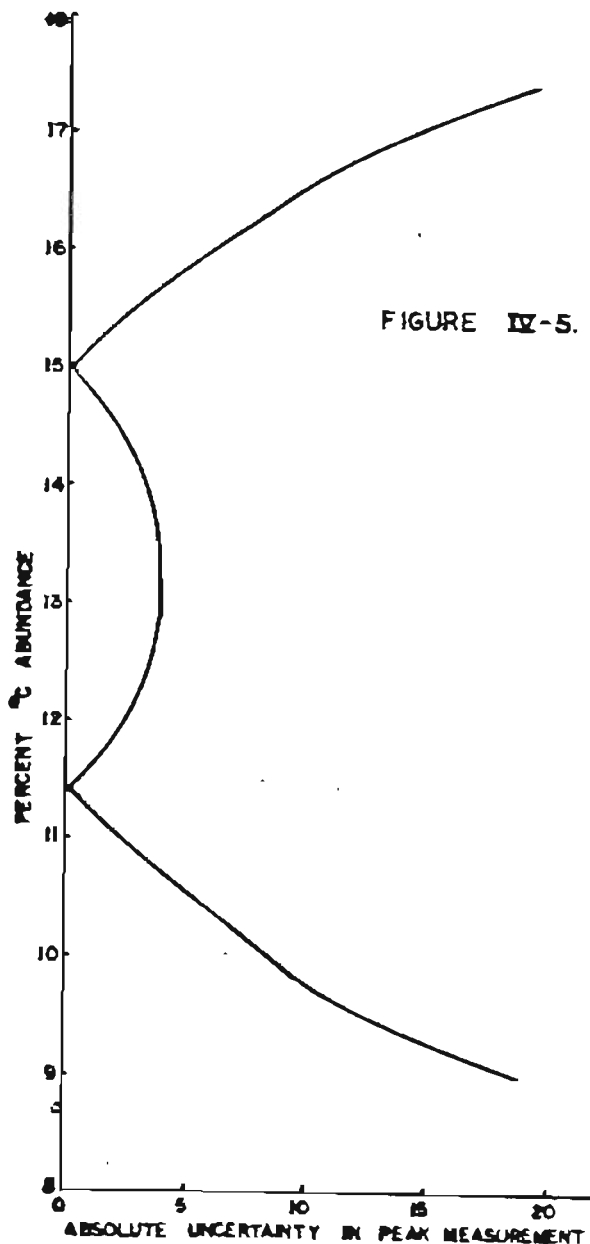
1. Overview

The approach to reduction of isotopic mass spectral data developed in Part II is based on the polynomial character of the equations describing the relative ion intensities in an ion region. When individual isotopic abundance values are sufficiently different from one another, this analytical technique is capable of identifying accurate abundance values for each carbon site. It therefore appears to be an appropriate data reduction method for determination of isotope effects operative on biosynthetic processes such as the amino acid series described above.

2. ICCD evaluation

The utility of the ICCD is described in Part IIIC. Figure IV-5 illustrates the appropriate ICCD for sample  $^{13}\text{C}$  abundance values obtained by calculations described in Part IV-C-3 and tabulated in Table IV-2. The example illustrated,  $\text{C}_2(15.0, 11.4)$ , exhibits a 24% isotope effect. With uncertainties not greater than  $\pm 3$  units per ion intensity measure-

ment these  $^{13}\text{C}$  abundance values will be clearly differentiated by the polynomial data reduction technique. This degree of accuracy is commonly obtained with measuring techniques employed in this investigation (See Appendix B2a).



### 3. Advantages of the polynomial approach

#### a. Individual $^{13}\text{C}$ abundance values

Determination of the average  $^{13}\text{C}$  abundance values for sets of ions of varying size will give evidence of a biological isotope effect. However, this isotope effect might also be observed by observation of the actual individual  $^{13}\text{C}$  abundance values. Determination of these values in the case of the amino acids should be possible using the polynomial data reduction approach. In addition to the expected progressive variation produced by the algae preference for  $^{12}\text{C}$ , any other variations produced by biosynthetic pathways more complex than simple linear addition of one carbon units would be visible. (An example of such variation may be seen in Part V-B-2d.)

#### b. Treatment of overlapping ion clusters

A common complication in treatment of isotopic mass spectra is the presence of overlapping ion clusters within a single region (See Part II-B-3). The processes producing these overlapping clusters are not always controllable or reproducible. Therefore, comparison of enriched with natural abundance samples such as is done in the amino acid analysis does not always eliminate their effect.

Such a complexity may be responsible for the discrepancy illustrated in Figure IV-6. In this figure the average percent  $^{13}\text{C}$  abundance obtained using equation (IV-9) is plotted versus the number of carbons per ion. The slope indicates the isotope effect. Most points lie cleanly on the linear curve; however, for eight carbon ions three points are indicated. The central point indicating the value quoted

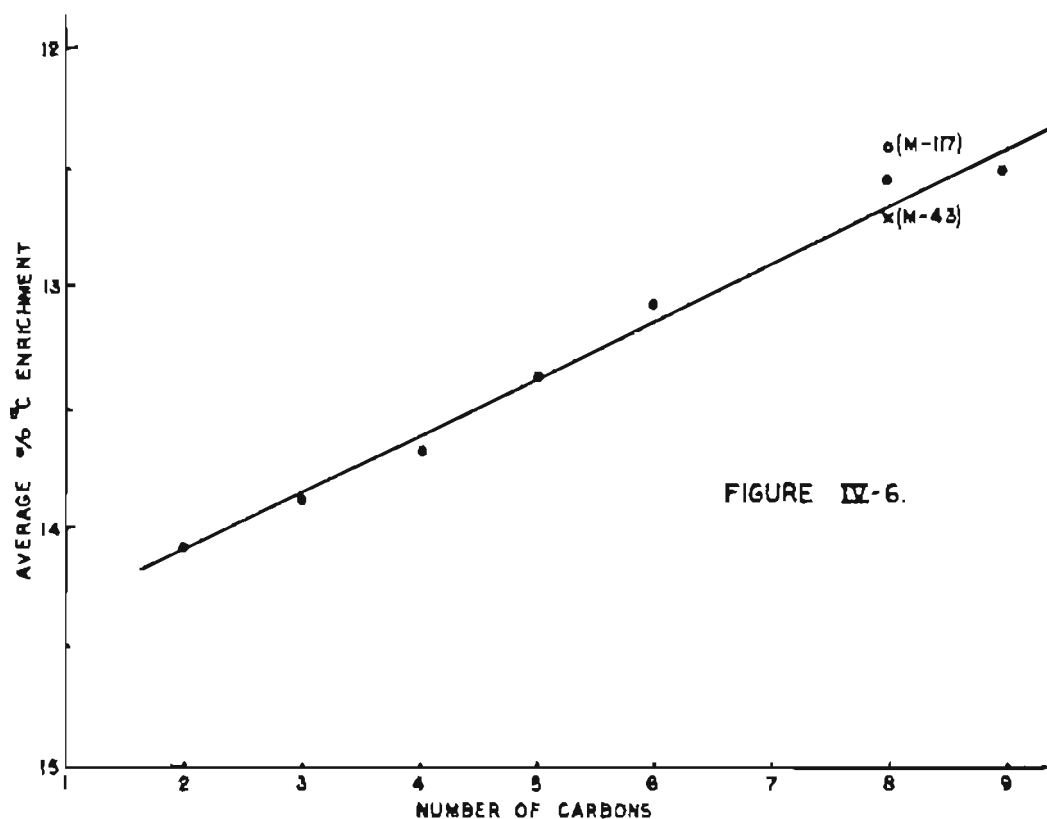


FIGURE IV-6.

by Vandenhoevel and Cohen is actually the average of values obtained from two different sets of ions containing eight amino acid carbons, one deriving from the molecular ion minus 43 mass units, methyl plus CO, the other from the molecular ion minus 117 mass units, carbtrimethylsilyloxy.<sup>18</sup> The value obtained from the M-117 ions is clearly in error.

The polynomial data reduction approach is capable of including cases of overlapping ion clusters (See Part II-C-3). If this particular complexity is the cause of the error in the M-117  $^{13}\text{C}$  abundance values

<sup>18</sup>Trimethylsilyl derivatives were used.

obtained, the polynomial approach would be expected to produce more accurate results.

#### F. Conclusion

Use of the polynomial data reduction technique for mass spectral isotopic analysis is therefore expected to have several advantages over the technique employed by Vandenneuvel and Cohen in this amino acid analysis (130,131). It is capable of obtaining more accurate results. Under favorable circumstances it produces isotopic enrichment values for individual sites rather than averages. It is more generally applicable being useful for ions of all sizes and at either high or low enrichment levels. It is capable of avoiding error by treating cases of overlapping ion clusters.

Therefore, when computer aid is available, mass spectral isotopic analysis is clearly advanced by application of the polynomial data reduction techniques developed herein.

PART V  
APPLICATION OF THE POLYNOMIAL DATA REDUCTION  
TECHNIQUE TO EXPERIMENTALLY OBTAINED DATA

A. Introduction

As a final test of the utility of this statistically-based approach to reduction of isotopic mass spectral data, biosynthetically  $^{13}\text{C}$  enriched samples were analyzed and the results obtained compared with those produced by independent proton and  $^{13}\text{C}$  nuclear magnetic resonance. Values obtained by mass spectrometry were found to be comparable to those produced by the other techniques and to have a greater degree of precision. This analytical approach employing the statistically-based data reduction method was also shown to produce useful results where the mass spectral fragmentation pathway was not clearly defined.

B. Fusaric Acid - a biosynthetic product.

1. Introduction

The biosynthesis of fusaric acid (Figure V-1), a metabolite of



FIGURE V-1 Fusaric Acid

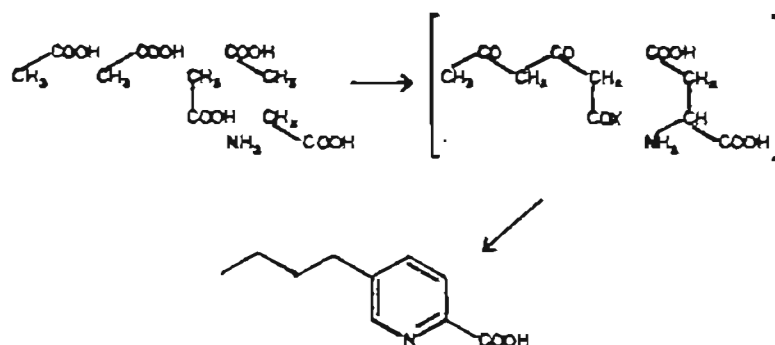
Fusarium oxysporum Schlecht has previously been studied using both  $^{14}\text{C}$  and  $^{13}\text{C}$  as tracer elements. The radiotracer experiments with  $^{14}\text{C}$  proceeded in the usual way with (a) administration of the labeled substrate to the organism, (b) isolation of the metabolite, fusaric acid, and (c)

determination of the distribution of the radioactivity through a series of chemical degradations (149,150). The numerous chemical manipulations necessary to accomplish analysis of a  $^{14}\text{C}$ -labeled metabolite allow location of labeled sites but often preclude quantitative determination of the degree of enrichment (117,151). Such quantitative determinations may be of value in ascertaining the origin of various sections of the sample molecule. The numerous chemical reactions, in themselves, are time-consuming (151).

Enrichment levels and labeling patterns of metabolites produced with  $^{13}\text{C}$ -labels may be determined by nuclear magnetic resonance spectrometry (NMR). The magnetic resonance of the  $^{13}\text{C}$  nuclei may be observed directly ( $^{13}\text{CMR}$ ) or the "satellite" signals produced by the spin-spin coupling of the  $^{13}\text{C}$  nuclei and protons directly bonded to them may be observed in a proton magnetic resonance spectrum ( $^1\text{HMR}$ ). In contrast to the laborious chemical manipulations of a  $^{14}\text{C}$  analysis, the  $^1\text{HMR}$  analysis of the  $^{13}\text{C}$  labeled fusaric acid required only one chemical reaction, the conversion to the derivative alcohol to allow determination of the  $^{13}\text{C}$  content of the C(7) carbon (3). Three other positions C(2), C(5), and C(9) were invisible without further chemical conversion; however, these measurements did not prove vital to proof of the biosynthetic hypothesis.

Also, in contrast to the  $^{14}\text{C}$  work, the  $^1\text{HMR}$  analysis provided information regarding the degree of enrichment at particular sites which was useful to the proof of the biosynthetic hypothesis. The C(4) position of fusaric acid produced when acetate- $1\text{-}^{13}\text{C}$  was administered as a

precursor was shown to contain about 4%  $^{13}\text{C}$ , while C(6), C(8), and C(10) enrichments were approximately 9%  $^{13}\text{C}$  (3). This difference in enrichment levels is evidence of a difference in biosynthetic origin, thus supporting the hypothesis shown in Figure V-2 in which carbons 5,6,8,9,10 and 11 are derived from the head to tail addition of acetate and the others are derived indirectly from acetate via an aspartate intermediate.



Can. J. Biochem. 46, 1293, (1968).

FIGURE V-2.

Biosynthetic Hypothesis for Fusic Acid

Mass spectrometry provides a third method of analysis for labeled metabolites. Normally radioactive enrichment is not obtained at levels sufficient for easy mass spectral analysis; however, in some cases, such analysis can be accomplished (132). Compounds labeled with stable isotopes may often be rapidly and efficiently analyzed with the aid of a mass spectrometer. A series of degradation reactions may be produced by electron impact and the concentration of the heavy isotope determined through measurement of the relative abundance of the various fragment ions sorted by the mass to charge ratio.

As described in Part I, previous  $^{13}\text{C}$  mass spectral analyses have largely involved compounds enriched at a single site. Since

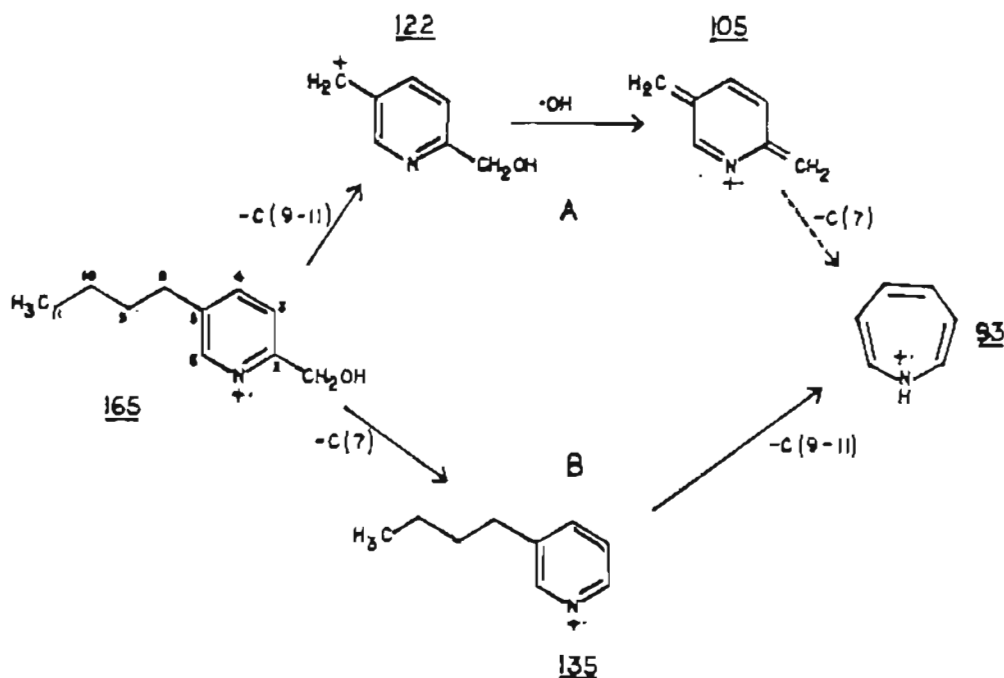
biosynthesis commonly produces metabolites with multiple sites of carbon enrichment, mass spectral analysis has found limited application in the field (See Part I-2-c). The statistical approach to data reduction employed here has particular application to cases of multiple enrichment and, therefore, to problems in biosynthesis. Fusaric acid provided an excellent test case because it had previously been studied by other analytical techniques and because the fragmentation pattern of the fusaryl alcohol derivative available was rather straightforward (149-151).

## 2. Results and discussion

### a. Mass spectral fragmentation pattern

Fusaryl alcohol is composed of a pyridine ring with two substituents: (1)  $-\text{CH}_2\text{OH}$  and (2)  $n\text{-C}_4\text{H}_9$  (Figure V-1). The primary pathways for fragmentation involve loss of 1, 2, or 3 carbon units from the hydrocarbon side chain and loss of  $-\text{OH}$  or  $\text{CO}$  from the other substituent. Figure V-3 illustrates hypothetical structures for the molecular ion and the four most abundant fragment ions. The ion of  $m/z$  136 results from loss of  $\text{C}(7)$  and the oxygen. Loss of the propyl group  $\text{C}(9-11)$ , from this ion makes possible the protonated anilium ion at  $m/z$  93. Loss of the propyl group,  $\text{C}(9-11)$ , from the molecular ion also makes possible a substituted anilium ion at  $m/z$  122. Other ions are visible representing loss of methyl- or ethyl- groups from the molecular ion; however, they obviously do not have the stability of the anilium ion and are therefore found at lower concentrations. Loss of a hydroxy group from  $m/z$  122 produces the structure of  $m/z$  105.

FIGURE V-3.  
Principle ions in the EIMS Fragmentation of Fusaryl Alcohol



The regions of the spectrum containing the low molecular weight fragments are of low intensity and individual regions are made more complex by fragments of undetermined carbon skeleton origin and by contaminant interference. The isotopic content of the separating low  $m/z$  fragments is calculated by subtraction of isotopic concentration values of parent and daughter ion at higher  $m/z$ . The exact fragmentation pathways including intramolecular rearrangements and/or hydrogen additions and subtractions are not of major importance. Rather, carbon skeleton identities provide the basis for the necessary subtractions of isotopic content.

Ion regions were chosen for analysis in this investigation on the basis of intensity, simplicity and applicability to desired carbon skeleton changes. The molecular ion region and fragment regions surrounding

m/z 122 and m/z 93 were studied specifically. The intense ion region at m/z 136 was neglected because it contained ion clusters differing by number of oxygen (Table V-1). The computer program in the version used herein is incapable of dealing with this situation.

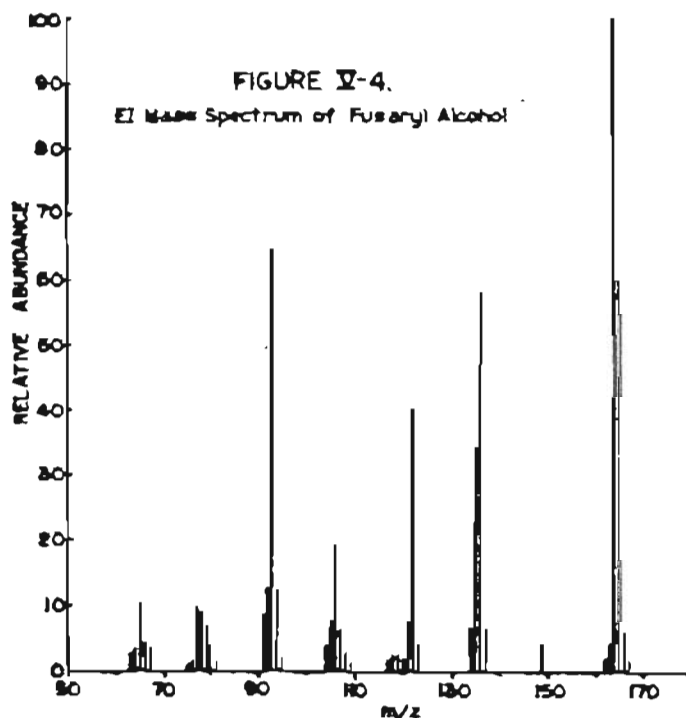
TABLE V-1  
HIGH RESOLUTION ION INTENSITY RECORDINGS  
FOR SELECTED IONS OF THE  
FUSARYL ALCOHOL EI MASS SPECTRUM

Spectrum No.		IDD	IIEE	IIIEE	IVEE
m/z	formula				
134	C <sub>8</sub> H <sub>8</sub> NO	29	19	18	19
	C <sub>9</sub> H <sub>12</sub> N	27	23	22	25
135	C <sub>8</sub> H <sub>9</sub> NO	9	7	7	7
	C <sub>9</sub> H <sub>13</sub> N	448	209	207	207
136	C <sub>8</sub> H <sub>10</sub> NO	7	5	5	5
	C <sub>9</sub> H <sub>14</sub> N	500	500	500	500

The <sup>13</sup>C abundance at C(7) will be equal to the difference in the <sup>13</sup>C abundance for ions at m/z 122 and 93 even though they are probably not directly related by any fragmentation pathway. The sum of the <sup>13</sup>C abundance values of C(9), C(10) and C(11) will be equal to the difference in the values for the ions of m/z 165 and 122. Of course, the sum of the <sup>13</sup>C abundances for the carbons of the pyridine ring plus carbon 8 from the hydrocarbon side chain will be equal to the total isotopic abundance for the ion of m/z 93.

A typical bar graph mass spectrum of a sample of fusaryl

alcohol containing isotopes only at natural abundance is shown in Figure V-4. Ions occur in groups surrounding intense peaks at masses 164, 136, 122 and 93. Other less intense groups (less stable ions) occur but are not used in this investigation. Each group of ions is denoted a "spectral region" as each may actually be composed of more than one "ion cluster", a term used here to signify an ion and its isotopically related counterparts.



b. High resolution mass spectrum

A high resolution spectrum of fusaryl alcohol was obtained in order to concretely identify the major ion clusters as well as minor overlapping clusters within specific regions. This high resolution spectrum is tabulated in Table V-2. Column A gives the empirical formula for observed ions; column B gives relative intensity data obtained from

TABLE V-2  
HIGH RESOLUTION EI MASS SPECTRUM OF FUSARYL ALCOHOL

A Empirical Formula	B Relative Intensity <sup>a</sup>	C Exact Mass <sup>b</sup>	D Observed Mass <sup>c</sup>
C <sub>6</sub> H <sub>5</sub> N	4.0	91.0422	d
C <sub>7</sub> H <sub>7</sub>	3.0	.0548	91.0550
<sup>13</sup> CC <sub>5</sub> H <sub>5</sub> N	5.8	92.0456	92.0497
C <sub>6</sub> H <sub>6</sub> N		.0500	
C <sub>6</sub> H <sub>7</sub> N	8.0	93.0578	93.0573
<sup>13</sup> CC <sub>5</sub> H <sub>7</sub> N	5.3 <sup>e</sup>	94.0612	94.0647
C <sub>6</sub> H <sub>8</sub> N		.0657	
C <sub>3</sub> HN <sub>3</sub> O	1.0	95.0120	95.0119
<sup>13</sup> CC <sub>5</sub> H <sub>8</sub> N	1.0	.0690	.0689
C <sub>7</sub> H <sub>6</sub> N	2.4	104.0500	d
C <sub>7</sub> H <sub>7</sub> N	4.2	105.0578	105.0576
C <sub>7</sub> H <sub>8</sub> N	5.6	106.0657	d
<sup>13</sup> CC <sub>6</sub> H <sub>8</sub> N	2.3	107.0690	107.0728
C <sub>7</sub> H <sub>9</sub> N		.0735	
C <sub>6</sub> H <sub>6</sub> NO <sup>f</sup>	2.4	108.0449	108.0448 <sup>g</sup>
<sup>13</sup> CC <sub>6</sub> H <sub>9</sub> N <sup>f</sup>		.0769	.0785 <sup>g</sup>
C <sub>7</sub> H <sub>10</sub> N <sup>f</sup>		.0813	
C <sub>8</sub> H <sub>7</sub> N <sup>f</sup>	1.4	117.0578	117.0577 <sup>g</sup>
C <sub>9</sub> H <sub>9</sub> <sup>f</sup>		.0704	.0697 <sup>g</sup>
C <sub>8</sub> H <sub>8</sub> N <sup>f</sup>	1.4	118.0657	118.0654 <sup>g</sup>
C <sub>7</sub> H <sub>6</sub> NO	1.0	120.0449	120.0436
C <sub>8</sub> H <sub>10</sub> N <sup>f</sup>	1.0	.0813	.0813 <sup>g</sup>
C <sub>7</sub> H <sub>7</sub> NO	3.6	121.0528	121.0527
C <sub>7</sub> H <sub>8</sub> NO	7.3	122.0606	d
<sup>13</sup> CC <sub>6</sub> H <sub>8</sub> NO	2.5	123.0639	123.0639
C <sub>8</sub> H <sub>8</sub> NO	7.6 <sup>h</sup>	134.0605	d
C <sub>9</sub> H <sub>12</sub> N	7.3 <sup>h</sup>	.0907	134.0978 <sup>g</sup>

$^{13}\text{CC}_7\text{H}_8\text{NO}^{\text{f}}$	4.9 <sup>h</sup>	135.0639	135.0678 <sup>g</sup>
$\text{C}_8\text{H}_9\text{NO}^{\text{f}}$		.0683	
$^{13}\text{CC}_8\text{H}_{12}\text{N}^{\text{f}}$	9.8 <sup>h</sup>	.1003	.1039 <sup>g</sup>
$\text{C}_9\text{H}_{13}\text{N}$		.1040	
$\text{C}_8\text{H}_{10}\text{NO}^{\text{f}}$	3.0 <sup>h</sup>	136.0762	136.0763 <sup>g</sup>
$\text{C}_9\text{H}_{14}\text{N}$	7.4 (10.5 <sup>h</sup> )	.1126	.1123 <sup>g</sup>
$^{13}\text{CC}_8\text{H}_{14}\text{N}$	8.8 <sup>h</sup>	137.1160	137.1160 <sup>g</sup>
$^{13}\text{C}_1\text{C}_7\text{H}_{14}\text{N}^{\text{f}}$	3.2 <sup>h</sup>	138.1194	138.1193 <sup>g</sup>
$\text{C}_{10}\text{H}_{12}\text{NO}^{\text{f}}$	3.3 <sup>h</sup>	162.0919	162.0892 <sup>g</sup>
$\text{C}_{10}\text{H}_{13}\text{NO}^{\text{f}}$	4.5 <sup>h</sup>	163.0997	d
$\text{C}_{10}\text{H}_{14}\text{NO}^{\text{f}}$	7.5 (10.5 <sup>h</sup> )	164.1075	164.1079 <sup>g</sup>
$\text{C}_{10}\text{H}_{15}\text{NO}$	7.0	165.1154	165.1147
$^{13}\text{CC}_9\text{H}_{15}\text{NO}$	2.3	166.1187	166.1191

(Notes to Table V-2)

<sup>a</sup>Relative intensity values quoted here are derived from data recorded on photoplates and is only given for reference purposes. All calculations were done using intensity data derived from photomultiplier measurements.

<sup>b</sup>Exact masses are calculated from established masses as given in the reference manual for the 21-110B mass spectrometer used herein (7/64).

<sup>c</sup>Observed masses were based on calculations using selected identifiable ions from the fusaryl alcohol spectrum itself as standards.

<sup>d</sup>Denoted standard as described in c.

<sup>e</sup>Observed as an irregularly shaped peak suggesting an unresolved doublet.

<sup>f</sup>Identified from a second, more intense spectrum.

<sup>g</sup>Calculated from standards in the other spectrum described in f.

<sup>h</sup>Relative intensity values from spectrum described in f.

photoplate recordings and is listed here purely for reference purposes; column C gives exact masses calculated from a PFK internal standard and selected reference ions within the sample itself. All ions are easily identifiable.

Resolution ( $\sim 20,000$ ) was insufficient to separate  $^{13}\text{C}$  containing ions from  $^{12}\text{C}$  ions containing an additional hydrogen (See Part II-B-3). Therefore, intensities identified as either type ion might be conceived actually to contain either or both.

c. Analysis - sample with natural isotopic abundance

(1) Determination of ionic intensity identity from  
unit resolution data

Ions may occur within a region having the same nominal mass and carbon skeleton but differing by number of  $^{13}\text{C}$  atoms and number of hydrogens. These require resolution of  $\sim 50,000$  for separation. When such resolution is unavailable, the identity of a particular ionic intensity may sometimes be established by calculations done utilizing data of only unit mass resolution.

Table V-3 summarizes results of ion cluster contribution calculations for the molecular ion region of four spectra of a fusaryl alcohol sample containing  $^{13}\text{C}$  at natural abundance.

TABLE V-3  
 RELATIVE EIMS ION CLUSTER INTENSITIES OF THE FUSARYL ALCOHOL  
 MOLECULAR ION REGION

Spectrum No.	IJ	IVJ	IP	IIIP
m/z				
161	.53	.58	.24	.58
162	.68	.66	.83	.66
163	4.07	3.84	3.94	3.84
164	63.50	63.88	63.11	63.88
165	30.72	31.05	31.15	31.05
166	-	-	-	-
167	-	-	-	-
168	-	-	-	-
169	-	-	-	-

Five ion clusters are observed to originate at m/z 161-165. Table V-4 lists raw and normalized data for these same spectra. In the most intense spectrum, IJ, ionic intensity was observed for nine m/z values; however, even in this case calculations show the presence of only five ion clusters. Observed intensity at m/z 166-169 is therefore identified as resulting from ions isomeric to those at m/z 161-165 rather than from ions containing additional hydrogen.

TABLE V-4  
EIMS ION INTENSITY DATA OF THE FUSARYL ALCOHOL  
MOLECULAR ION REGION

Spectrum No.	IJ	IVJ	IP	IIIP
A. Raw Data				
m/z				
161	5	4	2	2
162	7	5	7	6
163	39	27	33	30
164	601	443	520	474
165	359	266	321	286
166	41	29	35	33
167	4	2	4	2
168	2	-	-	-
169	3	-	-	-
B. Normalized Data				
161	4	5	2	2
162	6	6	7	6
163	32	30	32	32
164	500	500	500	500
165	299	300	309	302
166	34	33	34	35
167	3	2	4	2
168	2	-	-	-
169	2	-	-	-

(2) Calculation of  $^{13}\text{C}$  natural abundance - a test of accuracy

Mass spectral data obtained from a fusaryl alcohol sample containing  $^{13}\text{C}$  only at natural abundance provides an excellent opportunity for a test of the accuracy of the techniques used herein. Figure V-5 reproduces the computer print-out for results of one particular spectral recording. The curve indicated by the asterisks represents the change

FIGURE V-5.

Computer Print-out. Determination of  $^{13}\text{C}$  Natural Abundance

```

LOOP: YES, MAX-STOP: YES, WD 1171-5, MINZ: 100-3, P1: .001, DP: .
11-3/5, 1(A) = 0.36000 X(7) = 3/300,
A, I'S
110, 11, 1, 1,
* 5 = 1.10001 1 1 1 1 0 1 1 * 1 X 1 1
* 5 = 1.10101 1 1 1 1 0 1 1 * 1 X 1 1
* 5 = 1.10201 1 1 1 1 0 1 1 * 1 X 1 1
* 5 = 1.10301 1 1 1 1 0 1 1 * 1 X 1 1
* 5 = 1.10401 1 1 1 1 0 1 1 * 1 X 1 1
* 5 = 1.10501 1 1 1 1 0 1 1 * 1 X 1 1
* 5 = 1.10601 1 1 1 1 0 1 1 * 1 X 1 1
* 5 = 1.10701 1 1 1 1 0 1 1 * 1 X 1 1
* 5 = 1.10801 1 1 1 1 0 1 1 * 1 X 1 1
* 5 = 1.10901 1 1 1 1 0 1 1 * 1 X 1 1
* 5 = 1.11001 1 1 1 1 0 1 1 * 1 X 1 1

```

in the residual as described in Part II-C-4 at  $m/z$  166 as the trial %  $^{13}\text{C}$  value is progressively increased. Since the ion intensity at  $m/z$  166 has been shown to be due entirely to  $^{13}\text{C}$  isotopic isomers of lower  $m/z$  ions, a residual equal to zero within limits of error will result when the appropriate value for the abundance of  $^{13}\text{C}$  is used. For this sample that value is shown to lie between 1.106 and 1.107%  $^{13}\text{C}$ .

Table V-5 summarizes results from five recordings. The established value for  $^{13}\text{C}$  natural abundance of 1.108%  $^{13}\text{C}$  lies within the range of the result,  $1.14 \pm .04\%$   $^{13}\text{C}$ .

TABLE V-5  
 POLYNOMIAL FACTOR ANALYSIS OF FUSARYL ALCOHOL,  
 NATURAL ISOTOPIC ABUNDANCE, SPECTRA

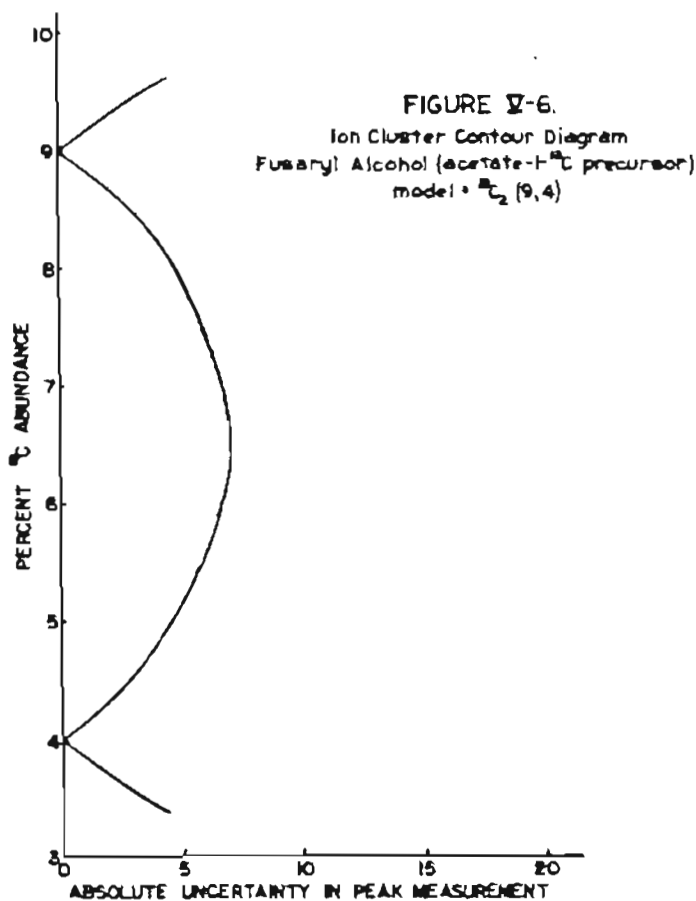
Spectrum No.	% <sup>13</sup> C
IJ	1.18
IVJ	1.11
IP	1.10
IIIP	1.19
Average	<u>1.14</u> ± .04% <sup>13</sup> C

d. Analysis - isotopically enriched sample

(1) ICCD evaluation

A sample of fusaryl alcohol enriched in <sup>13</sup>C by production with an acetate-1-<sup>13</sup>C precursor was available for analysis. According to the biosynthetic hypothesis such a precursor would be expected to produce five labeled sites (151). Two levels of enrichment would be expected. Carbons 7 and 4, introduced into fusaric acid via an aspartate intermediate, should exhibit approximately equal enrichment levels. Carbons 6, 8, and 10 should also have enrichment levels equal to each other but higher than the enrichment levels of carbons 7 and 4.

The ICCD, Figure V-6, indicates that at uncertainty levels obtained, ± 2 units/intensity measurement, and at abundance levels indicated by <sup>1</sup>HMR results, the presence of two different isotopic abundance levels should be clearly defined by the data.



## (2) Determination of $^{13}\text{C}$ abundance levels

When the number of labeled sites is assumed from the biosynthetic hypothesis to be five, the presence of two enrichment levels may be demonstrated. Figure V-7 pictures a portion of the computer print-out indicating, again from the residual at  $m/z$  166, that some carbon sites contain 9 percent  $^{13}\text{C}$ . The second  $^{13}\text{C}$  abundance level of 4 percent is similarly determined. These results are supported by  $^1\text{HMR}$  results as discussed above.

FIGURE V-7.

Computer Print-out: Determination of  $^{13}\text{C}$  Abundance  
Rusaryl Alcohol (acetate- $^{13}\text{C}$  precursor)

```

LOOP: YES, MAX-STOP: YES, NO FIT: Y-N-6, MIN: 1180-11, D1: 2, P2:
I150/S, I(K) = 60.0000 X(K) 150/140,
NA, Z'S
I5, I5, 4, 1,
# 7 = 5.40001 | | | | 0 | * | | | | |
# 7 = 5.60001 | | | | 0 | X* | | | | |
# 7 = 5.80001 | | | | 0 | |* | | | | |
# 7 = 6.00001 | | | | 0 | X* | | | | |
# 7 = 6.20001 | | | | 0 | X* | | | | |
# 7 = 6.40001 | | | | 0 | X* | | | | |
# 7 = 6.60001 | | | | 0 | X* | | | | |
# 7 = 6.80001 | | | | 0 | X* | | | | |
# 7 = 7.00001 | | | | 0 | X | |* | | | | |
# 7 = 7.20001 | | | | 0 | X | |* | | | | |
# 7 = 7.40001 | | | | 0 | X | |* | | | | |
# 7 = 7.60001 | | | | 0 | X | |* | | | | |
# 7 = 7.80001 | | | | 0 | X | |* | | | | |
# 7 = 8.00001 | | | | 0 | X | |* | | | | |
# 7 = 8.20001 | | | | 0 | X | |* | | | | |
# 6 = 8.40001 | | | | 0 | X | |* | | | | |
# 6 = 8.60001 | | | | 0 | X | |* | | | | |
# 6 = 8.80001 | | | | 0 | X | |* | | | | |
# 6 = 9.00001 | | | | 0 | X | |* | | | | |
# 6 = 9.20001 | | | | 0 | X | |* | | | | |
# 6 = 9.40001 | | | | 0 | X | |* | | | | |
# 6 = 9.60001 | | | | 0 | X | |* | | | | |
STOP: YES,
--3 = 9.80001

```

### (3) Location of $^{13}\text{C}$ labeled sites

Information leading to the location of labeled sites may be obtained by subtraction of the isotopic abundances of ion regions as previously described. Analysis of ions in the regions  $m/z$  164, 122, and 93 as accomplished herein permits the  $^{13}\text{C}$  abundance at carbon 7 to be calculated directly ( $m/z$  122 minus 93). Abundance values for other carbons are obtained as sums of the abundance values of individual carbon sites composing various fragments. That is for the isotopic generating function

$$(a_x + b_x)^n$$

the values,  $b_x$ , obtained will approximate the average %  $^{13}\text{C}$  per carbon in the given ion. Therefore, the value  $nb_x$  will approximate the sum of the actual enrichment values for the carbons involved.

Table V-6 tabulates the values obtained for the three ions.

TABLE V-6  
ISOTOPIC ANALYSIS OF THE EIMS ION REGIONS OF  $^{13}\text{C}$  ENRICHED FUSARYL ALCOHOL  
Biosynthetic Precursor = Acetate-1- $^{13}\text{C}$   
Isotopic Generating Function<sup>a</sup> -  $(a_x + b_x)^n$

Ion Region	C #'s	n	$b_x$	$nb_x$
164	2-11	10	4.7	47.0
122	2-8	7	5.02	35.1
93	2-6,8	6	5.2	31.2

<sup>a</sup>Binomial expression the expansion of which gives the mass spectrum of each model

Symbols:  $a_x$  =  $^{12}\text{C}$  abundance

$b_x$  =  $^{13}\text{C}$  abundance

n = number of carbons in ion

Appropriate subtraction produces a value of 3.9%  $^{13}\text{C}$  for carbon 7. The fragment containing carbons 9-11 is shown to have abundance values totaling 11.9. The biosynthetic hypothesis would suggest that only carbon 10 is labeled. If this is so and carbons 9 and 11 then contain  $^{13}\text{C}$  at natural abundance levels of 1.1% each, carbon 10 evidently contains 9.7%  $^{13}\text{C}$ . These results are comparable to those obtained above in the calculation utilizing data from the molecular ion region. (See Figure V-7) Carbon-13 enrichment levels have thus been established for two different carbons, one from each of the two segments suggested in the biosynthetic hypothesis. The results of 3.9% and 9.7%  $^{13}\text{C}$  are also in agreement with NMR results of  $4 \pm 0.6\%$   $^{13}\text{C}$  and  $9 \pm 0.8\%$   $^{13}\text{C}$  (3).

Quantitative values obtained in this way should not be expected to approach the accuracy demonstrated above for determination of the natural  $^{13}\text{C}$  abundance value. The isotopic generating function

$$(a_x + b_x)^n$$

used here to obtain the average  $^{13}\text{C}$  enrichment per carbon, is obviously inaccurate for it represents the case in which all carbon sites within a given fragment are equally enriched. At low enrichment levels however, the error introduced by such an approximation is not great. Results in Table V-7 illustrate this point. Six different models are assumed and the average percent  $^{13}\text{C}$  per carbon calculated for each case. The average deviation from the mean is seen to be only  $\pm 0.1\%$   $^{13}\text{C}$ . Model 6 was applied to data from two randomly selected spectral recordings and a variation of this same order of magnitude was observed.

TABLE V-7  
ISOTOPIC ANALYSIS OF THE EIMS C<sub>10</sub> ION REGION OF A <sup>13</sup>C ENRICHED FUSARYL  
ALCOHOL

Biosynthetic Precursor = Acetate-1-<sup>13</sup>C  
Isotopic Generating Function<sup>a</sup> -  $(a_x + b_x)^{m_a} (a_c + b_c)^{n - m - m_a}$

Model No.	m <sub>a</sub>	b	m	b <sub>x</sub>	Ave. % <sup>13</sup> C
1	-	-	10	4.7	4.70
2	-	-	1	33.6	4.35
3	-	-	5	8.25	4.68
4	2	4.0	3	11.3	4.75
5	3	9.0	2	7.3	4.72
6	3	10.0	2	5.7(6.2) <sup>b</sup>	4.69(4.80) <sup>b</sup>
Average					4.65±0.10

<sup>a</sup>Binomial expression the expansion of which yields the mass spectrum of each model

Symbols: a<sub>x</sub> = <sup>12</sup>C abundance being calculated

b<sub>x</sub> = <sup>13</sup>C abundance being calculated

a = assumed <sup>12</sup>C abundance

b = assumed <sup>13</sup>C abundance

a<sub>c</sub> = natural abundance of <sup>12</sup>C (98.89%)

b<sub>c</sub> = natural abundance of <sup>13</sup>C (1.11%)

m = number of carbons for which isotopic abundance is being calculated

m<sub>a</sub> = number of carbons of assumed isotopic abundance

n = total number of carbons in ion

<sup>b</sup>Result obtained from second spectral recording of same sample

### 3. Conclusion

Mass spectral isotopic analysis, a relatively rapid and clean technique, is shown to provide valuable information bearing on a biosynthesis of fusaric acid, even without unique isolation of individual carbon atoms. Application of the polynomial factor data reduction approach described herein provides clear evidence of multiple enrichment levels in fusaric acid produced from a  $^{13}\text{C}$  enriched acetate precursor. These multiple enrichment levels argue for formation from at least two separate biogenetic units each produced by addition of the acetate precursor.

#### C. Sepedonin - a fungal tropolone

##### 1. Introduction

Mass spectrometry as an analytical technique for isotopic analysis has suffered previously from the limitation that the chemistry underlying the mass spectrum of the compound of interest is not always clearly understood (73,129,152). In some cases a particular ion may be derived from more than one portion of the molecule and competing reaction rates are operative. The mass spectrum of sepedonin, (Figure V-8) is an example of such a situation.

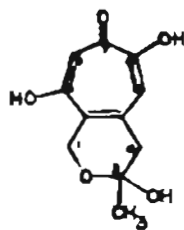
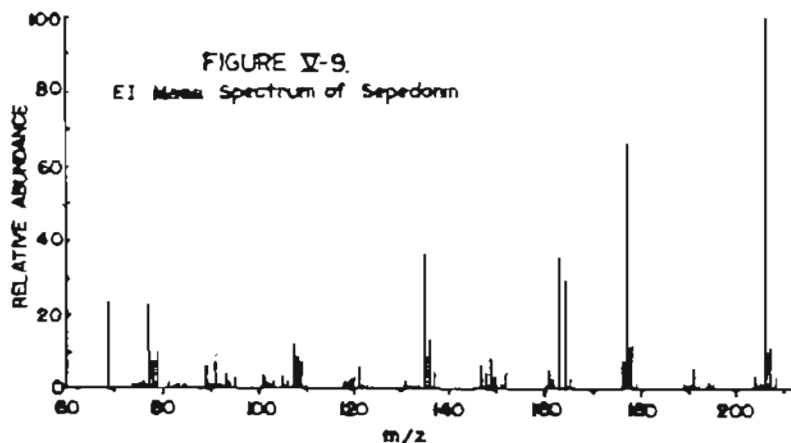


FIGURE V-8. Sepedonin

## 2. Results and discussion

### a. Mass spectral fragmentation pattern

A typical bar graph spectrum of a natural abundance sample of sepedonin is shown in Figure V-9. No molecular ion is visible; however,



an ion region occurs at  $m/z$  204 due to anhydrosepedonin ( $C_{11}H_8O_4$ ). This dehydration is thought to occur spontaneously with decomposition of the sample as well as within the mass spectrometer. The base peak at  $m/z$  206 may be due to the addition of  $2H$  to anhydrosepedonin. The resonance possible for sepedonin, Figure V-10, is the basis for the nonspecific fragmentation pattern. Loss of  $-HCO$  to produce the intense ion of  $m/z$  177 ( $C_{10}H_9O_3$ ) may occur from any one of at least three competing carbon sites

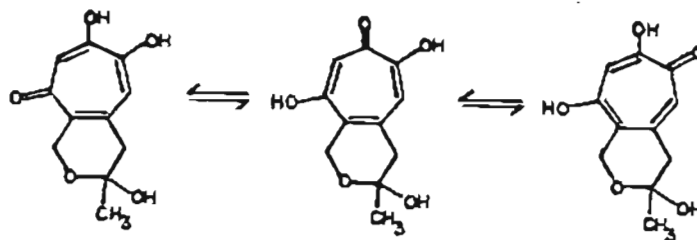
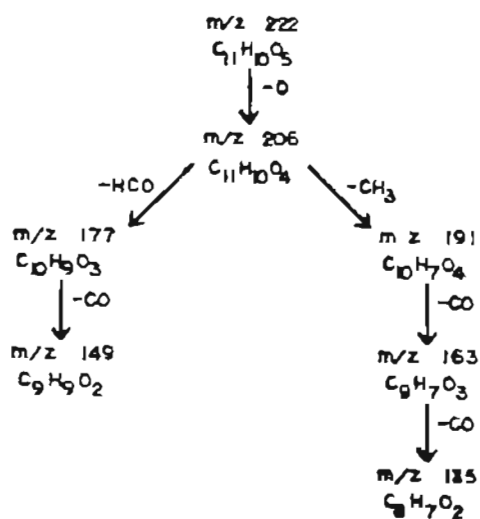


FIGURE V-10.  
Resonance Structures of Sepedonin

and loss of a second -CO fragment to produce the ion of  $m/z$  149 ( $C_9H_9O_2$ ) may be likewise nonspecific. Loss of the methyl group from the  $m/z$  206 ion produces the ion at  $m/z$  191 ( $C_{10}H_7O_4$ ) which may in turn lose a non-specific-CO to produce the ion at  $m/z$  163 ( $C_9H_7O_3$ ) followed by a second -CO to arrive at the ion  $m/z$  135 ( $C_8H_7O_2$ ). This fragmentation pattern is summarized in Figure V-11.

FIGURE V-11.  
EIMS Fragmentation Pathway of Sepedonin - Principle ions



b. High resolution mass spectrum

As might be expected for a molecule with such a complex fragmentation pattern, interfering ions of differing carbon and oxygen number due to loss of various hydrocarbon and water fragments occur. The high resolution spectrum displayed in Table V-8 identifies these ions. Again, as in the case of fusaryl alcohol, ions due to the presence of  $^{13}C$  isotope and to the  $^{12}C$  analog plus hydrogen are unresolved and both probably occur in many places where one is noted.

TABLE V-8  
HIGH RESOLUTION ELECTRON IMPACT MASS SPECTRUM OF  
SEPEDONIN (NAT. ABUND.)

INTENSITY	POSITION	MASS	FORMULA	ACTUAL MASS
1.3	91.2294	129.0333 <sub>5</sub>	C <sub>9</sub> H <sub>5</sub> O	129.0341
0.8	91.8293	130.0052 <sub>4</sub>	(C <sub>8</sub> H <sub>2</sub> O <sub>2</sub> )	(130.0055)
3.5	91.8507	130.0421 <sub>5</sub>	C <sub>9</sub> H <sub>6</sub> O	130.0419
6.3	92.4351	131.0497 <sub>St5</sub>	C <sub>9</sub> H <sub>7</sub> O	131.0497
5.6	93.0849	132.0576 <sub>5</sub>	C <sub>9</sub> H <sub>8</sub> O	132.0575
6.4	93.6662	133.0103 <sub>4</sub>	(C <sub>4</sub> H <sub>5</sub> O <sub>5</sub> )	(133.0137)
1.3	93.6767	133.0276 <sub>4</sub>	C <sub>8</sub> H <sub>5</sub> O <sub>2</sub>	133.0290
3.7	93.6930	133.0564 <sub>St5</sub>	<sup>13</sup> C <sub>2</sub> C <sub>7</sub> H <sub>7</sub> O	133.0564
5.7	94.2880	134.0373 <sub>5</sub>	C <sub>8</sub> H <sub>6</sub> O <sub>2</sub>	134.0368
0.8	94.8841	135.0217 <sub>4</sub>	(C <sub>11</sub> H <sub>3</sub> )	135.0235
8.7	94.8979	135.0446 <sub>St4</sub>	C <sub>8</sub> H <sub>7</sub> O <sub>2</sub>	135.0446
7.6	95.5037	136.0508 <sub>4</sub>	C <sub>8</sub> H <sub>8</sub> O <sub>2</sub>	136.0524
		136.0524 <sub>St3</sub>	C <sub>8</sub> H <sub>8</sub> O <sub>2</sub>	136.0524
1.8	96.0873	137.0237 <sub>4</sub>	C <sub>7</sub> H <sub>5</sub> O <sub>3</sub>	137.0238
9.3	96.1083	137.0587 <sub>4</sub>	C <sub>8</sub> H <sub>9</sub> O <sub>2</sub>	137.0602
			<sup>13</sup> CC <sub>7</sub> H <sub>8</sub> O <sub>2</sub>	137.0558
0.7	96.6773	138.0107 <sub>4</sub>	(C <sub>10</sub> H <sub>2</sub> O)	(138.0106)
2.0	96.7109	138.0670 <sub>4</sub>	C <sub>8</sub> H <sub>10</sub> O <sub>2</sub>	138.0680
			<sup>13</sup> CC <sub>7</sub> H <sub>9</sub> O <sub>2</sub>	138.0636
0.7	97.2790	139.0210 <sub>4</sub>	(C <sub>10</sub> H <sub>3</sub> O)	139.0184
-----				
4.8	100.8028	145.0115 <sub>4</sub>		
1.4	100.8140	145.0307 <sub>4</sub>	C <sub>9</sub> H <sub>5</sub> O <sub>2</sub>	145.0289
2.2	101.3988	146.0372 <sub>4</sub>	C <sub>9</sub> H <sub>6</sub> O <sub>2</sub>	146.0367
6.4	101.9824	147.0450 <sub>4</sub>	C <sub>9</sub> H <sub>7</sub> O <sub>2</sub>	147.0446
6.6	102.5633	148.0517 <sub>4</sub>	C <sub>9</sub> H <sub>8</sub> O <sub>2</sub>	148.0524
1.6	103.1227	149.0243 <sub>4</sub>		
7.4	103.1433	149.0602 <sub>St4</sub>	C <sub>9</sub> H <sub>9</sub> O <sub>2</sub>	149.0602

INTENSITY	POSITION	MASS	FORMULA	ACTUAL MASS
1.0	103.6892	150.0125 <sub>4</sub>	(C <sub>11</sub> H <sub>2</sub> O)	(150.0106)
1.1	103.6994	150.0304 <sub>4</sub>	(C <sub>8</sub> H <sub>6</sub> O <sub>3</sub> )	150.0317
4.9	103.7207	150.0676 <sub>4</sub>	C <sub>9</sub> H <sub>10</sub> O <sub>2</sub>	150.0680
			<sup>13</sup> CC <sub>8</sub> H <sub>9</sub> O <sub>2</sub>	150.0636
1.0	104.2923	151.0682 <sub>4</sub>	<sup>13</sup> CC <sub>8</sub> H <sub>10</sub> O <sub>2</sub>	150.0714
1.4	104.8253	152.0042 <sub>4</sub>		
2.3	104.8444	152.0475 <sub>4</sub>	(C <sub>8</sub> H <sub>8</sub> O <sub>3</sub> )	152.0473
-----				
2	108.8803	157.0063 <sub>7</sub>	n/1	
6	110.0142	159.0435 <sub>7</sub>	C <sub>10</sub> H <sub>7</sub> O <sub>2</sub>	159.0446
5	110.5732	160.0526 <sub>7</sub>	C <sub>10</sub> H <sub>8</sub> O <sub>2</sub>	160.0524
3	111.1093	161.0234 <sub>7</sub>	C <sub>9</sub> H <sub>5</sub> O <sub>3</sub>	161.0238
7	111.1288	161.0587 <sub>7</sub>	C <sub>10</sub> H <sub>9</sub> O <sub>2</sub>	161.0602
2	111.6647	162.0322 <sub>7</sub>	C <sub>9</sub> H <sub>6</sub> O <sub>3</sub>	162.0317
3	111.6828	162.0651 <sub>7</sub>	C <sub>10</sub> H <sub>10</sub> O <sub>2</sub>	162.0680
			<sup>13</sup> CC <sub>9</sub> H <sub>9</sub> O <sub>2</sub>	162.0635
9	112.2171	163.0337 <sub>7</sub>	C <sub>9</sub> H <sub>7</sub> O <sub>0</sub>	163.0395
1	112.7465	164.0062 <sub>7</sub>		
9	112.7680	164.0456 <sub>7</sub>	C <sub>9</sub> H <sub>8</sub> O <sub>3</sub>	164.0473
			<sup>13</sup> CC <sub>8</sub> H <sub>7</sub> O <sub>3</sub>	164.0429
2	112.8017	164.1073 <sub>7</sub>	(C <sub>7</sub> H <sub>16</sub> O <sub>8</sub> )	(164.1049)
0	113.2967	165.0148 <sub>7</sub>	C <sub>9</sub> H <sub>9</sub> O <sub>3</sub>	165.0551
7	113.3160	165.0502 <sub>7</sub>	<sup>13</sup> CC <sub>8</sub> H <sub>8</sub> O <sub>3</sub>	165.0507
1	113.3505	165.1136 <sub>7</sub>	n/1	
2	113.8612	166.0528 <sub>7</sub>	<sup>13</sup> CC <sub>8</sub> H <sub>9</sub> O <sub>3</sub>	166.0585
			<sup>13</sup> C <sub>2</sub> C <sub>7</sub> H <sub>8</sub> O <sub>3</sub>	166.0540
1	113.8661	166.0618 <sub>7</sub>	C <sub>9</sub> H <sub>10</sub> O <sub>3</sub>	166.0629
-----				
2	118.6772	175.0406 <sub>7</sub>	C <sub>10</sub> H <sub>7</sub> O <sub>3</sub>	175.0396
1	118.6906	175.0659 <sub>7</sub>	(C <sub>7</sub> H <sub>11</sub> O <sub>5</sub> )	175.0606
7	119.2096	176.0487 <sub>7</sub>	C <sub>10</sub> H <sub>8</sub> O <sub>3</sub>	176.0474

INTENSITY	POSITION	MASS	FORMULA	ACTUAL MASS
1	119.7199	177.0177 <sub>7</sub>	C <sub>9</sub> H <sub>5</sub> O <sub>4</sub>	177.0188
9	119.7396	177.0552 <sub>St7</sub>	C <sub>10</sub> H <sub>9</sub> O <sub>3</sub>	177.0552
			<sup>13</sup> CC <sub>9</sub> H <sub>8</sub> O <sub>3</sub>	177.0507
8	120.2680	178.0615 <sub>7</sub>	<sup>13</sup> CC <sub>9</sub> H <sub>9</sub> O <sub>3</sub>	178.0586
			C <sub>10</sub> H <sub>10</sub> O <sub>3</sub>	178.0630
4	120.7934	179.0649 <sub>7</sub>	<sup>13</sup> C <sub>2</sub> C <sub>8</sub> H <sub>9</sub> O <sub>3</sub>	179.0620
			<sup>13</sup> CC <sub>9</sub> H <sub>10</sub> O <sub>3</sub>	179.0664
-----				
5	122.8433	183.0067 <sub>7</sub>	(C <sub>11</sub> H <sub>3</sub> O <sub>3</sub> )	183.0082
0	124.9185	187.0408 <sub>7</sub>	C <sub>11</sub> H <sub>7</sub> O <sub>3</sub>	187.0396
2	125.4327	188.0472 <sub>7</sub>	C <sub>11</sub> H <sub>8</sub> O <sub>3</sub>	188.0474
3	125.9464	189.0553 <sub>7</sub>	C <sub>11</sub> H <sub>9</sub> O <sub>3</sub>	189.0552
1	126.4582	190.0624 <sub>7</sub>	C <sub>11</sub> H <sub>10</sub> O <sub>3</sub>	190.0630
			<sup>13</sup> CC <sub>10</sub> H <sub>9</sub> O <sub>3</sub>	190.0586
7	126.9509	191.0344 <sub>St7</sub>	C <sub>10</sub> H <sub>7</sub> O <sub>4</sub>	191.0344
			<sup>13</sup> CC <sub>9</sub> H <sub>7</sub> O <sub>4</sub>	192.0378
3	127.4578	192.0410 <sub>7</sub>	C <sub>10</sub> H <sub>8</sub> O <sub>4</sub>	192.0422
5	128.4760	194.0589 <sub>7</sub>	C <sub>10</sub> H <sub>10</sub> O <sub>3</sub>	194.0579
3	128.9511	195.0059		
1	128.9792	195.0620 <sub>7</sub>	C <sub>10</sub> H <sub>11</sub> O <sub>3</sub>	195.0657
			<sup>13</sup> CC <sub>9</sub> H <sub>10</sub> O <sub>3</sub>	195.0613
-----				
0	131.4772	200.0797 <sub>2</sub>		
-----				
1	132.9454	203.0589 <sub>2</sub>		
7	133.4276	204.0422 <sub>St2</sub>	C <sub>11</sub> H <sub>8</sub> O <sub>4</sub>	204.0422
6	133.9201	205.0489 <sub>2</sub>	C <sub>11</sub> H <sub>9</sub> O <sub>4</sub>	205.0500
			<sup>13</sup> CC <sub>10</sub> H <sub>8</sub> O <sub>3</sub>	205.0456
9	134.4125	206.0579 <sub>St2,1</sub>	C <sub>11</sub> H <sub>10</sub> O <sub>4</sub>	206.0579
1	134.8740	207.0058 <sub>2</sub>		
8	134.9012	207.0618 <sub>2</sub>	<sup>13</sup> CC <sub>10</sub> H <sub>10</sub> O <sub>4</sub>	207.0613

INTENSITY	POSITION	MASS	FORMULA	ACTUAL MASS	
5	} <sup>d</sup>	135.3877	208.0646 <sub>St1</sub>	<sup>13</sup> C <sub>2</sub> C <sub>9</sub> H <sub>10</sub> O <sub>4</sub>	208.0647
1		135.3903	208.0690 <sub>1</sub>	C <sub>11</sub> H <sub>12</sub> O <sub>4</sub>	208.0735
0		135.8737	209.0668 <sub>1</sub>	<sup>13</sup> C <sub>3</sub> C <sub>8</sub> H <sub>10</sub> O <sub>4</sub>	209.0681

c. Biosynthetic hypothesis

A biosynthetic hypothesis characterized by head to tail addition of acetate to form a C<sub>10</sub> unit followed by insertion of a one carbon unit is outlined in Figure V-12 (153). Such a scheme is analogous to

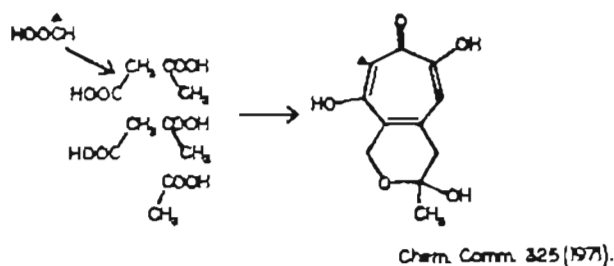


FIGURE V-12.

Biosynthetic Hypothesis for Sepedonin

pathways demonstrated for other fungal tropolones (154). Evidence in support of this hypothesis has been obtained from both <sup>1</sup>HMR and <sup>13</sup>CMR spectra from labeled samples of sepedonin (153,155). These labeled samples have been produced through the use of both <sup>13</sup>C enriched formate and acetate precursors.

The spin-spin coupling of <sup>13</sup>C and its bonded proton produces satellite peaks in the proton nuclear magnetic resonance spectrum which allow investigation of the 1, 4, 5, 8 and methyl carbon sites of the sepedonin molecule (155). Other carbon sites, specifically carbons 3,6,7,9 and the bridge carbons, are invisible since there are no directly

bonded protons. The  $^1\text{HMR}$  results are summarized in Table V-9 for samples produced from the indicated precursors. All positions labeled by the

TABLE V-9  
PROTON MAGNETIC RESONANCE RESULTS FOR  
CARBON-13 ENRICHED SEPEDONINS<sup>a</sup>

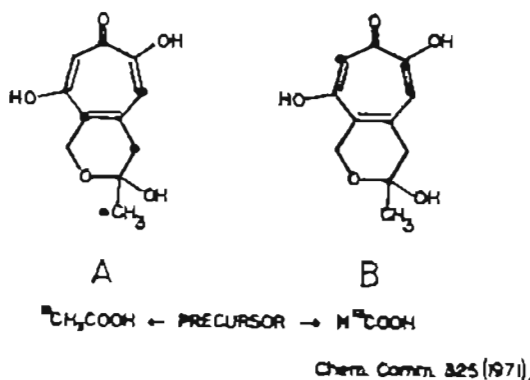
Carbon No.	Group	$\tau$ Value	$^{13}\text{CH}_3$ COOH Precursor	$\text{H}^{13}\text{COOH}$
	-CH <sub>3</sub>	8.33	4.3	1.2
4	-CH <sub>2</sub> -	7.08	3.7	1.0
1	-CH <sub>2</sub> -	4.91	1.0	1.0
5	=CH-	3.14	3.9	1.1
8	=CH-	2.85	1.1	20.6

<sup>a</sup>McInnes, Smith, Vining and Wright, Chem. Comm., 1968, 1669.

acetate precursors are shown to contain about the same amount of  $^{13}\text{C}$  within given error limits. The formate is shown to incorporate  $^{13}\text{C}$  in at least the C-8 position. All evidence obtained by  $^1\text{HMR}$  supports the biosynthetic hypotheses (Figure V-12). Relative standard deviations in the  $^{13}\text{C}$  enrichment values are relatively large, on the order of 15%

Carbon-13 nuclear magnetic resonance spectra produced eleven carbon resonances, all singlets (153). The results of this study are summarized in Figure V-13. Sepedonin produced by the formate  $^{-13}\text{C}$  precursor is shown to incorporate label only at the C-8 position. Sepedonin produced by acetate-2- $^{13}\text{C}$  precursor contains enrichment at alternating carbon sites, the methyl and carbons-4,5,7, and 9a. Nuclear Overhauser

FIGURE V-13.  
 $^{13}\text{C}$ MR Results for  $^{13}\text{C}$ -Enriched Sepedonins



effects precluded quantitative determination of enrichment levels from  $^{13}\text{C}$ MR spectra; however, estimates based on the C-5 and C-8 resonances were in agreement with  $^1\text{H}$ MR results.

d. Ion cluster contributions from natural  $^{13}\text{C}$  abundance data

The nonspecific mass spectral fragmentation pathway described above would ordinarily rule out mass spectrometry as an isotopic analysis technique for sepedonin samples except for determination of the total  $^{13}\text{C}$  enrichment; i.e.  $^{13}\text{C}$  enrichment values for specific carbon sites could not be studied individually. However, the polynomial factor data reduction technique may be applied to the anhydrosepedonin region alone ( $m/z$  204-209) to obtain information regarding the number of labeled sites and a quantitative measure of enrichment levels.

Ion cluster contribution values for the  $m/z$  206 region may be calculated from natural  $^{13}\text{C}$  abundance sepedonin samples for later comparison with those from enriched samples. Table V-10 tabulates results from three different spectra. A high degree of reproducibility was

TABLE V-10  
 EIMS ION CLUSTER INTENSITY RESULTS FOR m/z 206 REGION  
 SEPEDONIN-NATURAL  $^{13}\text{C}$  ABUNDANCE

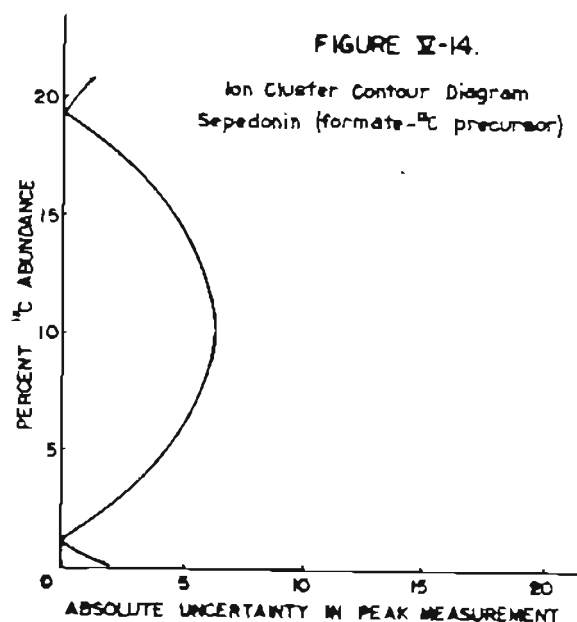
Spectrum No.	Mass Number					
	204	205	206	207	208	209
IY	9.9	1.6	86.4	-	1.7	-
IIY	9.7	1.6	86.6	-	1.7	-
IIIIY	10.3	1.6	86.1	-	1.6	-
Ave.	$10.0 \pm 0.3$	$1.6 \pm 0.0$	$86.4 \pm 0.3$	-	$1.7 \pm 0.03$	-

achieved. This is reasonable considering the stability of the ions involved. Ion clusters are observed originating at m/z 204, 205, 206 and 208. Ionic intensity observed at m/z 207 and 209 and above is then strictly due to entities containing one or more  $^{13}\text{C}$  atoms.

e. Analysis - sample isotopically enriched by formate - $^{13}\text{C}$  precursor

(1) ICCD evaluation.

The ICCD shown in Figure V-14 shows clearly that at uncertainty levels obtained in this sepedonin data ( $\pm 2$  units per ion intensity measurement) and at enrichment levels encountered here, variations in the model should be clearly determined as they are in Table V-11. The isotopic abundance is expected to approach 20%  $^{13}\text{C}$  at the labeled site; therefore uncertainties must be greater than  $\pm 6$  units per measurement before results will be obscured.



- (2) Determination of the number of different  $^{13}\text{C}$  abundance levels

A mass spectrum was obtained in the base peak ( $m/z$  206) region for a sample of sepedonin produced from a  $^{13}\text{C}$ -enriched formate precursor. During data reduction various possible models were selected and the resultant ion cluster intensities calculated. These calculations are summarized in Table V-11. Of these models only the last two, two enriched sites and one enriched site, contain ion clusters qualitatively identical to the result obtained from natural abundance sample calculations and only the last one, that with only one enriched site, produces intensities in quantitative agreement with those of the natural abundance sample. Therefore, it is shown that formate is incorporated into only one site in the sepedonin molecule. This is in agreement with the biosynthetic hypothesis as well as with  $^1\text{HMR}$  and  $^{13}\text{CMR}$  results (153-155).

TABLE V-11  
 EIMS ION CLUSTER INTENSITY RESULTS FOR m/z 206 REGION - SEPEDONIN-FORMATE <sup>13</sup>C PRECURSOR  
 Isotopic Generating Function<sup>a</sup> -  $(a_x + b_x)^m (a_c + b_c)^{n-m}$

Model			Mass Number						
m	b <sub>x</sub> max min		204	205	206	207	208	209	210
11	2.1		8.9	2.8	78.9	9.2	-	0.3	-
	3.1		9.9	2.0	88.0	-	-	-	-
10	2.2		8.9	2.8	78.9	9.2	-	0.3	-
	3.3		9.9	2.0	88.0	-	-	-	-
9	2.32		8.9	2.8	78.9	9.2	-	0.3	-
	3.52		9.9	2.0	87.0	-	-	-	-
8	2.5		8.9	2.8	79.0	9.0	-	0.3	-
	3.8		9.8	2.0	87.8	-	-	-	-
7	2.7		8.9	2.8	79.1	8.9	-	0.4	-
	4.2		9.9	2.0	87.9	-	-	-	-
6	3.0		8.9	2.7	79.2	8.8	-	0.4	-
	4.7		9.9	2.0	87.9	-	-	0.4	-
5	3.0		8.7	2.9	77.8	10.1	-	0.4	-
	5.4		9.9	2.0	87.9	-	-	0.4	-
4	4.0		8.9	2.7	79.4	8.5	-	0.4	-
	6.4		9.9	2.0	87.7	-	-	0.4	-
3	6.0		9.2	2.5	82.1	5.9	-	0.4	-
	8.0		9.8	2.0	87.5	-	-	0.5	-
2	8.0		9.2	2.5	81.5	6.3	-	0.4	-
	11.2		9.8	1.9	87.4	-	0.6	-	-
1	19.4		9.7	1.9	86.6	-	1.7	-	-

<sup>a</sup> Binomial expression the expansion of which yields the mass spectrum of each model

Symbols: a<sub>x</sub> = <sup>12</sup>C abundance to be calculated  
 b<sub>x</sub> = <sup>13</sup>C abundance to be calculated  
 a<sub>c</sub> = <sup>12</sup>C natural abundance (98.89%)  
 b<sub>c</sub> = <sup>13</sup>C natural abundance (1.11%)  
 m = number of carbons for which isotopic abundance is to be calculated  
 n = total number of carbons in ion

### (3) Quantitative determination of <sup>13</sup>C enrichment level

Table V-12 lists quantitative results obtained from three separate spectra of the formate -<sup>13</sup>C produced sepedonin. The sample is shown to contain  $19.3 \pm 0.6\%$  (relative standard deviation) percent <sup>13</sup>C.

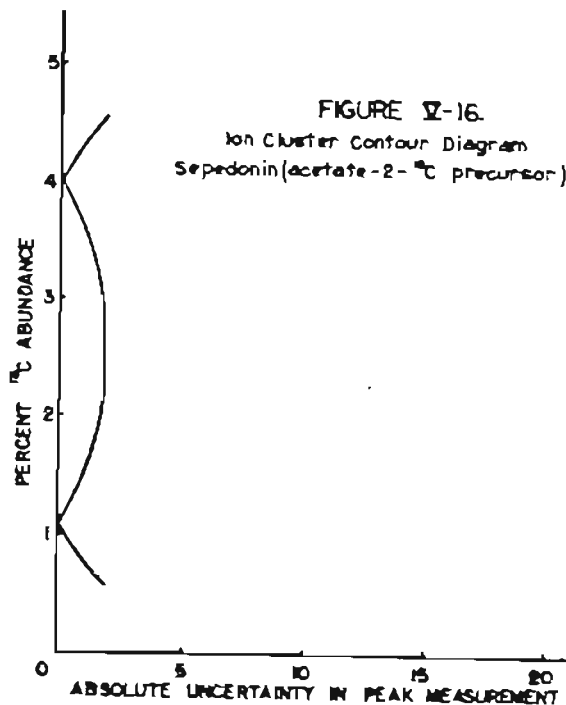


with  $^1\text{HMR}$  results of  $20.6 \pm 15\%$  (relative standard deviation) percent  $^{13}\text{C}$  (155). Both results were based on an average of three measurements.

f. Analysis - sample isotopically enriched by acetate- $2\text{-}^{13}\text{C}$  precursor

(1) ICCD evaluation

A sample of sepedonin produced by an acetate  $2\text{-}^{13}\text{C}$  precursor was also available for analysis. However, according to  $^1\text{HMR}$  results an isotopic abundance level of less than 4%  $^{13}\text{C}$  per labeled site was to be expected (155). As observed in the ICCD, Figure V-16, this abundance level should not be high enough to distinguish between various models at



the obtainable level of uncertainty. Table V-13 illustrates that this is so. No clear distinction can be made between ion cluster intensity results for the various models.

TABLE V-13  
 EIMS ION CLUSTER INTENSITY RESULTS FOR m/z 206 REGION - SEPEDONIN-ACETATE-2-<sup>13</sup>C PRECURSOR  
 Isotopic Generating Function<sup>a</sup> -  $(a_x + b_x)^m (a_c + b_c)^{n-m}$

MODEL		MASS NUMBER						
m	b <sub>x</sub>	204	205	206	207	208	209	210
11	2.1	8.01	1.50	87.69	-	2.62	-	-
10	2.2	8.02	1.49	87.71	-	2.62	-	-
9	2.3	8.00	1.51	87.54	-	2.66	-	-
8	2.4	7.97	1.53	87.21	-	2.73	-	-
7	2.6	7.98	1.52	87.31	-	2.72	-	-
6	2.9	8.00	1.50	87.60	-	2.67	-	-
5	3.2	7.99	1.51	87.40	-	2.72	-	-
4	3.7	7.98	1.52	87.30	-	2.76	-	-
3	4.6	7.99	1.50	87.44	-	2.77	-	-
2	6.2	7.97	1.51	87.26	-	2.88	-	-
1	10.8	7.95	1.51	87.06	-	3.13	-	-

<sup>a</sup>Binomial expression the expansion of which yields the mass spectrum of each model

- Symbols: a<sub>x</sub> = <sup>12</sup>C abundance to be calculated  
 b<sub>x</sub> = <sup>13</sup>C abundance to be calculated  
 a<sub>c</sub> = <sup>12</sup>C natural abundance  
 b<sub>c</sub> = <sup>13</sup>C natural abundance  
 m = number of carbons for which isotopic abundance is being calculated

(2) Quantitative determination of  $^{13}\text{C}$  enrichment level

When the correct model is assigned (five  $^{13}\text{C}$  enriched carbon sites) as expected from the biosynthetic hypothesis or obtained from NMR results, the quantitative result obtained of  $3.13 \pm 2.3\%$  (Table V-14) (relative standard deviation) is only slightly lower than the  $^1\text{HMR}$  result of  $3.9 \pm 15\%$  (relative standard deviation) and considerably more precise (155). There is no reason to assume that the  $^1\text{HMR}$  result is more accurate.

TABLE V-14  
 $^{13}\text{C}$  ISOTOPIC ENRICHMENT RESULTS FOR FOUR EIMS SPECTRA  
 SEPEDONIN-ACETATE-2- $^{13}\text{C}$  PRECURSOR

Mass No.	Ion Intensities				Ave.
	IJ	IIJ	IIIJ	IVJ	
204	47	43	78	165	
205	20	20	34	66	
206	518	463	765	1590	
207	122	106	179	359	
208	33	29	49	105	
209	7	7	12	23	
210	2	2	3	7	
% C	3.215	3.095	3.19	3.03	$3.13 \pm 2.3\%$ <sup>a</sup>

<sup>a</sup>Relative standard deviation

### 3. Conclusion

Isotopic analysis by mass spectrometry has traditionally been viewed as useless for molecules without a fragmentation pattern which uniquely isolates identifiable carbons. However, this sample analysis of two different  $^{13}\text{C}$ -enriched sepedonins clearly illustrates that isotopic mass spectral analysis can be a valuable tool even in these difficult cases. It is capable of producing quantitative results with a high degree of precision and of ascertaining the number of enriched sites when stable isotope enrichment levels are appropriate to the uncertainty of measurement. At the currently attainable high  $^{13}\text{C}$  enrichment levels, this should rarely present a problem.

Mass spectrometry has been shown to be a widely applicable analytical technique for stable isotope labeling experiments associated with study of biosynthetic problems and need no longer be so severely restricted in its application.

References

1. F. W. Aston, *Phil. Mag.* 39, 1920, 611.
2. IUPAC, *Inorg. Chem. Div., Pure Appl. Chem.* 1976, 75-95.
3. R. Park and H. N. Dunning, *Geochim. Cosmochim. Acta* 22, 99 (1961).
4. J. N. Weber and D. M. Raup, *Geochim. Cosmochim. Acta* 30, 681 (1966).
5. W. Stahl in *Recent Developments in Mass Spectroscopy*, (1969).
6. V. Smejkal, F. D. Cook and H. R. Kronse, *Geochim. Cosmochim. Acta* 35, 787 (1971).
7. J. L. Holmes, *Isotopes in Organic Chemistry* 1, 61 (1975).
8. M. F. Grostic and K. L. Rinehart, Jr. in *Mass Spectrometry; Techniques and Applications*, G.W.A. Mihne, ed., Wiley, N.Y., 1971, p. 217.
9. M. Tanabe in *Biosynthesis*, 2, 241 (1973).
10. K. Muysers and U. Smidt in *Biochemical Applications of Mass Spectrometry*, G. R. Walker, ed., Wiley, N.Y., 1972, p. 241.
11. S. Ratner in *Biochemical Applications of Mass Spectrometry*, G. R. Walker, ed., Wiley, N.Y., 1972, p. 1.
12. R. M. Caprioli in *Biochemical Applications of Mass Spectrometry*, G. R. Walker, ed., Wiley, N.Y., 1972, p. 735.
13. M. Strolin Benedetti and P. Strolin, *Pharmacologie Clinique*, 1, 15 (1973).
14. D. Rittenberg and T. D. Price in *Ann. Rev. of Nuc. Science*, Vol. 1, *Ann. Rev. Inc. with Nat'l Acad. Sc.*, Stanford, 1957, p. 569.
15. H. G. Boettger in *Biochemical Applications of Mass Spectrometry*, G. R. Walker, ed., Wiley, N.Y., 1972, p. 789.

16. A. L. Hammond, *Science*, 176, 1315 (1972).
17. N. A. Matwiyoff and D. G. Ott, *Science* 181, 1125 (1973).
18. S. Meyerson and E. K. Fields, *Science* 166, 325 (1969).
19. R. Bentley, N. C. Saba, C. C. Sweeley, *Anal. Chim.* 37, 1118 (1965).
20. T. E. Gaffney, C.-G. Hammar, B. Hohnstedt and R. E. McMahon, *Anal. Chem.* 43, 307 (1971).
21. B. D. Dombek, J. Lowther and E. Carberry, *J. Chem. Ed.*, 48, 729 (1971).
22. O. Borgen and B. Larsen, *Acta Chem. Scand.* 26, 3391 (1972).
23. D. D. Tunnicliff, P. A. Wadsworth and D. O. Schissler, *Anal. Chem.* 37, 543 (1965).
24. D. D. Tunnicliff and P. A. Wadsworth, *Anal. Chem.* 40, 1826 (1968).
25. W. H. Christie and H. S. McKown, *Chem. Instrum.* 3, 99 (1971).
26. R. J. Robinson, C. G. Warner and R. S. Gohlke, *J. Chem. Ed.* 47, 467 (1970).
27. B. Boone, R. K. Mitchum and S. E. Scheppele, *Int. S. Mass Spectrom. Ion. Phys.* 5, 21 (1970).
28. E. McLaughlin and R. W. Rozett, *J. Organometallic Chem.* 52, 261 (1973).
29. D. Mueller-Sohnius, K. Cammann and H. Koehler, *Int. J. Mass Spectrom. Ion Phys.* 15, 155 (1974).
30. Y. N. Sukkarev and Y. S. Nekrasov, *Org. Mass Spectrom.* 1976, 1232.
31. K. Biemann, P. Bommer and D. M. Desiderio, *Tetrahedron Lett.* 26, 1725 (1964).
32. R. M. Hilmer and J. W. Taylor, *Anal. Chem.* 46, 1038 (1974).

33. Yu N. Sukharev and Yu S. Nekrasov, *Org. Mass Spectrom* 1976, 1239.
34. A. J. Everett in "Computers for Spectroscopists, R.A.G. Carrington, ed., Wiley, N.Y., 1974, p. 215.
35. D. Henneberg, K. Casper, E. Ziegler and B. Weimann, *Angew. Chem. Int. Ed.* 11, 357 (1972).
36. C. R. McKinney, J. M. McCrea, S. Epstein, H. A. Allen and H. C. Urey, *Rev. Sci. Instrum.* 21, 724 (1950).
37. J. Bigeleisen and T. L. Allen, *J. Chem. Phys.*, 19, 760 (1951).
38. R. N. Clayton and E. T. Degens, *Bull. Am. Ass. Petrol. Geol.* 43, 890 (1959).
39. D. P. Stevenson, *J. Chem. Phys.* 19, 17 (1951).
40. K. Biemann, *Mass Spectrometry-Organic Chemical Applications*, McGraw-Hill, New York (1962).
41. A. Buchholz, "Mass Spectral and Nuclear Magnetic Resonance Studies of Compounds Labeled with Carbon-13," University Microfilms, Ann Arbor, Michigan (1967).
42. J. L. Brauman, *Spectral Analysis*, J. A. Blackburn, ed., M. Dekker (1970) p. 235-237.
43. G. D. Daves, Jr., W. E. Buddenbaum and B. S. Earl, Northwest Regional Meeting, American Chemical Society, Corvallis, Oregon, April, 1972.
44. E. Hugentobler and J. Loliger, *J. Chem. Ed.*, 49, 610 (1972).
45. C. Genty, *Anal. Chem.* 45, 505 (1973).
46. R. W. Rozett, *Anal. Chem.* 47, 348 (1975).
47. W. E. Buddenbaum, B. S. Earl and G. D. Daves, Jr., Proc. First Int. Conf. Stable Isotopes in Chem., Biol., Med., Argonne Nat'l Lab., May 9-11, 1973.

48. W. E. Buddenbaum and G. D. Daves, Jr., 21st Annual Conf. on Mass Spectrom. and Allied Topics, San Francisco, Calif., May 20-25, 1973.
49. R. W. Rozett, Anal. Chem. 46, 2085 (1974).
50. R. L. Middaugh, Inorg. Chem., 7 1011 (1968).
51. J. F. Pickup and K. McPherson, Anal. Chem. 48, 1885 (1976).
52. H. Yamamoto and J. A. McCloskey, Anal. Chem., 49, 281 (1977).
53. C. E. Melton and G. A. Ropp, J. Am. Chem. Soc. 80, 5573 (1958).
54. J. H. Beynon, R. A. Saunders, A. Topham and A. E. Williams, J. Chem. Soc., 6403 (1965).
55. A. K. Bose, K. G. Das, P. T. Funke, I. Kugajevsky, O. P. Shukla, K. S. Khanchandani and R. J. Suhadolnik, J. Am. Chem. Soc., 90, 1038 (1968).
56. A. L. Burlingame, B. Balogh, J. Welch, S. Lewis and D. Wilson, J. Chem. Soc., Chem. Comm., 318, (1972).
57. M. Tanabe, T. Hamasaki, D. Thomas and L. Johnson, J. Am. Chem. Soc. 93, 273 (1971).
58. S. Meyerson and P. N. Rylander, J. Am. Chem. Soc. 79, 1058 (1957).
59. F. M. Dean, J. Goodchild, R. A. W. Johnstone and B. J. Millard, J. Chem. Soc. (C), 2232, (1967).
60. M. Marx and C. Djerassi, J. Am. Chem. Soc. 90, 678 (1968).
61. T. H. Kinstle and J. G. Stam, J. Chem. Soc. (D) 185, (1968).
62. N. G. Foster and R. W. Higgins, Org. Mass Spectrom. 191, (1968).
63. R. M. Roberts and T. L. Gibson, J. Am. Chem. Soc. 93, 7340 (1971).
64. R. A. W. Johnstone, B. J. Millard, F. M. Dean, and A. W. Hill, J. Chem. Soc. (C) 1912, (1966).

65. O. Beeck, J. W. Otros, D. P. Stevenson and C. D. Wagner, J. Chem. Phys. 16, 255 (1948).
66. D. P. Stevenson, C. D. Wagner, O. Beeck and J. W. Otros, J. Chem. Phys. 16, 993 (1948).
67. J. W. Otros, D. P. Stevenson, C. D. Wagner and O. Beeck, J. Chem. Phys. 16, 745 (1948).
68. H. H. Voge, C. D. Wagner and D. P. Stevenson, J. Catalysis, 2, 58 (1963).
69. R. E. Honig, Phys. Rev. A, 75, 1319 (1949).
70. G. P. Happ and D. W. Stewart, J. Am. Chem. Soc. 74, 4404, 1952).
71. Paul N. Rylander and Seymour Meyerson, J. Am. Chem. Soc., 78, 5799 (1956).
72. Paul N. Rylander, Seymour Meyerson and H. M. Grubb, J. Am. Chem. Soc. 79, 842 (1957).
73. Seymour Meyerson and Paul N. Rylander, J. Chem. Phys. 27, 901 (1957).
74. Seymour Meyerson and Paul N. Rylander, J. Phys. Chem. 62, 2 (1958).
75. A. Langer and C. P. Johnson, J. Phys. Chem. 61, 891 (1957).
76. C. P. Johnson and A. Langer, J. Phys. Chem. 61, 1010 (1957).
77. Seymour meyersen and Paul N. Rylander, 4th Annual stim Meeting on Mass Spectrometry, Cincinnati, Ohio, 1956 paper No. 49.
78. G. J. Karabatsos, F. M. Vane and S. Meyerson, J. Am. Chem. Soc., 83, 4297 (1961).
79. G. J. Karabatsos, F. M. Vane and S. Meyerson, J. Am. Chem. Soc. 85, 733 (1963).
80. J. D. Roberts, R. E. McMahon and J. S. Hine, J. Am. Chem. Soc., 72 (1963)

81. G. J. Karabatsos, C. E. Orzech, Jr., and S. Meyerson, *J. Amer. Chem. Soc.* 86, 1994 (1964).
82. W. H. McFadden, K. L. Stevens, S. Meyerson, G. J. Karabatsos and C. E. Orzech, Jr., *J. Phys. Chem.* 69, 1742 (1965).
83. R. A. W. Johnstone and B. J. Millard, *Z. Naturforschg.* 21a, 604 (1966).
84. R. A. W. Johnstone and B. J. Millard, *J. Chem. Soc. (C)*, 1955 (1966).
85. A. V. Robertson, M. Marx and C. Djerassi, *J. Chem. Soc. (D)* 414, (1968).
86. A. V. Robertson and C. Djerassi, *J. Am. Chem. Soc.* 90, 6992 (1968).
87. K. L. Rinehart, Jr., A. C. Buchholz and G. E. VanLear, *J. Am. Chem. Soc.* 90, 1073 (1968).
88. P. D. Woodgate and C. Djerassi, *Tet. Lett.* 22, 1875 (1970).
89. G. G. Meisels, J. Y. Park and B. G. Giessner, *J. Am. Chem. Soc.* 91, 1555 (1969).
90. K. D. Berlin and R. D. Shupe, *Org. Mass Spectrom.* 447, (1969).
91. B. Davis, D. H. Williams and A. N. H. Yeo, *J. Chem. Soc. (B)* 81, (1970).
92. R. G. Cooks and S. L. Bernasek, *J. Am. Chem. Soc.* 92, 2129 (1970).
93. M. E. Rennekamp, W. O. Perry and R. G. Cooks, *J. Am. Chem. Soc.* 94, 4985 (1972).
94. J. D. Henion and D. G. I. Kingston, *J. Chem. Soc. (D)*, 258 (1970).
95. P. M. Draper and D. B. Machean, *Can. J. Chem.* 48, 746 (1970).
96. A. S. Siegel, *Org. Mass Spectrom.* 1417, (1970).
97. N. A. Uccella, I. Howe and D. H. Williams, *J. Chem. Soc. (B)* 1933, (1971).

98. V. A. Koptug, I. S. Isaev and M. I. Gorfinkel, Akad. Nauk. SSSR (Sev. Khim.) 845, (1970).
99. A. T. Balaban and D. Farasiu, J. Am. Chem. Soc. 89, 1958 (1967).
100. R. M. Roberts, A. A. Khalaf and R. N. Greene, J. Am. Chem. Soc. 86, 2864 (1964).
101. D. Farcasiu, Rev. Chim. (Bucharest) 10, 457 (1965).
102. F. G. Jiminez and R. I. Reed, Rev. Latinoamer. Quim. 6, 175 (1975).
103. F. Fajula and F. G. Gault, J. Am. Chem. Soc., 98, 7690 (1976).
104. K. L. Rinehart, Jr., A. C. Buchholz, G. E. Vanhear and H. L. Cantrill, J. Am. Chem. Soc. 90, 2983 (1968).
105. A. S. Siegel, J. Am. Chem. Soc. 92, 3277 (1970).
106. F. deJong, H. J. M. Sinnige and M. J. Janssen, Org. Mass Spectrom. 3, 1539 (1970).
107. A. Venema, N. M. M. Nibbering and T. J. deBoer, Org. Mass Spectrom. 3, 1589 (1970).
108. I. Horman, A. N. H. Yeo and D. H. Williams, J. Am. Chem. Soc. 92, 2131 (1970).
109. W. O. Perry, J. H. Beynon, W. E. Baftinger, J. W. Amy, R. M. Caprioli, R. N. Renaud, L. C. Leitch and S. Meyerson, J. Am. Chem. Soc. 92, 7236 (1970).
110. R. A. Davidson and P. S. Skell, J. Am. Chem. Soc. 95, 6843 (1973).
111. F. A. White, Mass Spectrometry in Science and Technology, John Wiley and Sons, Inc., New York, (1968).
112. M. S. Benedetti and P. Strolin, Pharmacologie Clinique 1, 15 (1973).
113. E. Flaumenhaft, R. A. Uphaus and J. J. Katz, Biochim. Biophys. Acta 215, 421 (1970).

114. C. T. Gregg, J. Y. Hutson, J. R. Prine, D. G. Oh and J. E. Furdiner, *Life Sciences* 13, 775 (1973).
115. C. Gregg, D. Smith, D. Oh, J. Malanify, B. McInteer, N. Matwiyoff and D. Neubert, *Proceedings Ninth International Congress of Biochemistry*, Stockholm (1973).
116. R. F. Tavares, "Studies on Some Compounds Labeled with  $^{13}\text{C}$  and  $^{15}\text{N}$ ," doctoral dissertation, University Microfilms, Inc., Ann Arbor, Michigan, (1968).
117. A. K. Bose, K. S. Khanchendani, P. T. Funke and M. Anchel, *J. Chem. Soc. (D)*, 1347, (1969).
118. E. Costa, *J. Psychiat. Res.* 11, 295 (1974).
119. L. Sweetman, W. L. Nyhan, P. D. Klein and P. A. Szczepanik, *Proceedings of the First International Conference on Stable Isotopes in Chemistry, Biology and Medicine*, Argonne Nat'l Lab., May, 1973. U. S. Atomic Energy Comm. Rept. No. CONF-730525, (1973).
120. M. Sano, Y. Yotsui, H. Abe and S. Sasaki, *Biomed. Mass Spectrom.* 3, 1 (1976).
121. T. Whelan, W. M. Sackett and C. R. Benedict, *Biochem. Biophys. Res. Comm.* 41, 1205 (1970).
122. B. N. Smith and S. Epstein, *Plant Physiol.* 47, 380 (1971).
123. B. S. Jacobson, B. N. Smith, S. Epstein and G. G. Laties, *J. Gen. Physiol.* 55, 1 (1970).
124. B. S. Jacobson, B. N. Smith and A. V. Jacobson, *Biochem. Biophys. Res. Comm.* 47, 398 (1972).

125. W. W. Shreeve, C. H. Wu, M. S. Roginsky, D. G. Ott, C. T. Gregg, R. Uphoff, J. D. Shoop and R. P. Eaton, Symposium on New Developments in Radiopharmaceuticals and Labeled Compounds, Copenhagen, 1973, Vol. 2., p. 281, Int. Atomic Energy Agency, Vienna, 1973.
126. V. H. Kollman, J. L. Hanners, J. Y. Hutson, T. W. Whaley, D. G. Ott and C. T. Gregg, *Biochem. Biophys. Res. Comm.* 50, 826 (1973).
127. P. D. Klein, J. K. Haumann and W. Eisler, *Anal. Chem.* 44, 490 (1972).
128. A. K. Bose, K. S. Khanchandani, R. Tavares and P. T. Funke, *J. Am. Chem. Soc.* 90, 3593 (1968).
129. George R. Waller, Ragnar Ryhage and Seymour Meyerson, *Anal. Biochem.* 16, 277 (1966).
130. W. J. A. Vandenheuvel and Jack S. Cohen, *Biochim. Biophys. Acta* 208, 251 (1970).
131. W. J. A. Vandenheuvel, J. L. Smith and J. S. Cohen, *Advances in Chromotography, Sixth International Symposium Proceedings*, (1970).
132. Walter Heinrich Johnson, Jr., CERN (*Eur. Organ. Nucl. Res.*) 1970 CERN 70-30 (Vol. 1), 307-19 (Eng.) in *Chem. Abst.* 74, 106156y, p. 106161 (1971).
133. K. Biemann, *Mass Spectrometry - Organic Chemical Applications*, McGraw-Hill, N.Y. (1962).
134. Oliver A. Schaeffer, *J. Chem. Phys.* 18, 1501 (1950).
135. M. A. Baldwin, F. W. McLafferty and Donald M. Jerina, *J. Am. Chem. Soc.* 97, 6169 (1975).
136. Jean Pierre Leicknam, *Commis. Energ. At. (Fr)*, Rapp. No. 3134, 103 pp. (1967) (Fr.). Taken from *Chem. Abst.* 68, 117954j (p. 11381) (1968).

137. F. L. Mohler and V. H. Dibeler, *Phys. Rev.* 72, 158 (1947).
138. Lorin P. Hills, Marvin L. Vestal and Jean H. Futrell, *J. Chem. Phys.* 54, 3834 (1971).
139. J. H. Beynon, D. F. Brothers and R. G. Cooks, *Anal. Chem.* 46, 1299 (1974).
140. John H. Beynon, J. E. Corn, William E. Baitinger, R. M. Caprioli, Robert A. Benkeser, *Org. Mass Spectrom* 3, 1371 (1970).
141. Ian Howe and Dudley H. Williams, *Chem. Comm.* 1971, 1195.
142. Fred L. Mohler, Vernon H. Dibeler, Laura Williamson and Helen Dean, *J. Res. Natl B. of Stand.* 48, 188 (1952).
143. Maurice M. Bursey and F. W. McLafferty, "Linear Free Energy Relationships of Ion Abundances in Mass Spectra" (~1964).
144. Maurice M. Bursey and F. W. McLafferty, *J. Am. Chem. Soc.*, 89, 1 (1967).
145. R. Graham Cooks, Ian Howe and Dudley H. Williams, *Org. Mass Spectrom* 2, 137 (1969).
146. J. H. Beynon, *Mass Spectrometry and Its Application to Organic Chemistry*, Elsevier, Amsterdam (1960).
147. F. W. McLafferty, *Interpretation of Mass Spectra*, 2nd Edition, W. A. Benjamin, Inc., Reading, Mass. (1973).
148. V. L. Avona and C. F. Eck, "Proceedings of the Second International Conference on Stable Isotopes in Chemistry, Biology and Medicine," October, 1975, Oak Brook, Ill., E. R. Klein and P. D. Klein, ed., ERDA CONF. 751027, National Technical Information Service, Springfield, VA., 1976, p. 705.

149. R. D. Hill, A. M. Unrau and D. T. Canvin, *Can. J. Chem.* 44, 2077 (1966).
150. T. A. Dobson, D. Desaty, D. Brewer and L. C. Vining, *Can. J. Biochem.* 45, 809 (1967).
151. D. Desaty, A. G. McInnes, D. G. Smith and L. C. Vining, *Can. J. Biochem.* 46, 1293 (1968).
152. H. M. Grubb and S. Meyerson, *The Mass Spectrometry of Organic Ions*, F. W. McLafferty, Ed, Academic Press, Inc., New York, N.Y. 1963.
153. A. G. McInnes, D. G. Smith and L. C. Vining, *Chem. Comm.* 325 (1971).
154. A. I. Scott, H. Guilford and Eunlee, *J. Am. Chem. Soc.* 93, 3534 (1971).
155. A. G. McInnes, D. G. Smith, L. C. Vining and J.L.C. Wright, *Chem. Comm.* 1669 (1968).
156. W. F. Hadon, H. C. Lukens and R. E. Elsken, *Anal. Chem.* 45, 682 (1973).
157. J. F. Holland, C. C. Sweeley, R. E. Thrush, R. E. Teets and M. A. Bieber, *Anal. Chem.* 45, 308 (1973).
158. K. L. Rinehart, Jr., A. C. Buckholz, G. E. VanLear and H. L. Cantrill, *J. Amer. Chem. Soc.* 90, 2983 (1968).
159. H. R. Inle and A. Neubert, *Int. J. Mass Spectrom. Ion. Phys.* 7, 189 (1971).
160. P. V. Divekar, H. Raistrick, T. A. Dobson and L. C. Vining, *Can. J. Chem.* 43, 1835 (1965).

## APPENDIX

## A. Computer analysis technique

## 1. Preliminary remarks

Isotopic abundance mass spectral data is most commonly obtained in the form of height measurements of oscillograph peaks which correspond to ionic abundances at given masses. (See Appendix B-1-a) Reduction of this data to yield abundance values of various isotopes and a description of the isotopic distribution within the molecular ion may be accomplished through utilization of the polynomial nature of the generating functions which describe the regions of ionic intensity (See Part II-C). The calculations involved are time-consuming and repetitive and are, thus, most efficiently accomplished with computer aid. Application of this polynomial nature is a new approach and, therefore, required development of the following computer programs.

Two different manipulations of the polynomial nature of the isotopic generating functions were described above (See Part II-C). Each requires its own computer program.

The programs are written in Focal-11 for a 4K PDP-11/20 system. The 4K limit of this particular system required treatment of a spectrum by individual ion regions. Each ion region could contain up to eight observable ion intensities formed by ions composed of up to five different types of atoms, that is, different elements with corresponding isotopic distributions and/or different isotopic distributions of a particular element. Larger clusters and more complex ion regions may be treated on systems with increased memory configuration. The program is

entered via paper tape and data is entered via a teletype. Output is received either through the teletype or through a graphic computer terminal. All program/programmer interaction proceeds with a conversational format. This format was chosen to enable the computer to best serve as an aid to the thought processes of the user rather than as a "black box" data processor.

2. One parameter approach - a limited application of the polynomial formulation

Initially a simple curve fitting application of the polynomial nature of the isotopic generating function was developed (See Part II-C-1-3). This is termed the "one parameter approach" in that only one unknown value may be accurately determined at one time. For example, use of the one parameter approach allows definite determination of one unknown abundance value for a given number of carbon sites or the number of enriched carbon sites containing a given isotopic abundance. Exact determination of more than one unknown abundance value or the number of enriched sites of an unknown isotopic content is outside the scope of this approach. The single value obtained in cases of multiple enrichment levels will approximate the average isotopic abundance of the ion. The more information known, the more accurate the approximation will be. A description of the program format follows and will serve to illustrate its application.

The first portion of the program proper involves input and manipulation of intensity data and corresponding absolute errors. Data required for input are the number of ions in the ion region to be

considered, the  $m/z$  of the lowest mass ion, and raw data consisting of relative intensities of ions by nominal mass. The data including  $m/z$  values, raw intensity values, and normalized intensity values are then printed out and the absolute error in raw intensity values entered individually. The total region intensity (sum over intensity values) and the absolute measuring error is then computed and printed out.

The second portion of the program involves input and manipulation of isotopic abundance data. It is to this portion that the program repeatedly returns for changes in the one parameter being varied in this approach. Data input required includes the number,  $N$ , of atom types as previously defined, the number of a particular atom type within a molecule, and the relative abundances expected for the heavy isotopes of that atom type. For example, if the ion under consideration were water,  $H_2O$ , with all isotopes at natural abundance levels one would first enter  $N=2$  (atom types) and then, for the hydrogens, 2 followed by 0.015, the relative abundance of deuterium and zero, the abundance of tritium being insignificant. For oxygen one would enter 1 followed by 0.037 and 0.204, the relative natural abundances of  $O^{17}$  and  $O^{18}$ , respectively. The portion of the ion region due to these known isotopic abundance values is then calculated.

The third portion of the program involves calculation of a spectrum from given isotopic abundance data for comparison with the observed intensity data. Input data required are the mass number at which the calculation is to begin, the quantity by which the unknown isotopic abundance is to be varied, the isotopic abundance at which to cease

iterations, the number of unknown atom types, and the isotopic abundance at which calculations are to begin. A print out may be requested of the information upon which calculations are currently being based.

The program then calculates a spectrum based on the given initial isotopic abundance and the intensity of the first ion in the region, subtracts that calculated spectrum from the observed intensities, recalculates the spectrum based on the intensity of the remainder of the second ion, subtracts and continues until all intensities in the specified region are utilized.

The results including the calculated size of each ion cluster in the region and the error are printed out.

The program then automatically varies the isotopic abundance by the specified amount and repeats the above calculations continuing in this manner until the specified limit is reached or until subtraction of the calculated spectrum from the observed produces a negative ion intensity thereby indicating that a maximum isotopic abundance has been reached. In this case, the computer prints the phrase "Max % at Mass...." indicating the maximum isotopic abundance which will possibly yield a spectrum consistent with that observed and the  $m/z$  of the limiting ion intensity.

The resulting table of varying isotopic abundance values with corresponding ion cluster intensities and errors may be used for manual comparison with observed data (See Appendix B-2). A similar analysis may be carried out for other regions of the spectrum, thereby obtaining corroborating evidence for a particular solution.

This simple approach has proven remarkably effective in

defining the set of solutions possible within observable uncertainties. It requires only minimal computer capabilities and serves as an efficient aid to the thought processes of the individual researcher.

3. Factor approach - a more general application of the polynomial formulation

A more valuable application of the polynomial formulation was developed based on extraction of the factors of equation (II-14), p. 71. The approach is more general in that more than one unknown isotopic abundance may be accurately determined at a time.

The computer program which facilitates application of the factor approach begins identically with that corresponding to the one parameter approach, i.e. input and manipulation of ion intensity data followed by input and manipulation of isotopic abundance data for known portions of the molecule.

The program then asks for several parameters by which to adjust its calculations: Shall calculations be iterative? Shall calculations cease when a maximum isotopic abundance value,  $b_x$ , is reached for a given polynomial,  $P_{M+L}^R$ ? Shall a plot of  $b_x$  vs.  $P_{M+L}^R$  be constructed? And, if so, which value of L shall determine the polynomial of interest? For which value of  $a_x$ , the abundance of the light isotope, shall iterations cease? By what increment shall  $b_x$  or, if present,  $c_x$ , the abundance of the isotope two mass units above the light isotope, be varied? How many atom types, n, are being investigated? What shall be the beginning values for  $b_x$  and  $c_x$ ?

For iterative calculations of varied isotopic abundance values,

the indicated plot is then constructed or the calculated cluster abundance values with corresponding values of  $P_{M+L}(\lambda)$  printed.

If the plot of  $b_x$  vs.  $P_{M+L}^R(\lambda)$  is constructed, intersections at zero on the  $P_{M+L}^R(\lambda)$  coordinate will occur for correct values of  $b_x$  (see Part III-D-2).

## B. Experimental

### 1. Instrumentation

#### a. Mass spectrometer and related systems

Mass spectra were obtained using a Dupont/Consolidated Electrodynamics Corporation double-focusing mass spectrometer, Model 21-110B, operated at 70 eV. Low resolution (unit mass separation) spectra were recorded on a CEC recording oscillograph, Model 5-124. High resolution ( $\sim 1$  in 20,000) spectra obtained for the purpose of exact mass determination were recorded directly onto Ilford  $Q_2$  photographic plates. In those instances where ion intensity values were needed at high resolution, the regions of interest were recorded on the CEC oscillograph.

Solid samples were introduced through a vacuum lock via a direct introduction probe, the tip of which was heated separately from the ion source.

Liquid samples were introduced through a volatile sample inlet system which consisted of two valves, one to the rough pump and the other to a glass line leading directly into the ion source. Total volume of the inlet system was less than 40 cc. Sample flow could be roughly

adjusted at the valve to the ion source.

b. Computing system

Computations were done using programs written in Focal-11 for a Digital Equipment Corporation PDP 11 with a minimum 4 K memory configuration (See Appendix A). Additional auxiliary equipment included an ASR 33 teletype, a Tektronix graphic computer terminal, Model T-4002, and a Sykes Compu/corder 100.

2. Methods

a. Mass spectral recording techniques

Three distinct problems were identified in attempts to obtain accurate ion intensity measurements:

(1) An ion containing one  $^{13}\text{C}$  atom will lie at the same nominal mass as the ion produced by addition of hydrogen to the corresponding  $^{12}\text{C}$  isomer. Separation of these two ions of differing molecular formulas requires a resolution of approximately 1 in 50,000 at mass 200. Accurate intensity values are not obtainable at this resolution with the equipment employed (156).

(2) As conventionally recorded on an oscillograph, peak areas, rather than peak heights, are proportional to ion intensities.<sup>18</sup> Peak shapes will change with changing mass as well as with changes in instrument parameters. Therefore, peak areas are not readily obtainable

---

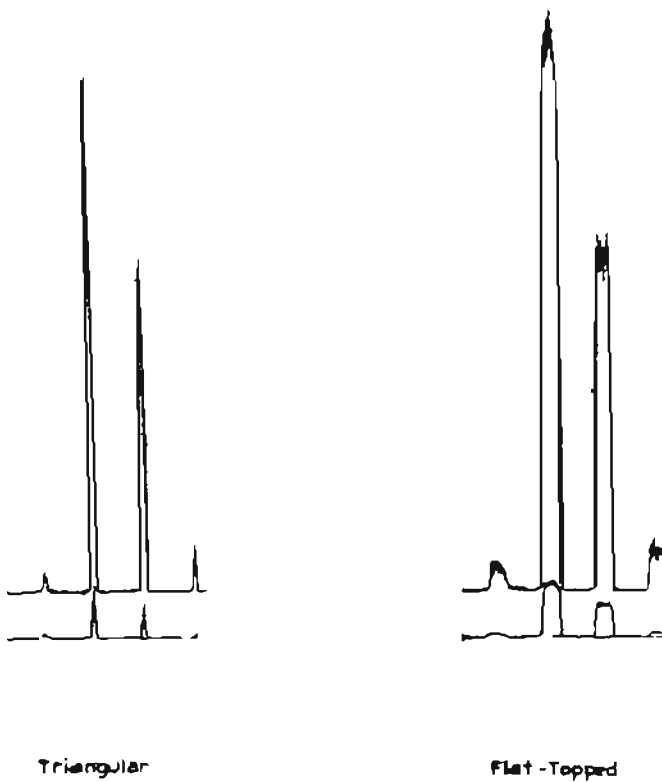
<sup>18</sup>This opinion, clearly apparent in experimental measurements done for this investigation, is commonly held (40,147). However, for an interesting contrary opinion see work done by Holland and Sweely, et al. (157).

without instrumental modifications. Peak heights, on the other hand, are easily measurable.

(3) Instrument noise, particularly that originating in the electron multiplier of our detection system resulted in non-constant peak ratios. That is exact peak height was dependent upon noise level at the instant of recording. In theory, this problem might seemingly have been solved by averaging multiple scans (55,128). However, in practice, such multiple scans are not always comparable especially within the rather extended time frame required with the previously described equipment (41,116,129,145). Ion clusters will be produced by processes other than fragmentation; i.e. ion-molecule reactions, dehydrations, oxidations, reductions, etc. For samples subject to such reactions the conditions controlling the reaction rates must be carefully stabilized (pressure, temperature, time, presence of impurities). Where sufficient stabilization is not obtainable as here, the accuracy of any measurement will be degraded when averaging in the suggested manner is attempted.

A single, temporary solution to these three problems of varied origin was developed through the simple technique of scanning with wide slit width and slow magnet speed thereby producing an oscillograph recording characterized by broad, flat-topped peaks of unit mass resolution (Figure A-1). Rinehart (158) and Djerassi (88) have each also reported using this technique in some applications. A peak height is then a measure of the sum of all ion intensities at a given unit mass since the

FIGURE A-1.  
 Representative Oscillograph Peak Shapes For EI Mass Spectra  
 Recorded With Different Exit:Entrance Slit Widths.



entire ion beam will strike the detector at once.<sup>19</sup> Computations may then treat observables as the sum of the ion intensities at a given nominal mass. There is no need to obtain peak areas since peak width is now proportional to the speed of scanning the magnetic field, not to

---

<sup>19</sup>The technique of scanning with wide slit widths bears some resemblance to ion counting technique which is known to significantly increase sensitivity of measurement (159).

the ion intensity. Experience demonstrated that a fairly accurate estimate of the instrument noise average can be made visually.

Data in Tables A-1 and A-2 illustrate the superiority of this recording technique. Experiments using intensity ratios of ions of known elemental composition show that for highest accuracy this method requires (a) the entrance slit be wide enough to yield nominal mass resolution; (b) the exit slit be wide enough to allow the entire beam to pass; (c) the ratio of entrance to exit slit width be such that flat-top rather than triangular peaks be produced; and (d) the ion beam intensity be such that the electron multiplier is not saturated. When these conditions obtain results are of superior accuracy and precision.

With available equipment strip chart intensity data were produced with a dynamic range of 500 units (most intense/weakest peak) with an average instrumental error of  $\pm 1$  unit.

#### b. Computational techniques

Computations were done using original computer programs especially designed for the statistical approach described herein. Descriptions of these programs are contained in Appendix A.

### 3. Materials

#### a. Fusaryl alcohol

Fusaryl alcohol samples enriched at specific sites with  $^{13}\text{C}$  were kindly provided for mass spectral analysis by Drs. D. G. Smith and A. G. McInnes (151) and were analyzed on a mass spectral system as described above using the volatile sample inlet system. Highly volatile impurities in the samples were reduced by the use of the vacuum system

TABLE A-1  
M/M + 1 ION INTENSITY RATIOS FROM MASS SPECTRA OF ACETYL ACETONE PARENT ION REGION  
DEMONSTRATING CHANGE IN M/M + 1 WITH CHANGE IN SLIT WIDTH

Slit Adjustment	Triangular Peaks	Both Slit Wide Open	Entry Slit: Exit Slit (1:2)
M/M + 1 (1)	15.0	15.1	17.2
(2)	15.2	15.6	17.3
(3)	14.6	16.2	17.5
Average	$14.9 \pm .2^{bc}$	$15.6 \pm .4^{ab}$	$17.3 \pm .1^{bd}$

<sup>a</sup>Values low and precision poor due to saturation of the electron multiplier in the detection system.

<sup>b</sup>Precision given as standard deviation.

<sup>c</sup>Precision poor due to electron multiplier noise and values low due to need for peak area measurements as opposed to peak height measurements.

<sup>d</sup>Theoretical value = 17.3. Precision improved by visual averaging of instrumental noise on top of the flat peak.

TABLE A-2  
 ION INTENSITY RATIOS FROM MASS SPECTRA OF FUSARYL ALCOHOL PARENT ION REGION  
 DEMONSTRATING QUALITY OF VISUAL AVERAGING POSSIBLE WITH USE OF WIDE SLIT WIDTHS

Peak Shape <sup>a</sup>	Triangular <sup>b</sup>	Flat-Topped <sup>c</sup>
Ion Intensity Ratios <sup>d</sup>	1.58	1.65
	1.62	1.66
	1.47	1.65
	$1.56 \pm .05^e$	$1.65 \pm .005^e$

<sup>a</sup>Refers to appearance of ion intensity peaks as recorded by a CEC oscillograph.

<sup>b</sup>Triangular peaks were observed when slit widths were adjusted so that no finite time existed when the entire ion beam was incident upon the detector.

<sup>c</sup>Flat-topped peaks were observed when the exit slit was adjusted so that the entire ion intensity was incident upon the dector for a finite time.

<sup>d</sup>Ratio of ion intensities of mass 164/165.

<sup>e</sup>Precision as standard deviation.

of the mass spectrometer prior to analysis. The disappearance of these impurities was monitored through periodic spectral recordings on the oscillograph.

The fusaryl alcohol sample itself was maintained in a water-ice bath throughout the recording period to limit its volatility. Instrument parameters were approximately as follows: inlet temperature, 45°C; source temperature, 220°C; pressure  $2-6 \times 10^{-7}$  torr.

b. Sepedonin

Sepedonin samples also were provided by Drs. D. G. Smith and A. G. McInnes (153,155,160) and were analyzed using a mass spectral system as described above utilizing the direct introduction probe for these solid samples. The sample itself was held in a capillary tube inserted into the probe tip. Instrument parameters were approximately as follows: source temperature 140°-160°C; pressure,  $2 \times 10^{-7}$  torr.

Care was exercised to maintain instrumental parameters as constant as possible because the sepedonin samples suffered from instability of several sources. Immediate dehydration of sepedonin produced the most intense region of the spectrum. No true molecular ion was visible. This dehydration coupled with reduction of the dehydration product resulted in severely time dependent spectra. The time dependence could be roughly correlated with the temperature of the direct introduction probe.

## VITA

The author, Bari Shown Earl, was born in Las Vegas, Nevada on April 3, 1944. She attended the University of Nevada, Las Vegas where she received financial assistance from the First Western Savings and Dorothea Brinker Scholarship Funds and earned the degree Bachelor of Science in Chemistry in 1968. She was listed in Who's Who Among Students in American Colleges and Universities, 1967-68 for her achievements during her undergraduate studies. At the University of Nevada, Las Vegas, she was employed as a research assistant to Dr. Robert Smith and as Supervisor of Chemical Stockrooms from 1966-68. Following graduation from UNLV, she was employed as a pathology laboratory technician by the University of Oregon Dental School. She entered the Oregon Graduate Center for Study and Research and obtained the degree Master of Science in Organic Chemistry in 1972 and pursued her doctoral research. Manuscripts based on this work are in preparation. She is a member of the American Chemical Society and Phi Kappa Phi.

Mrs. Earl is married to John Lawrence Earl, D.M.D. They have four children, Laura Melissa, Donna Melinda, Molly Beth, and Emily Melaina..